THESIS APPROVAL

GRADUATE SCHOOL, KASETSART UNIVERSITY

Master of Engineering (Chemical Engineering)

DEGREE

Chemical Engineering — **FIELD**

Chemical Engineering — **DEPARTMENT**

TITLE: Investigation of Accuracy of Different Procedures for Estimating the Gas Diffusivity and the First Order Irreversible Reaction Rate Constant From TAP Pulse Responses

NAME: Miss Rapeeporn Ekjamnong

THIS THESIS HAS BEEN ACCEPTED BY

______________________________ **THESIS ADVISOR**

(Associate Professor Phungphai Phanawadee, D.Sc.)

______________________________ **THESIS CO-ADVISOR**

(Associate Professor Metta Chareonpanich, D.Eng.)

______________________________ **DEPARTMENT HEAD**

(Associate Professor Phungphai Phanawadee, D.Sc.)

APPROVED BY THE GRADUATE SCHOOL ON ______________________________

______________________________ **DEAN**

(Associate Professor Gunjana Theeragool, D.Agr.)

THESIS

INVESTIGATION OF ACCURACY OF DIFFERENT PROCEDURES FOR ESTIMATING THE GAS DIFFUSIVITY AND THE FIRST ORDER IRREVERSIBLE REACTION RATE CONSTANT FROM TAP PULSE RESPONSES

RAPEEPORN EKJAMNONG

A Thesis Submitted in Partial Fulfillment of
the Requirements for the Degree of
Master of Engineering (Chemical Engineering)
Graduate School, Kasetsart University
2011

Rapeeporn Ekjamnong 2011: Investigation of Accuracy of Different Procedures for Estimating the Gas Diffusivity and the First Order Irreversible Reaction Rate Constant from TAP Pulse Responses. Master of Engineering (Chemical Engineering), Major Field: Chemical Engineering, Department of Chemical Engineering. Thesis Advisor: Associate Professor Phungphai Phanawadee, D.Sc. 119 pages.

A transient experiment called "temporal analysis of products" (TAP) has been increasingly applied for heterogeneous catalytic reaction studies. The kinetic parameters from the TAP experimental response can be determined by using different estimation procedures including 1) determination of the kinetic parameters after transport parameter determination, and 2) determination of the kinetic and transport parameters simultaneously. In this work, the effect of different procedures on the accuracy of estimated transport and kinetic parameters are theoretical investigated for the first order irreversible reaction case under a non-ideal inlet flow condition. A more accurate procedure is the one which gives a lower deviation of the estimated parameters from the real values. Simulation results show that for the one-zone reactor, the first procedure provides the most accurate of estimated diffusivity and reaction rate constant. In addition, the exit flow rate curve fitting gives more accurate results than the unit-area normalized response fitting. Similar results are obtained for three-zone reactor case.

Student's signature Thesis Advisor's signature ___ / ___ / _____

ACKNOWLEDGEMENTS

Firstly I would like to express my sincere gratitude to Associate Professor Dr. Phungphai Phanawadee, who has been an excellent advisor, and has supported me in every way. I have also benefited from his broad knowledge and logical way of thinking. His understanding, encouraging and personal guiding have provided a good basis for the present thesis and life.

I am deeply grateful to my thesis co-advisor, Associate Professor Dr. Metta Chareonpanich, and my thesis committees, Associate Professor Dr. Apinya Duangchan and Dr. Monrudee Phongaksorn for their valuable comments and suggestions.

My sincere thanks are due to all of my friends and colleagues, for their suggestions, support and encouragement during study and research work.

I am especially appreciated my parents, my sister and brother for their heartfelt love and continuing support and encouragement throughout my life.

The financial support from the National Nanotechnology Center under the National Science and Technology Development Agency, the National Center of Excellence for Petroleum, Petrochemicals, and Advanced Materials, and the Kasetsart University Research and Development Institute is also gratefully acknowledged.

Rapeeporn Ekjamnong
March 2011

TABLE OF CONTENTS

TABLE OF CONTENTS (Continued)

Page

LIST OF TABLES

LIST OF TABLES (Continued)

Page

Appendix Table

LIST OF FIGURES

LIST OF FIGURES (Continued)

Figure **Page**

LIST OF FIGURES (Continued)

LIST OF FIGURES (Continued)

LIST OF FIGURES (Continued)

Figure **Page**

LIST OF FIGURES (Continued)

Figure **Page**

LIST OF FIGURES (Continued)

Figure **Page**

Appendix Figure

LIST OF ABBREVIATIONS

A	=	cross-sectional area of the microreactor (cm^2)
a_s	=	surface concentration of active sites of catalyst (mol cm^2 of catalyst)
C	=	gas concentration (mol/cm^3)
C^*	=	dimensionless gas concentration
d	=	ratio of dimensionless diffusivity defined by $d \equiv \dfrac{D_{e,est}}{D_{e,real}}$
d_i	=	ratio of dimensionless diffusivity of gas in inert zone defined by $d_i \equiv \dfrac{D_{e,est}^{inert}}{D_{e,real}^{inert}}$
d_c	=	ratio of dimensionless diffusivity of gas in catalyst zone defined by $d_c \equiv \dfrac{D_{e,est}^{cat}}{D_{e,real}^{cat}}$
ΔD_e	=	quantity defined by $\Delta D_e \equiv \dfrac{D_{e,est} - D_{e,real}}{D_{e,real}}$
$\bar{d}$	=	average diameter of the interstitial voids between the pellets in the reactor (cm)
D_e	=	effective Knudsen diffusivity (cm^2/s)
D_e^{cat}	=	effective Knudsen gas diffusivity in the catalyst zone
D_e^{inert}	=	effective Knudsen gas diffusivity in the inert zone
d_{pellet}	=	average pellet diameter (cm)
F	=	dimensional exit flow rate of gas (mol/s)
F^*	=	dimensionless exit flow rate of gas
k	=	adsorption/reaction rate constant (cm^3 of gas/mol s)

LIST OF ABBREVIATIONS (Continued)

k'	=	apparent adsorption/reaction rate constant (s^{-1})
L	=	microreactor length (cm)
MW	=	molecular weight
N_p	=	number of moles or molecules of gas in the inlet pulse
R	=	gas constant (= 8.314 J/mol K)
S_v	=	surface area of catalyst per volume of catalyst (cm^{-1})
t	=	time (s)
t_{open}		opening duration time (s)
T	=	absolute temperature at each reactor axial coordinate (K)
X	=	gas conversion
z	=	reactor axial coordinate (cm)

Greek letters

κ	=	dimensionless adsorption/reaction rate constant
$\Delta\kappa$	=	quantity defined by $\Delta\kappa \equiv \frac{\kappa_{est} - \kappa_{real}}{\kappa_{real}}$
$\delta(t-0^+)$	=	Dirac delta function placed at $t = 0^+$
$\delta(\tau-0^+)$	=	Dirac delta function placed at $\tau = 0^+$
ε_b	=	fractional voidage of the packed-bed
τ	=	dimensionless time
τ'	=	tortuosity factor
ξ	=	dimensionless reactor axial coordinate

Subscripts

est	=	estimated parameters
real	=	real parameters

INVESTIGATION OF ACCURACY OF DIFFERENT PROCEDURES FOR ESTIMATING THE GAS DIFFUSIVITY AND THE FIRST ORDER IRREVERSIBLE REACTION RATE CONSTANT FROM TAP PULSE RESPONSES

INTRODUCTION

Steady-state and transient experiments have been used for kinetic study of heterogeneous catalytic reactions. The data obtained from steady-state conditions contains information on the overall process. Transient techniques are usually applied to reveal more information on the mechanism of the reactions. A transient experiment called "temporal analysis of products" (TAP) (Gleaves *et al*., 1988; Gleaves *et al*., 1997) has been increasing applied for studying heterogeneous catalytic reaction (Gleaves *et al*., 2010). The TAP experiment is performed by injecting a narrow gas pulse by a pulse valve into an evacuated microreactor containing catalyst particles. The gas exiting the reactor is monitored as a function of time with a mass spectrometer producing a transient response. The intensity of the response is proportional to the exit flow rate of the corresponding gas. The size and the shape of the experimental response depend on transport characteristics and chemical kinetics of the system. Quantitative interpretation of TAP response data requires mathematical models that describe the transport and chemical processes in the reactor. The simplest reactor is the one-zone reactor which is a reactor uniformly packed with catalyst or inert particles. Another type of reactor is the three-zone reactor which contains a catalyst bed sandwiched between two inert beds. The advantage of the three-zone reactor is that the temperature distribution in the catalyst bed is more uniform than the one-zone reactor.

Estimation of transport and kinetic parameters in TAP experiments can be accomplished by comparing the experimental response with the model response based on the least square fit. Different types of response curves may be used for parameter estimation including the exit flow rate curve and the unit-area normalized response.

The exit flow rate curve fitting concerns both the size and shape of the response. The use of the exit flow rate to interpret the TAP experimental data needs the information of the absolute calibration factor and the pulse intensity required in the mathematical model (Huinink, 1995). These two parameters are not easily determined precisely and can vary depending on the operating conditions. Due to this disadvantage, the unit-area normalized curve fitting method concerning only the shape of the response is practically more common.

The estimation of the kinetic parameter is often performed after the diffusivity is predetermined from a diffusion experiment (Gleaves *et al.*, 1997). However some researchers estimate the kinetic parameters by determining the transport and kinetic parameters simultaneously (Soick *et al.*, 2000). The kinetic parameters extracted from TAP experiment is expected to be as accurate as possible. It is of great interest to investigate how the different estimation procedures affect the accuracy. If all the assumptions or the ideal conditions e.g., the Dirac delta inlet flow condition, zero concentration at the reactor outlet and uniform temperature distribution in the reactor, applied in the mathematical model are exactly true, the estimated parameters from different procedures would be identical, since the experimental and the model responses would coincide. A way to compare those methods should be based on a well-defined condition, which can be accomplished by simulation. We can assume a non-ideal inlet condition in the model and calculate the response. The calculated response is assumed to be the experimental response. The parameters used in the calculation of this response are assumed to be real parameters. The parameter estimation from the experimental response is performed using the ideal model. The deviation of the estimated parameters from the real parameters can be determined and compared for different estimation procedures.

In this work, the first order irreversible reaction case will be focused. The TAP experimental responses are obtained from simulation assuming the triangular-shape inlet flow having the highest at the beginning and linearly decreasing to zero at the time the pulse valve closes. This inlet flow condition follows the specification of the pulse valve (Rothaemel *et al.*, 1996). The kinetic parameter from the TAP experimental response is determined by using different estimation procedures including determination of the kinetic parameter after transport parameter determination, and determination of the kinetic and transport parameters simultaneously. A more accurate procedure is the one which gives a lower deviation of the estimated parameters from the real ones. How well each estimation method can handle the non-ideal condition will be studied.

OBJECTIVE

The objective of this work is to investigate accuracy of different procedures for estimating the transport and kinetic parameters from TAP pulse responses for the irreversible reaction case.

Scope

The simulation work focuses on the case in which the temperature distribution in the reactor is uniform. The non-ideal inlet flow with a triangular shape is used to generate the experimental responses. The first order irreversible reaction case is focused with the gas conversion ranges from 0.01 to 0.99. The exit flow rate curves and the unit-area normalized response curves are applied for parameter estimations based on the least square fit. Both the one-zone and three-zone reactors are investigated. For the three-zone reactor, the ratios of length of the catalyst zone to the length of the reactor are 1/3 and 1/30.

LITERATURE REVIEW

Temporal analysis of products or TAP (Gleaves *et al*., 1988; Gleaves *et al*., 1997; Gleaves *et al*., 2010) has been recognized as an important transient experimental method for heterogeneous catalytic reaction studies (Pérez-Ramírez and Kondratenko, 2007). The basic TAP system (Figure 1) consists of: (1) pulse valve, (2) microreactor, (3) vacuum chamber, (4) mass spectrometer.

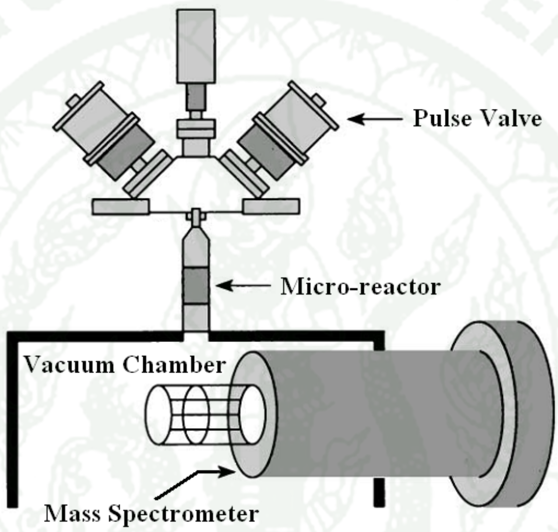

Figure 1 TAP reactor system

The TAP pulse-response experiment is performed by injecting a narrow gas pulse into an evacuated packed bed microreactor. The outlet of the reactor is maintained at low pressure (10^{-8} torr). The gas exiting the reactor is monitored as a function of time with a quadrupole mass spectrometer (QMS) producing a transient response at the QMS detector. Intensity of the response is proportional to the exit flow rate of the corresponding gas. Quantitative information of the phenomena in the reactor can be extracted from the size and the shape of the responses by the use of mathematical models that describe the processes in the reactor. The required mathematical solution therefore describes the gas exit flow rate. The experimental gas exit flow rate can be determined only when the absolute calibration factor has been obtained. Matching of the experimental and the model exit flow rates provides the estimated parameters. However, the use of the exit flow rate needs the information of the absolute calibration factor and the inlet pulse intensity that appears in the mathematical model (Huinink, 1995). Alternative approach for determining parameters is to use a pulse-intensity (PI) –normalized flow rate (Phanawadee, 1997) for curve fitting. The PI-normalized flow is the gas exit flow rate divided by the number of moles of the corresponding gas in the inlet pulse (F/N_p). To obtain the PI-normalized flow, a relative calibration factor is required (Phanawadee, 1997). Matching of two types of the responses including the exit flow rate curve and the pulse intensity (PI) normalized exit flow rate provides the same estimated parameters provided that the calibration factors are accurate. However, many researchers used the experimental response curve without converting into the exit flow rate curve (Svoboda *et al.*, 1992; Weerts *et al.*, 1996; Schuurman *et al.*, 1997; Fierro *et al.*, 2002). In this case, only the shape of the response is concerned. When only the shape is concerned, the two area-equated responses, or usually unit-area normalized responses, are compared. It should be noted for the diffusion-only case, the unit-area normalized responses of a non-reactive gas is the PI-normalized flow because area is unity due to the mass conservation.

The TAP experiment typically involves a small amount of inlet gas and the pressure in the reactor is so low that the gas transport through the reactor is Knudsen diffusion. An important characteristic of the Knudsen diffusion is that the diffusivities of the individual components of the gas mixture are independent of the gas composition of the mixture or the pressure. The effective Knudsen diffusivity of a gas in a packed bed can be determined by (Huizenga and Smith, 1986)

$$D_b = \frac{\varepsilon_b}{\tau'}\frac{\bar{d}}{3}\sqrt{\frac{8RT}{\pi MW}} \tag{1}$$

where $\bar{d}$ is the average diameter of the interstitial voids between the pellets in the reactor (m), ε_b is the void fraction in the bed, τ' is the tortuosity factor and MW is the molecular weight.

For spherical pellets,

$$\bar{d} = \frac{2\varepsilon_b}{3(1-\varepsilon_b)} d_{\text{pellet}} \tag{2}$$

where d_{pellet} is the average pellet diameter (m).

The effective Knudsen diffusivity of a gas can be calculated from the effective Knudsen diffusion coefficient of another gas in the same bed using the correlation

$$D_{e,1} \frac{\sqrt{MW_1}}{\sqrt{T_1}} = D_{e,2} \frac{\sqrt{MW_2}}{\sqrt{T_2}} \tag{3}$$

where D_e, MW, and T are the effective Knudsen diffusivity, molecular weight, and temperatures respectively, and subscripts 1 and 2 refer to gas 1 and gas 2 respectively.

Several types of microreactor configurations have been applied in the TAP experiments. A one-zone reactor (Figure 2) is the reactor in which its entire volume is uniformly packed with inert or catalyst particles. A more common reactor configuration is a three-zone reactor (Figure 3) in which the catalyst bed is sandwiched between beds of inert particles. The main advantage of the three-zone reactor is that the temperature distribution in the catalyst bed is more uniform.

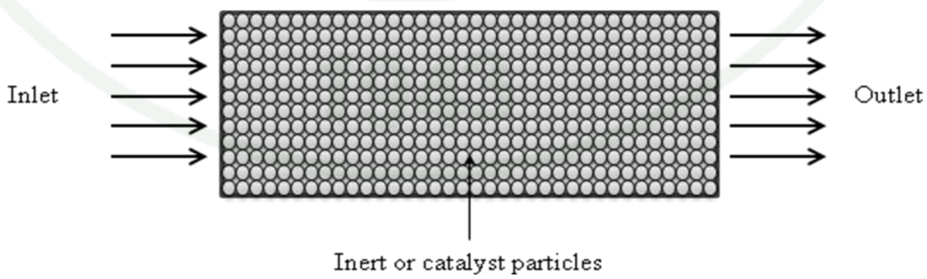

Figure 2 One-zone TAP reactor

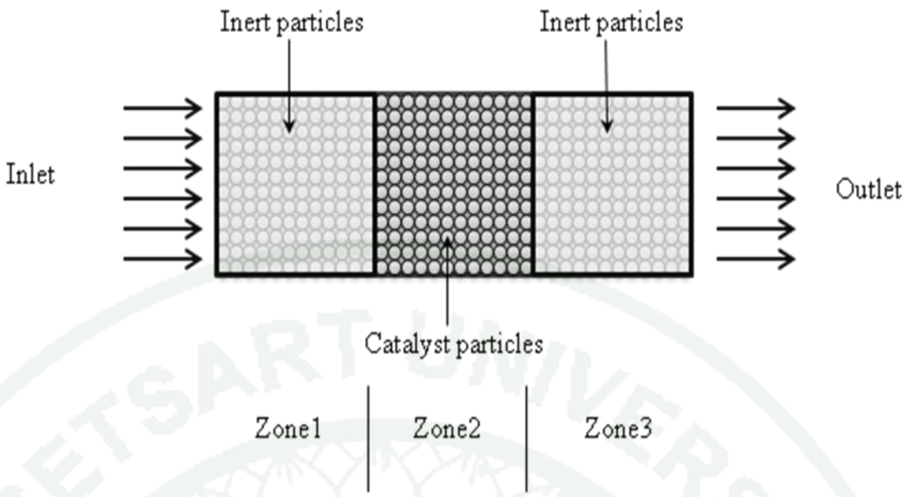

Figure 3 Three-zone TAP reactor

Mathematical model for the One-zone TAP Reactor

In the Knudsen flow regime, the equation of continuity for the diffusion of a non-reacting gas through the packed-bed uniformly packed with non-porous catalyst pellets is described by (Gleaves *et al.*, 1988, 1997)

$$\varepsilon_b \frac{\partial C}{\partial t} = D_e \frac{\partial^2 C}{\partial z^2} \tag{4}$$

If the reaction is first order in gas concentration, the equation for a reactant gas can be described by

$$\varepsilon_b \frac{\partial C}{\partial t} = D_e \frac{\partial^2 C}{\partial z^2} - \varepsilon_b k C \tag{5}$$

where C is the gas concentration on the bed (mol/cm^3), D_e is the effective Knudsen diffusivity in the bed (cm/s^2), t is the time (s), z is the axial coordinate (cm), ε_b is the void fraction in the bed, and k is the reaction rate constant (cm^3 of gas/mol s).

The set of initial and boundary conditions are described by (Gleaves *et al.*, 1988, 1997)

Initial conditions, $t = 0;$ $C = \delta(z - 0^+)\dfrac{N_P}{\varepsilon_b A}$ (6)

Boundary conditions, $z = 0;$ $\dfrac{\partial C}{\partial z} = 0$ (7)

$z = L;$ $C = 0$ (8)

where A is the cross-sectional area of the microreactor (cm^2), L is the length of the reactor (cm), N_P is the number of moles or molecules of gas in the inlet pulse (mol), and $\delta(z - 0^+)$ is the Dirac delta function placed at $z = 0^+$.

The initial condition given by Eq. (6) explains that N_P moles of gas is injected into the reactor at $t = 0$ and the corresponding gas concentration in the inlet pulse can be represented by the Dirac delta function placed at $z = 0^+$. The inlet boundary condition given by Eq. (7) corresponds to the absence of flux at the reactor entrance when the pulse valve is closed. The outlet boundary condition given by Eq. (8) specifies that the reactor outlet is held at vacuum conditions and therefore the gas concentration is zero. Using the above boundary and initial conditions, an analytical solution for the exit flow was obtained by the technique of separation of variables.

The exit flow rate of gas at the reactor outlet (F , mol/s) is determined by

$$F = -AD_e \left.\frac{\partial C}{\partial z}\right|_{z=L} \tag{9}$$

For the diffusion-only case, the set of Eqs. (4), (6)-(8) can be solved for C and by the use of Eq. (9), the solution can be determined and is described (Gleaves *et al.*, 1997) by

$$\frac{F}{N_p} = \frac{D_e \pi}{\varepsilon_b L^2} \sum_{n=0}^{\infty} \left\{ (-1)^n (2n+1) \exp\left(-(n+0.5)^2 \pi^2 \frac{tD_e}{\varepsilon_b L^2} \right) \right\} \tag{10}$$

Similarly, the solution for the irreversible reaction case is given by

$$\frac{F}{N_P} = \frac{D_e \pi}{\varepsilon_b L^2} \exp(-kt) \sum_{n=0}^{\infty} \left\{ (-1)^n (2n+1) \exp\left(-(n+0.5)^2 \pi^2 \frac{tD_e}{\varepsilon_b L^2} \right) \right\} \tag{11}$$

Many researchers have used another mathematical equivalent set of initial and inlet boundary conditions described by

Initial condition, $t = 0;$ $C = 0$ (12)

Inlet boundary condition, $z = 0;$ $-D_e \frac{\partial C}{\partial z} = \delta(t - 0^+) \frac{N_p}{A}$ (13)

Eq. (13) specifies that the inlet flux is represented by a delta function at $t = 0^+$.

With this set of equations, analytical solutions in the Laplace-domain can be derived. Laplace-domain solutions are used to determine moment expressions that are useful for parameter estimation. Researchers will use this method only when moment expressions are available.

Application of the Dirac delta to describe the inlet flow is normally considered to be good enough for modeling of typical TAP response data. However, a more realistic description of the inlet flow referring to a non-ideal case has also been applied (Zou *et al*., 1993). In this case, we can write

Non-ideal inlet boundary condition: $z = 0;$ $-D_e \frac{\partial C}{\partial z} = X(t - 0^+) \frac{N_p}{A}$ (14)

A simple type of the non-ideal inlet condition that follows the specification of the pulse valve (Rothaemel *et al*., 1996) is described by a triangular shape show in Figure 4. The quantity t_{open} is opening duration time of pulse valve (s).

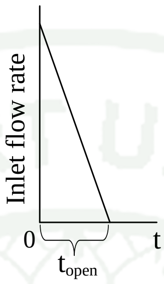

Figure 4 Non-ideal inlet flow condition

Mathematical model for the Three-zone TAP Reactor

Mass conservation of a gas in inert zone 1 and inert zone 3 packed with inert particles is described by

$$\varepsilon_b^{inert}\frac{\partial C}{\partial t} = D_e^{inert}\frac{\partial^2 C}{\partial z^2} \tag{15}$$

where D_e^{inert} is the effective Knudsen diffusivity in the inert zone (cm/s^2) and ε_b^{inert} is the void fraction in the inert zone.

Mass conservation of gas in zone 2 or catalyst zone that an irreversible 1st-order reaction takes place is described by,

$$\varepsilon_b^{cat}\frac{\partial C}{\partial t} = D_e^{cat}\frac{\partial^2 C}{\partial z^2} - \varepsilon_b^{cat} kC \tag{16}$$

where D_e^{cat} is the effective Knudsen diffusivity in the catalyst zone and ε_b^{cat} is the void fraction in the catalyst zone.

The ideal conditions are the same as those for the one-zone reactor given by Eqs. (6)–(8). Additional boundary conditions are required at the boundaries between zones 1 and 2 (z_1) and between zones 2 and 3 (z_2) and are described as follows:

$$z = z_1; \qquad C\big|_I = C\big|_{II} \tag{17}$$

$$z = z_1; \qquad -D_e^{inert} \left.\frac{\partial C}{\partial z}\right|_I = -D_e^{cat} \left.\frac{\partial C}{\partial Z}\right|_{II} \tag{18}$$

$$z = z_2; \qquad C\big|_{II} = C\big|_{III} \tag{19}$$

$$z = z_2; \qquad -D_e^{inert} \left.\frac{\partial C}{\partial z}\right|_{II} = -D_e^{cat} \left.\frac{\partial C}{\partial Z}\right|_{III} \tag{20}$$

The subscripts I, II, and III refer to zones 1, 2 and 3 respectively. Equations (17)-(20) correspond to continuity in the concentration and flux at the boundaries.

The exit flow of gas at the reactor outlet is given by

$$F = -AD_e^{inert} \left.\frac{\partial C}{\partial z}\right|_{z=L} \tag{21}$$

where F is the exit flow rate of the gas (mol/s).

Dimensionless model for the One-Zone TAP Reactor

To reduce the number of computational experiments performed in this study, the set of Eqs. (4)-(11), and (14) for the one-zone reactor can be transformed to generalized dimensionless equations (Gleaves *et al.*, 1997) using dimensionless variables and parameters defined by

Dimensionless axial coordinate;

$$\xi = \frac{z}{L} \tag{22}$$

Dimensionless concentration;

$$C^* = \frac{C}{N_P / \varepsilon_b AL} \tag{23}$$

Dimensionless time;

$$\tau = \frac{tD_e}{\varepsilon_b L^2} \tag{24}$$

Dimensionless reaction rate constant;

$$\kappa = k \frac{\varepsilon_b L^2}{D_e} \tag{25}$$

Eqs. (4)-(11), and (14) are then written in dimensionless form as follows:

Diffusion-only case;

$$\frac{\partial C^*}{\partial \tau} = \frac{\partial^2 C^*}{\partial \xi^2} \tag{26}$$

Diffusion with first order irreversible adsorption/reaction case;

$$\frac{\partial C^*}{\partial \tau} = \frac{\partial^2 C^*}{\partial \xi^2} - \kappa C^* \tag{27}$$

Dimensionless initial and boundary conditions;

$$\tau = 0; \qquad C^* = 0 \tag{28}$$

$$\xi = 0; \qquad -\frac{\partial C^*}{\partial \xi} = \delta(\tau - 0^+) \tag{29}$$

$$\xi = 1; \qquad C^* = 0 \tag{30}$$

For the case in which the inlet flow rate is non-ideal, we write

$$\xi = 0; \quad , \qquad -\frac{\partial C^*}{\partial \xi} = X(\tau) \tag{31}$$

The exit flow rate of the gas can be expressed in dimensionless form using the dimensionless variable defined by

$$F^* = F\,\frac{\varepsilon_b L^2}{N_P D_e} \tag{32}$$

where F^* is the dimensionless gas exit flow rate.

Eq. (9) is then written as

$$F^* = -\left.\frac{\partial C^*}{\partial \xi}\right|_{\xi=1} \tag{33}$$

The analytical solution for the dimensionless exit flow rate of the gas can be determined and is described by

Diffusion-only case;

$$F^* = \pi\sum_{n=0}^{\infty}\left\{(-1)^n(2n+1)\exp\left(-(n+0.5)^2\pi^2\tau\right)\right\} \tag{34}$$

Diffusion with first order irreversible reaction case;

$$F^* = \pi \exp(-\kappa\tau)\sum_{n=0}^{\infty}\left\{(-1)^n (2n+1)\exp\left(-(n+0.5)^2 \pi^2\tau\right)\right\} \tag{35}$$

Dimensionless model for the Three-zone TAP Reactor

The mathematical model for gas diffusion in the TAP reactor is described in a generalized dimensionless form by

Inert zone 1 and zone 3: $$r_{\varepsilon i}\frac{\partial C^*}{\partial \tau} = r_{Di}\frac{\partial^2 C^*}{\partial \xi^2} \tag{36}$$

Catalyst zone 2: $$\frac{\partial C^*}{\partial \tau} = \frac{\partial^2 C^*}{\partial \xi^2} \tag{37}$$

where C^* is the dimensionless concentration $\left(C^* \equiv C\big/\left(N_p/\varepsilon_b^{cat} AL\right)\right)$, $r_{\varepsilon i}$ is the ratio of the void fraction between inert zone and catalyst zone $\left(r_{\varepsilon i} \equiv \varepsilon_b^{inert}/\varepsilon_b^{cat}\right)$, r_{Di} is the ratio of the gas diffusivity between inert zone and catalyst zone $\left(r_{Di} \equiv D_e^{inert}/D_e^{cat}\right)$, τ is the dimensionless time $\left(\tau \equiv tD_e^{cat}/\varepsilon_b^{cat}L^2\right)$ and ξ is the dimensionless axial coordinate $\left(\xi_i \equiv l_i/L\right)$.

For diffusion combined with the first order irreversible reaction, we can write

$$\frac{\partial C^*}{\partial \tau} = \frac{\partial^2 C^*}{\partial \xi^2} - \kappa C^* \tag{38}$$

where k^* is dimensionless reaction rate constant $\left(\kappa \equiv k\varepsilon_b^{cat}L^2/D_e^{cat}\right)$.

Dimensionless boundary conditions;

$\xi = \xi_1$; $$C^*\big|_I = C^*\big|_{II} \tag{39}$$

$$-r_{Di}\frac{\partial C^*}{\partial \xi}\bigg|_I = -\frac{\partial C^*}{\partial \xi}\bigg|_{II} \tag{40}$$

$$\xi = \xi_2\,; \qquad C^*\big|_{II} = C^*\big|_{III} \tag{41}$$

$$-\left.\frac{\partial C^*}{\partial \xi}\right|_{II} = -r_{Di}\left.\frac{\partial C^*}{\partial \xi}\right|_{III} \tag{42}$$

The dimensionless exit flow rate can be calculated using

$$F^* = -r_{Di}\left.\frac{\partial C^*}{\partial \xi}\right|_{\xi=1} \tag{43}$$

where F^* is the dimensionless exit flow rate $\left(F^* \equiv \dfrac{F\varepsilon_b^{cat}L^2}{N_p D_e^{cat}}\right)$.

Application of the mathematical models for analysis in this study is presented in the next section.

CALCULATION METHODS

To compare the estimated parameters from different parameter estimation procedures, there must be simple quantities to indicate the differences. For the gas diffusivity, the estimated and the real diffusivities were compared using an indicating quantity defined by

$$\Delta D_e = \frac{D_{e,est} - D_{e,real}}{D_{e,real}} \times 100 \qquad (44)$$

To determined ΔD_e, the response calculated from a given $D_{e,real}$ under the non-ideal inlet condition was assumed to be the experimental response. The estimated diffusivity was then determined from the experimental response using the model with the ideal inlet condition. A good estimation procedure would gives a small magnitude of ΔD_e.

For the first order irreversible rate constant, we define a similar indicating quantity as

$$\Delta k = \frac{k_{est} - k_{real}}{k_{real}} \times 100 = \frac{\kappa_{est} - \kappa_{real}}{\kappa_{real}} \times 100 \qquad (45)$$

Typically, the diffusivity of the reactant gas is calculated from the diffusivity of the inert gas introduced into the reactor with the reactant gas using the correlation (Cunningham and Williams, 1980)

$$\frac{D_{e,reactant}}{D_{e,inert}} = \sqrt{\frac{MW_{inert}}{MW_{reactant}}} \qquad (46)$$

where $D_{e,reactant}$ and $MW_{reactant}$ are the effective Knudsen diffusivity and molecular weight of the reactant gas respectively. Since the ratio of the two diffusivities is proportional to the square root of the ratio of their molecular weights, ΔD_e of the two gases is the same.

Based on the least square fit, different types of response curves will be applied to estimate the transport and kinetic parameters, including the exit flow rate curve and the unit-area normalized response. The exit flow rate curve fitting is performed by comparing the experimental exit flow rate curve with the model exit flow rate curve. The fitting of unit-area normalized responses applies the experimental response without converting into the exit flow rate curve. The model exit flow rate and the experimental exit flow rate curve are unit-area normalized before matching to estimate the parameters.

Assuming the non-ideal inlet condition, the experimental exit flow rate curve was numerically calculated by the method of lines (MOL). The software used in our calculation is called Livermore Solver for Ordinary Differential equations with Automatic method switching for stiff and non-stiff problems (LSODA) (Petzold, 1983). The software is available at http://www.netlib.org. The computer programs are written in standard FORTRAN77. The calculation used 1000 grids to span the axial coordinate, and a time step of 0.001. Accuracy of the numerical calculation was investigated by comparing the diffusion mean residence time determined from the calculated exit flow rate using ideal inlet condition for a one-zone reactor with the analytical expression (Gleaves *et al*., 1997). The difference was not larger than 0.1%. The accuracy of the numerical calculation for the diffusion-only case under the non-ideal inlet condition was also investigated by checking the dimensionless exit flow rate curve of which the area must be unity according to the mass conservation. In this case, the numerical error was found to be less than 0.04%. In addition, the mean residence times determined from the calculated exit flow rate using non-ideal inlet condition were compared with those from the analytical expressions (Boonnumpha, 2005). For both diffusion-only and first order irreversible reaction cases, the difference was not larger than 0.1% for all gas conversions.

This study involves the investigation of accuracy of different procedures for estimating the transport and kinetic parameters from TAP pulse responses for the irreversible reaction case. Both the one-zone and three-zone reactors are investigated.

One-zone reactor

The reaction rate constant is determined from the TAP experimental responses by using two different estimation procedures including

1. Determination of the reaction rate constant after the diffusivity is predetermined

2. Determination of the diffusivity and the reaction rate constant simultaneously.

Since the inlet boundary condition involves $f(\tau)$ (Eq.(31)) describing the inlet gas flow rate and the shape of the inlet flow rate is triangular (Figure 4), the characteristic of $f(\tau)$ is governed by the magnitude of t_{open}, the opening duration time of the pulse valve. The quantity τ_{open}, dimensionless opening duration times of the pulse valve can be defined by

$$\tau_{open} \equiv \frac{t_{open} D_e}{\varepsilon_b L^2} \tag{47}$$

The simulation was performed for different magnitudes of τ_{open}. The magnitudes of τ_{open} obtained from various conditions are shown in Table 1. For example, the magnitude of τ_{open} is equal to 0.004 corresponding to the experiment with t_{open} = 500 µs, the reactor length is 4 cm, the bed fractional voidage is 0.5 (irregular shape) and the gas diffusivity is 68.40 cm^2/s for methane operated at 1000 ºC in a packed bed of spherical pellets whose diameter is 325 µm. The gas diffusivity in a packed bed of spherical pellets can be calculated by using Eqs. (1) and (2). It should be noted that the bed fractional voidage is 0.36 for spherical pellets and typical lengths in TAP reactor are 2.54 cm and 4 cm (Gleaves *et al*., 1997; Shektman *et al*., 2008). Different magnitudes of τ_{open} are obtained from different values of variable in Eq. (47). In this study, the magnitude of τ_{open} is in the range of 0.004 to 0.026.

Table 1 Calculated value of τ_{open} obtained from various conditions

Reactant	Diffusivity (cm^2/s)	t_{open} (μs)	Fractional voidage	Reactor length (cm)	τ_{open}
CH_4	68.40	500	0.50	4.00	0.004
CO_2	41.25	500	0.50	2.54	0.006
C_3H_8	41.25	500	0.50	2.54	0.009
CH_4	68.40	500	0.36	2.54	0.015
CO	89.56	500	0.36	2.54	0.020
C_2H_6	120.7	500	0.36	2.54	0.026

For the irreversible reaction case, the parameter that appears in Eq.(27) is κ. However, the gas conversion is practically the primary quantity that can be determined by the use of an internal standard or an inert gas (Zou *et al*., 1994). The gas conversion can be calculated from the reaction rate constant using

$$X = 1 - \frac{1}{\cosh\sqrt{\kappa}} = 1 - \frac{1}{\cosh\sqrt{k\varepsilon_b L^2 / D_e}} \tag{48}$$

In this study, ΔD_e and Δk will be reported to depend on the magnitude of gas conversion rather than κ for practical purpose.

For the one-zone reactor, the model exit flow rate curve can be calculated using analytical expressions. For the diffusion only case, the exact solution of the model exit flow rate under the ideal inlet condition is shown in Eq.(10). In the first procedure, the model exit flow rate was calculated using the equation:

$$\frac{F}{N_p} = \frac{D_{e,est}\pi}{\varepsilon_b L^2}\sum_{n=0}^{\infty}\left\{(-1)^n (2n+1)\exp\left(-(n+0.5)^2 \pi^2 \frac{tD_{e,est}}{\varepsilon_b L^2}\right)\right\} \tag{49}$$

Eq. (49) is used to determine $D_{e,est}$ in the first procedure. In this case, the exit flow rate curve fitting and the unit-area normalized response fitting give the same estimated diffusivity. The reason is that for the diffusion-only case the unit-area normalized response is in fact the curve of F/N_p and the area of this curve is unity. When the dimensionless form is applied, the model curve is calculated by

$$F^* = d\pi\sum_{n=0}^{\infty}\left\{(-1)^n (2n+1)\exp\left(-(n+0.5)^2 \pi^2 d\tau\right)\right\} \tag{50}$$

where
$$d = \frac{D_{e,est}}{D_{e,real}} \tag{51}$$

In this case, the estimated parameter is d. The quantity ΔD_e can be determined from the estimated d using

$$\Delta D_e = (d-1)\times 100 \tag{52}$$

It is noted that accuracy of the numerical calculation was also investigated by comparing the values of parameter d estimated using the model responses calculated from the analytical solution and that calculated by MOL. The difference between the two d 's was found to be less than 0.02%.

For the irreversible reaction case, the solution is given by Eq. (11). The model exit flow rate curve was estimated by using

$$\frac{F}{N_P}=\frac{D_{e,est}\pi}{\varepsilon_b L^2}\exp(-k_{est}t)\sum_{n=0}^{\infty}\left\{(-1)^n(2n+1)\exp\left(-(n+0.5)^2\pi^2\frac{tD_{e,est}}{\varepsilon_b L^2}\right)\right\} \tag{53}$$

The estimated parameters obtained by using Eq. (53) are $D_{e,est}$ and k_{est}. When the dimensionless form is used in this study, the model curve is calculated by

$$F^*=d\pi\exp(-\kappa_{est}\tau)\sum_{n=0}^{\infty}\left\{(-1)^n(2n+1)\exp\left(-(n+0.5)^2\pi^2 d\tau\right)\right\} \tag{54}$$

In this case, the estimated parameters are d and κ_{est}.

In the first procedure involving determination of the reaction rate constant after the diffusivity is predetermined, the calculation followed that reported in (Tantake *et al.*, 2007). The parameter d was predetermined from Eq. (50). The estimated reaction rate constant, κ_{est}, was then determined using Eq. (54). The estimated reaction rate constant was compared with the real rate constant providing Δk.

In the second procedure, the parameters d and κ_{est} were determined simultaneously from one reactive response using Eq. (54). The quantity ΔD_e was obtained from Eq. (52). The quantity Δk was obtained by using Eq (45). The schematic diagram of the calculation methods for the one-zone reactor is shown in Figure 5. When the unit-area normalized response fitting is applied, the model exit flow rate curve calculated from Eq. (54) is unit-area normalized before matching with the unit-area normalized experimental response. The quantities d and κ_{est} obtained from different methods will be compared.

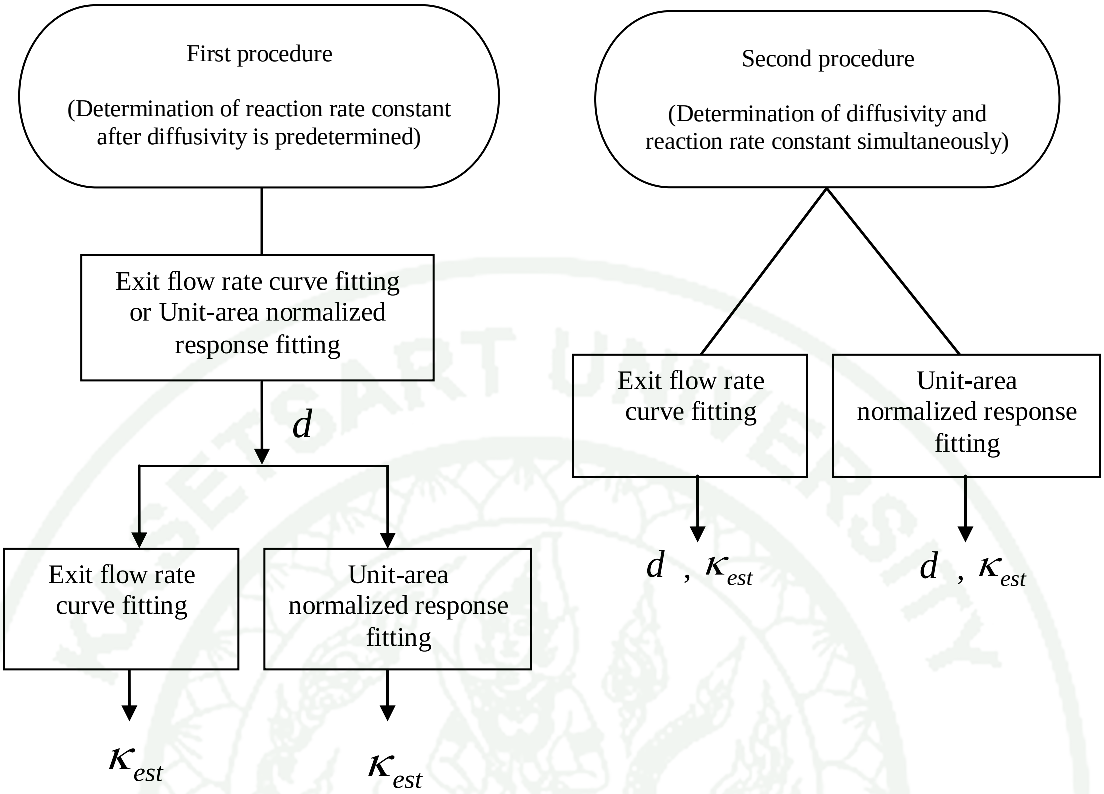

Figure 5 Schematic diagrams of the calculation methods for the one-zone reactor

Three-zone reactor

In the three-zone reactor, the catalyst pellets are uniformly packed between two beds of inert particles. The sizes of pellets are approximately 100-300 μm. According to Eqs. (1) and (2), the gas diffusivity is proportional to the sizes of pellets. It is possible that the sizes of the inert particles and the catalyst pellets are different resulting in the difference of gas diffusivities in different zones. In order to investigate the effect of different gas diffusivity in each zone on accuracy of estimated parameters, the ratio of the gas diffusivity of inert zone to catalyst zone was varied in the range of 1/3 to 3/1 in accordance with the sizes of the pellets. For the diffusion-only case, the gas diffusivity can be estimated using two different ways including determination of the gas diffusivity in the catalyst zone after the gas diffusivity in the inert zone is predetermined (Phanawadee *et al.*, 1999; Tantake *et al.*, 2007), and determination of the gas diffusivity in the inert zone and the gas diffusivity in the catalyst zone simultaneously.

For the former case, the parameter estimation in the three-zone reactor is performed by predetermination of gas diffusivity in the inert zone from the experiment using the one-zone reactor packed with the inert particles. After determining the gas diffusivity in the inert zone, the gas diffusivity in the catalyst zone is determined from the diffusion response obtained from the three-zone reactor. For the latter case, the diffusivities in both zones are estimating using one diffusion response from the three-zone reactor.

In the three-zone reactor case, the calculation procedures to be investigated therefore include

1. Determination of the kinetic parameter after transport parameter determination including

1.1 Determination of the reaction rate constant after the diffusivity of gas in the inert zone is predetermined from the one-zone reactor and the diffusivity of gas in the catalyst zone is determined from the diffusion response obtained from the three-zone reactor

1.2 Determination of the reaction rate constant after the diffusivities of gas in the inert zone and the catalyst zone are simultaneously determined from the diffusion response obtained from the three-zone reactor

2. Determination of the reaction rate constant, the diffusivity of gas in the inert zone and the diffusivity of gas in the catalyst zone simultaneously

This study observes three quantities including ΔD_e^{inert}, ΔD_e^{cat} and Δk obtained from different procedures. The magnitudes of ΔD_e^{inert}, ΔD_e^{cat} and Δk also depend on the ratio of the gas diffusivity of inert zone to catalyst zone (r_{Di}) in addition to τ_{open} and the gas conversion.

The model response for gas diffusion in the three-zone reactor is described in a generalized dimensionless form by

Inert zone 1 and zone 3: $$\frac{\partial C^*}{\partial \tau} = d_i r_{Di} \frac{\partial^2 C^*}{\partial \xi^2} \tag{55}$$

where $$d_i = \frac{D_{e,est}^{inert}}{D_{e,real}^{inert}} \tag{56}$$

and $$r_{Di} = \frac{D_{e,real}^{inert}}{D_{e,real}^{cat}} \tag{57}$$

Catalyst zone 2: $$\frac{\partial C^*}{\partial \tau} = d_c \frac{\partial^2 C^*}{\partial \xi^2} \tag{58}$$

where $$d_c = \frac{D_{e,est}^{cat}}{D_{e,real}^{cat}} \tag{59}$$

For diffusion combined with the first order irreversible reaction, we can write

$$\frac{\partial C^*}{\partial \tau} = d_c \frac{\partial^2 C^*}{\partial \xi^2} - \kappa_{est} C^* \tag{60}$$

The dimensionless exit flow rate can be calculated using

$$F^* = -d_i r_{Di} \left. \frac{\partial C^*}{\partial \xi} \right|_{\xi=1} \tag{61}$$

Figure 6 shows the schematic diagram of the calculation methods for the three-zone reactor. In the procedure 1.1, the diffusivity of gas in the inert zone was predetermined from the diffusion response obtained from the one-zone reactor. The model exit flow rate for the one-zone reactor case can be calculated using Eq. (54). In this case, the model exit flow rate one-zone reactor packed with the inert particles was calculated using the equation:

$$F^{*} = d_i \pi \sum_{n=0}^{\infty} \left\{ \left(-1\right)^n \left(2n+1\right) \exp\left(-\left(n+0.5\right)^2 \pi^2 d_i \tau\right) \right\} \tag{62}$$

The quantity ΔD_e^{inert} can be determined from the estimated d_i using

$$\Delta D_e^{inert} = (d_i - 1) \times 100 \tag{63}$$

For a three-zone reactor, no exact solution is available. To determine the model response, the same numerical method previously discussed was applied.
The diffusivity of gas in the catalyst zone was then determined from diffusion response obtained from the three-zone reactor using Eq. (58) with the set of the boundary conditions, Eqs. (39) and (40).

The quantity ΔD_e^{cat} can be determined from the estimated d_c using

$$\Delta D_e^{cat} = (d_c - 1) \times 100 \tag{64}$$

The estimated reaction rate constant was then determined from reactive response using Eq. (60) with the set of the boundary conditions. The estimated reaction rate constant was compared with the real rate constant providing Δk .

In the procedure 1.2, the parameters d_i and d_c were determined simultaneously using the model response for diffusion-only case in the three-zone reactor. The quantity ΔD_e^{inert} was obtained from Eq. (63). The quantity ΔD_e^{cat} was obtained from Eq. (64). The estimated reaction rate constant was then determined from reactive response, and Δk was obtained using Eq. (45).

In the procedure 2, the parameters d_i , d_c and κ_{est} were determined simultaneously using the model response obtained from the reactive case in the three-zone reactor. The quantities ΔD_e^{inert} , ΔD_e^{cat} and Δk were obtained from Eqs. (63), (64) and (45) respectively. The quantities d_i , d_c and κ_{est} obtained from different methods will be compared.

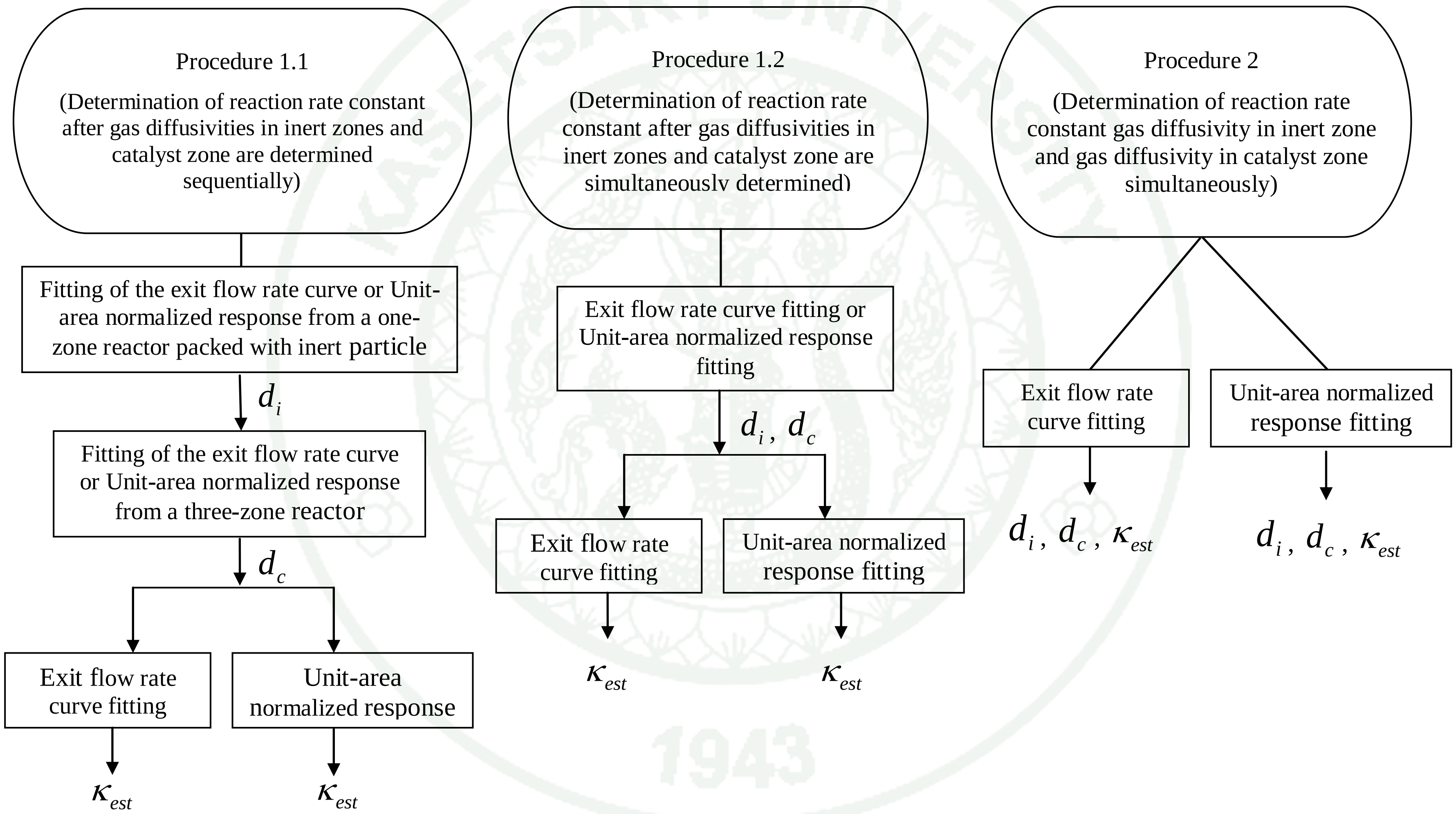

Figure 6 Schematic diagrams of the calculation methods for the three-zone reactor

RESULTS AND DISCUSSION

Deviations of estimated parameters from real values when using different estimation procedures will be compared. The calculation results for the one-zone reactor and three-zone reactor will be discussed respectively.

1. One-zone reactor

Figure 7 show the fitting of the simulated experimental and the model exit flow rate curves corresponding to the magnitude τ_{open} of 0.026. In this case, estimated value of d is equal to 0.967 with 95% confidence interval of 0.008%. The agreement between the two curves is excellent except at the peak. The fitting between the simulated and model curves for other magnitudes of τ_{open} are better than that in Figure 7.

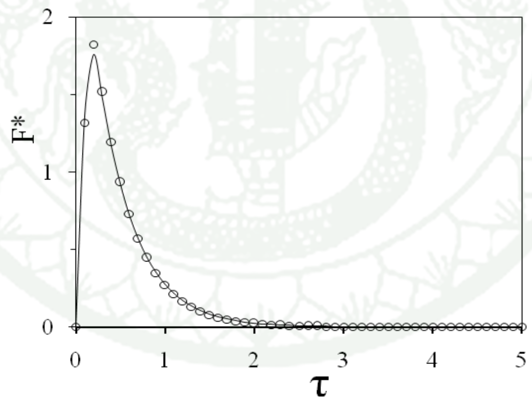

Figure 7 Comparison of the simulated experimental exit flow rate curve (circles) with the model exit flow rate curve (line) at τ_{open} = 0.026.

1.1 Effect of different procedures on accuracy of the estimated diffusivity

Figure 8 shows the plots of ΔD_e versus τ_{open} at x=0.01 (a), x=0.25 (b), x=0.5 (c), x=0.75 (d), x=0.99 (e) for the first procedure using the exit flow rate curve fitting (open circles), and second procedure using the exit flow rate curve fitting (open triangles) and the unit-area normalized response fitting (solid squares). Numerical values of ΔD_e are shown in Appendix B. The minus sign of ΔD_e corresponds to an underestimation of the gas diffusivity. The results show that all procedures underestimate the gas diffusivity throughout the range of the conversion. The relationship between ΔD_e and τ_{open} is close to linear for all procedures. When the magnitude of τ_{open} is increased, the quantities $|\Delta D_e|$ obtained from all procedures are also increased. At x=0.01 (Figure 8(a)), the quantities ΔD_e obtained from the first procedure and second procedure using the exit flow rate curve fitting are very close to each other. Figure 8(b), 8(c), 8(d) and 8(e) for x=0.25, 0.5, 0.75 and 0.99 respectively show that the first procedure gives lower $|\Delta D_e|$ compared with the second procedure throughout the range of τ_{open}. The quantities $|\Delta D_e|$ obtained from the first procedure are the same at all conversions since the diffusivity is predetermined using the diffusion response. For the second procedure, the quantities $|\Delta D_e|$ are increased with increasing conversion. The first procedure gives the lowest $|\Delta D_e|$ throughout the range of conversions. The second procedure using the unit-area normalized response fitting gives much higher $|\Delta D_e|$ than the second procedure using exit flow rate curve fitting. This can be clearly seen in Figure 9 which shows the selected case in which the magnitude of τ_{open} is equal to 0.015. For the second procedure using the exit flow rate curve fitting, $|\Delta D_e|$ slightly increases from 2 to 3% with increasing conversion at the conversions between 1 and 75%. For this procedure, large $|\Delta D_e|$ can be found in the range of conversion between 75 to 99% within $|\Delta D_e|$ does not exceed 6%. For the second procedure using the unit-area normalized response fitting, $|\Delta D_e|$ increases from 6 to 16% when the conversion is increased from 1 to 99%.

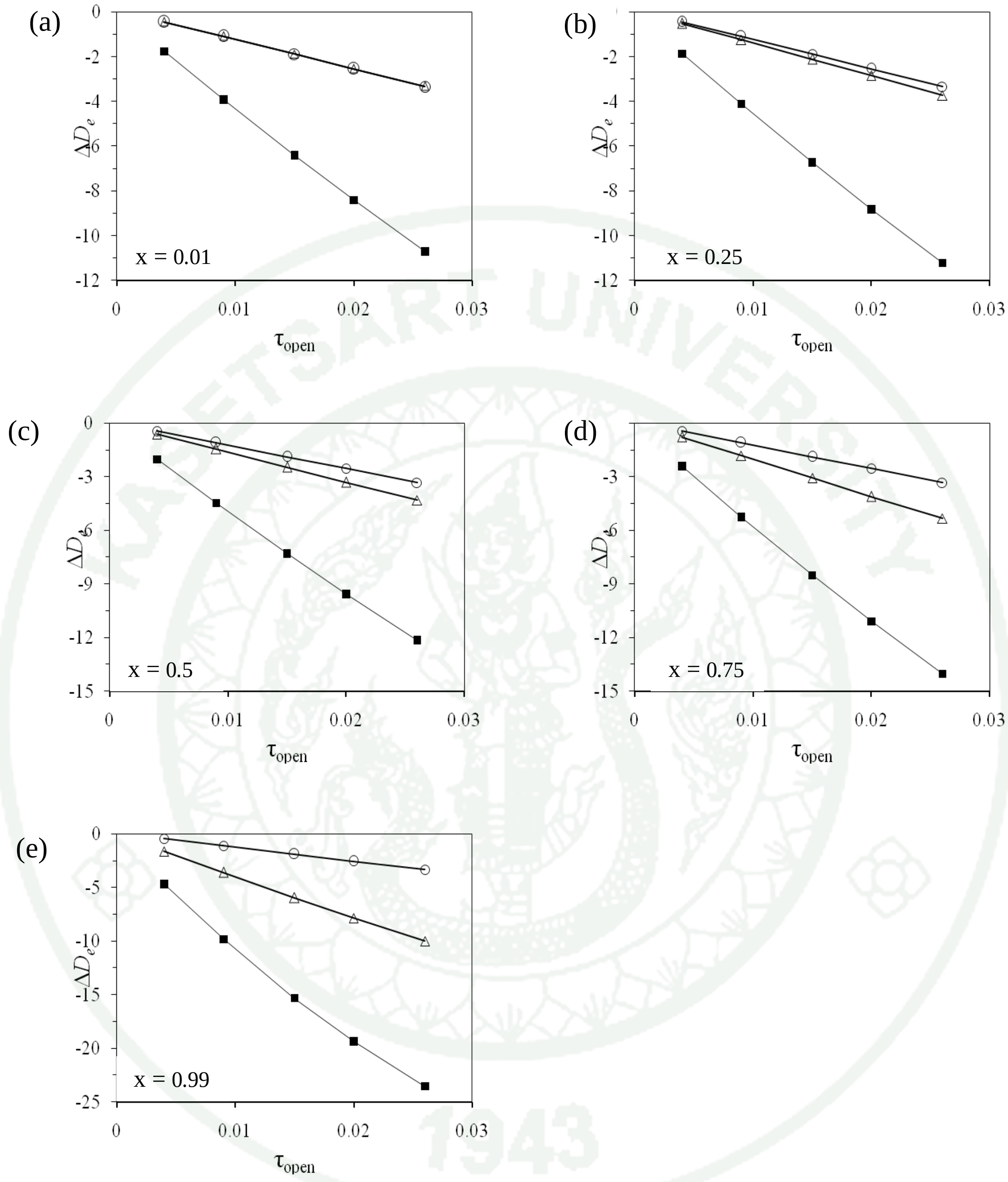

Figure 8 Plots of ΔD_e vs. τ_{open} at x=0.01 (a), x=0.25 (b), x=0.5 (c), x=0.75 (d), x=0.99 (e) for different procedures: first procedure using the exit flow rate curve fitting (open circles), second procedure using the exit flow rate curve fitting (open triangles) and second procedure using the unit-area normalized response fitting (solid squares)

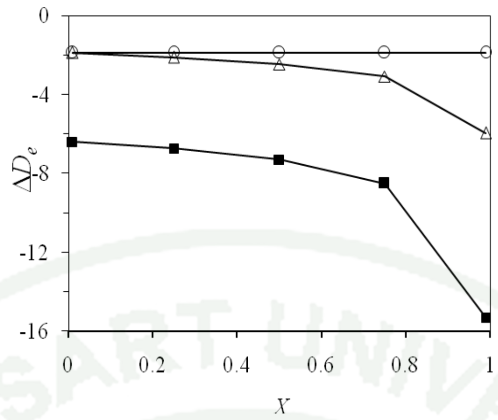

Figure 9 Plots of ΔD_e vs. conversions at τ_{open} =0.015 for different procedures: first procedure using the exit flow rate curve fitting (open circles), second procedure using the exit flow rate curve fitting (open triangles) and second procedure using the unit-area normalized response fitting (solid squares)

1.2 Effect of different procedures on accuracy of the estimated reaction rate constant

To determine the reaction rate constants, different estimation methods including the exit flow rate curve fitting, the unit area normalized response fitting are applied. When using the exit flow rate curve fitting, the simulated experimental and model exit flow rate curves are compared based on the method of least square fit providing the estimated reaction rate constants (κ_{est}). The comparison between the experimental and model exit flow rate curves for the magnitude τ_{open} of 0.026 when conversion equals to 50% is shown in Figure 10. The 95% confidence interval for the estimated rate constant from the curve fitting is narrow within ±0.24% of the estimated rate constant. It can be seen from the figure that the experimental exit flow rate curve fits well with the model curve despite the very large error of estimated reaction rate constant.

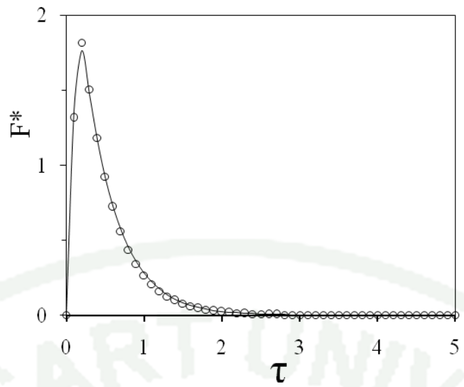

Figure 10 Comparison of the simulated experimental exit flow rate curve (circles) with the model exit flow rate curve (line) for τ_{open} =0.026 at X=0.5

Another curve fitting method applied to estimate the reaction rate constants involves comparing the unit-area normalized experimental exit flow rate curve with the unit-area normalized model exit flow rate curve based on the least square fit. The comparison between the unit-area normalized experimental response (circles) and the unit-area normalized model response (line) when using the unit-area normalized response fitting for the magnitude τ_{open} of 0.026 when conversion equals to 50% is shown in Figure 11. The good agreement between the two unit-area normalized responses is observed. The 95% confidence interval for the estimated rate constant from the curve fitting is narrow within ±0.17% of the estimated rate constant.

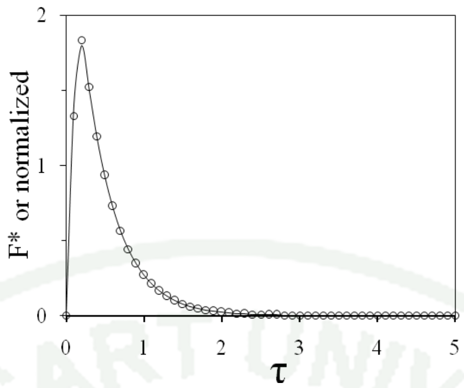

Figure 11 Comparison of the unit-area normalized experimental response (circles) with the unit-area normalized model response (line) for τ_{open} =0.026 at X=0.5

1.2.1 Accuracy of estimated reaction rate constant using exit flow rate curve fitting

Figure 12 shows Δk versus τ_{open} for the first procedure and the second procedure at conversion equal to 1%, 25%, 50%, 75% and 99% respectively. The linear relationship between Δk and τ_{open} is also observed. An underestimation of the reaction rate constant is obtained from the first procedure and the second procedure. At fixed reaction rate constant or conversion, when the magnitude of τ_{open} is increased, the quantities $|\Delta k|$ obtained from the first procedure and second procedure are also increased. In Figure 12(a) for conversion equal to 1%, $|\Delta k|$ is very large for the first and second procedures due to the small κ_{real} of 0.020168 at this conversion. The quantities Δk obtained from the first procedure and the second procedure are not different. At x > 0.01 (Figure 12(b), 12(c), 12(d) and 12(e)), the quantities $|\Delta k|$ obtained from the first procedure are lower than those obtained from the second procedure. When increasing the conversions, the differences of $|\Delta k|$ between the first procedure and the second procedure are also increased. The results show that the first procedure provides more accurate estimated reaction rate constants than the second procedure.

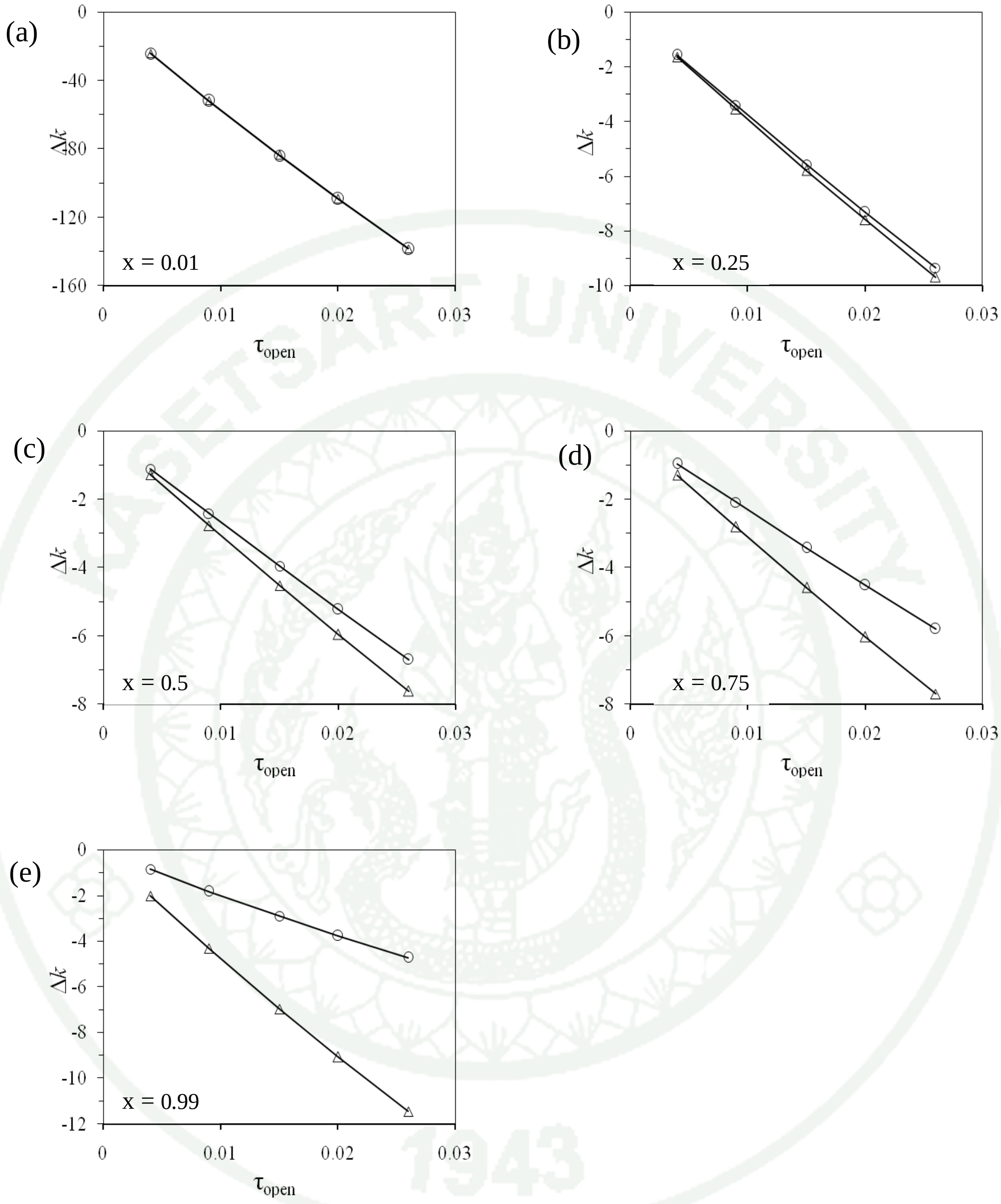

Figure 12 Plots of Δk vs. τ_{open} at x=0.01 (a), x=0.25 (b), x=0.5 (c), x=0.75 (d), x=0.99 (e) using the exit flow rate curve fitting for different procedures: first procedure (open circles) and second procedure (open triangles)

1.2.2 Accuracy of estimated reaction rate constant using unit-area normalized response fitting

Figure 13 shows the plots of Δk versus τ_{open} for the first procedure and the second procedure at conversion equal to 1%, 25%, 50%, 75% and 99% respectively. At fixed reaction rate constant or conversion, when the magnitude of τ_{open} is increased, $|\Delta k|$ increases as expected. In addition, the relationship between Δk and τ_{open} is close to linear for all different procedures. The second procedure generally overestimates the reactant rate constants for all conversion and $|\Delta k|$ obtained from the second procedure are considerably large compared with the first procedure. The very large $|\Delta k|$ is obtained from the second procedure throughout the range of τ_{open}. In Figure 13(a), when using the unit-area normalized response fitting, $|\Delta k|$ is very large at conversion equal to 1% for all different procedures, especially the second procedure. The very large $|\Delta k|$ at the lowest conversion is due to the small κ_{real} of 0.020168. The quantities $|\Delta k|$ obtained from the first procedure are much lower than those obtained from the second procedure except at conversion equal to 99%.

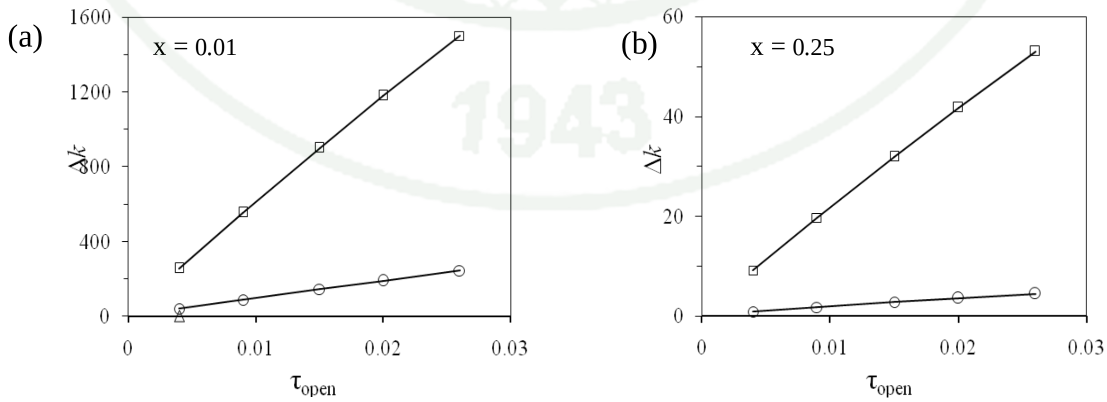

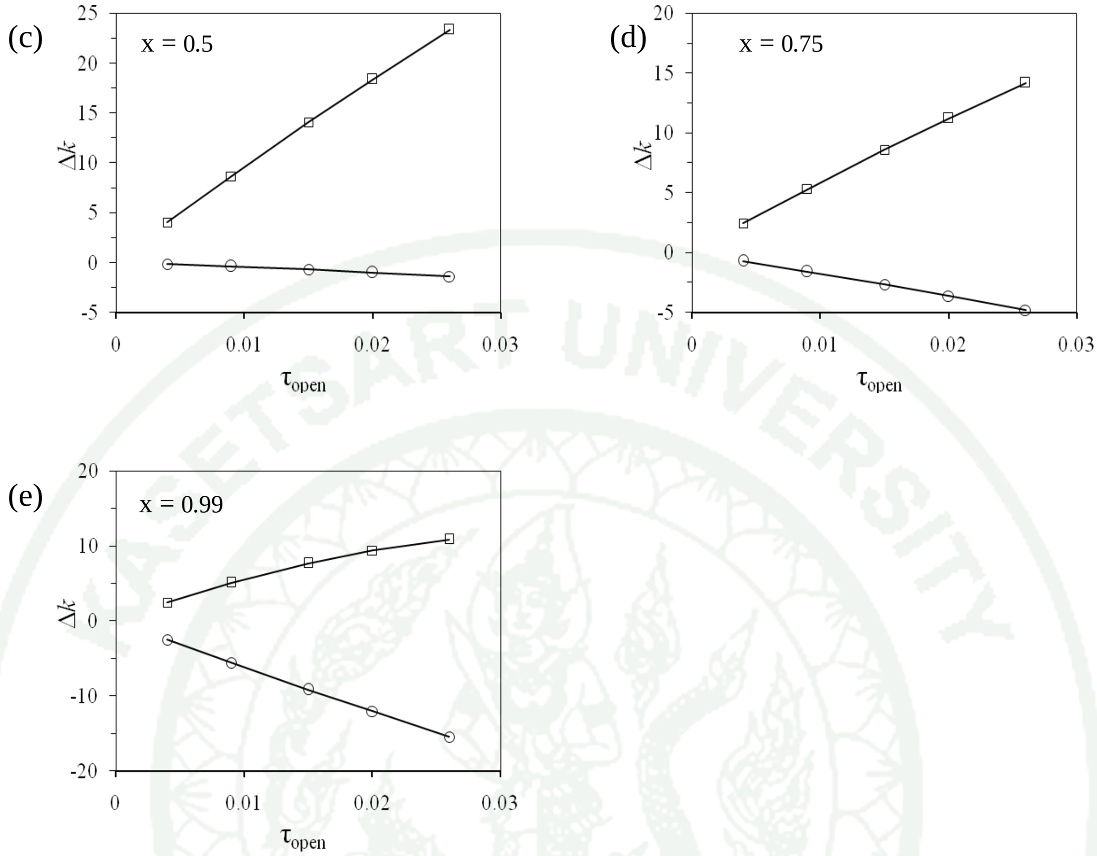

Figure 13 Plots of Δk vs. τ_{open} at x=0.01 (a), x=0.25 (b), x=0.5 (c), x=0.75 (d), x=0.99 (e) using the unit-area normalized response fitting for different procedures: first procedure (open circles) and second procedure (open squares)

When comparing the exit flow rate curve fitting with the unit-area normalized response fitting, the results show that $|\Delta k|$ obtained from the unit-area normalized response fitting is much larger than those obtained from the exit flow rate curve fitting. For example, $|\Delta k|$ obtained from the first and second procedures using the exit flow rate curve fitting for τ_{open} =0.026 at X=0.01 is 138.4% while those using the unit-area normalized response fitting is 245.3% for the first procedure and 1501% for the second procedure at the same τ_{open} and conversion.

2. Three-zone reactor ($L_{cat}/L_{reactor}$ =1/3)

For the three-zone reactor, the effects of r_{Di} , τ_{open} and conversion on accuracy of estimated parameters are investigated. The gas diffusivities and the reaction rate constant are also determined using the exit flow rate curve fitting and the unit-area normalized response fitting. For the gas diffusivities obtained from the procedure 1.1 and the procedure 1.2, only the exit flow rate curve fitting is applied due to the same response area of unity.

2.1 Effect of τ_{open} on accuracy of estimated parameters determined from different procedures

The simple cases shown in this section have the magnitude of r_{Di} equal to 1.0 and conversion equal to 0.5. The quantities ΔD_e^{inert} obtained from different procedures at r_{Di} = 1 and x=0.5 are shown in Figure 14. Numerical values of ΔD_e^{inert} are shown in Appendix C. The linear relationship between ΔD_e^{inert} and τ_{open} is observed for procedure 1.1 and procedure 2 using both of the exit flow rate curve fitting and the unit-area normalized response fitting. The underestimate of ΔD_e^{inert} is observed for procedure 2 using the unit-area normalized response fitting. But procedure 2 using the exit flow rate curve fitting give overestimate of ΔD_e^{inert}. The quantities $\left|\Delta D_e^{inert}\right|$ obtained from procedure 1.1 and procedure 2 using the unit-area normalized response fitting are increased with increasing the magnitude of τ_{open}. The magnitudes of $\left|\Delta D_e^{inert}\right|$ for τ_{open} ranging from 0.004 to 0.026 are considerably small and do not exceed 5% for procedure 1.1 and procedure 1.2. Procedure 1.1 gives the lowest $\left|\Delta D_e^{inert}\right|$ while procedure 2 using the unit-area normalized response fitting gives the highest of $\left|\Delta D_e^{inert}\right|$ at the same τ_{open}. For procedure 2, the exit flow rate curve fitting provides less $\left|\Delta D_e^{inert}\right|$ than the unit-area normalized response fitting.

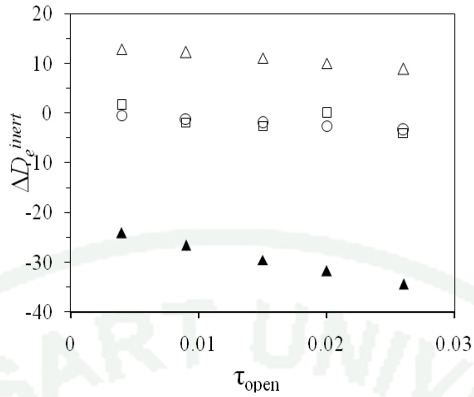

Figure 14 Plots of ΔD_e^{inert} vs. τ_{open} at r_{Di} = 1.0 and x=0.5 for different procedures: procedure 1.1 (open circles), procedure 1.2 (open squares), procedure 2 (open triangles) using the exit flow rate curve fitting and procedure 2 (solid triangles) using the unit-area normalized response fitting

Figure 15 shows the plots of ΔD_e^{cat} obtained from different procedures versus τ_{open} at r_{Di} = 1.0 and x=0.5. Numerical values of ΔD_e^{cat} are shown in Appendix D. The relationship between ΔD_e^{cat} and τ_{open} is close to linear for procedure 1.1and procedure 2 using both of the exit flow rate curve fitting and the unit-area normalized response fitting. The overestimate of ΔD_e^{cat} is observed for procedure 2 using the unit-area normalized response fitting. Procedure 2 using the exit flow rate curve fitting give underestimate of ΔD_e^{cat}. When the magnitudes of τ_{open} are increased, the quantities $\left|\Delta D_e^{cat}\right|$ obtained from procedure 1.1 and procedure 2 using the exit flow rate curve fitting also increase. Similarly to Figure 14, procedure 1.1 gives the lowest $\left|\Delta D_e^{cat}\right|$ for each τ_{open}. In addition, the magnitudes of $\left|\Delta D_e^{cat}\right|$ obtained from procedure 2 using the unit-area normalized response fitting are approximately 60% throughout the range of τ_{open} in this study.

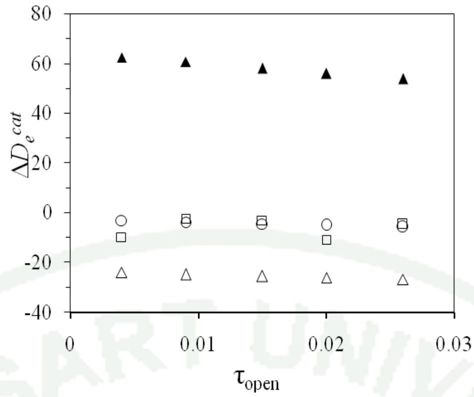

Figure 15 Plots of ΔD_e^{cat} vs. τ_{open} at r_{Di} = 1.0 and x=0.5 for different procedures: procedure 1.1 (open circles), procedure 1.2 (open squares), procedure 2 (open triangles) using the exit flow rate curve fitting and procedure 2 (solid triangles) using the unit-area normalized response fitting

Figure 16 shows the plots of Δk obtained from different procedures using the exit flow rate curve fitting versus τ_{open} at r_{Di} = 1.0 and conversion equal to 50%. Numerical values of Δk obtained from the exit flow rate curve fitting are shown in Appendix E. The relationship between Δk and τ_{open} is close to linear for all procedures. The underestimate of Δk is observed for all procedures. When increasing the magnitude of τ_{open}, the quantities $|\Delta k|$ determined from all different procedures also increase. The quantities $|\Delta k|$ obtained from all different procedures are not very different. The magnitudes of $|\Delta k|$ obtained all different procedures are small within which $|\Delta k|$ does not exceed 4%.

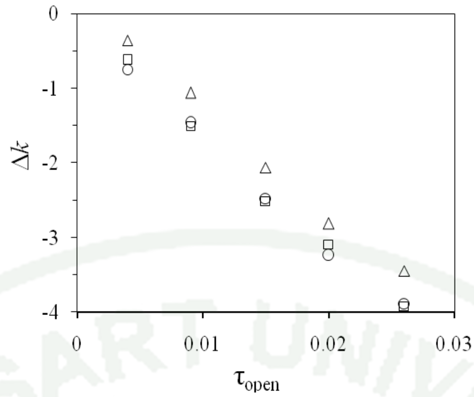

Figure 16 Plots of Δk vs. τ_{open} at conversion equal to 50% and r_{Di} = 1.0 using the exit flow rate curve fitting for different procedures: procedure 1.1 (open circles), procedure 1.2 (open squares) and procedure 2 (open triangles)

For the unit-area normalized response fitting, calculated values of Δk obtained from different procedures at r_{Di} = 1.0 and x = 0.5 are shown in Figure 17. Numerical values of Δk obtained from the unit-area normalized response fitting are shown in Appendix F. The overestimate of Δk is observed for all procedures. The quantities $|\Delta k|$ obtained from procedure 1.1 and procedure 1.2 are very close to each other. When the magnitudes of τ_{open} are increased, the quantities $|\Delta k|$ obtained from all procedures using the unit-area normalized response fitting also increase. The quantities $|\Delta k|$ obtained from procedure 1.1 and procedure 1.2 are very small. The largest error of $|\Delta k|$ is observed from procedure 2 using the unit-area normalized response fitting.

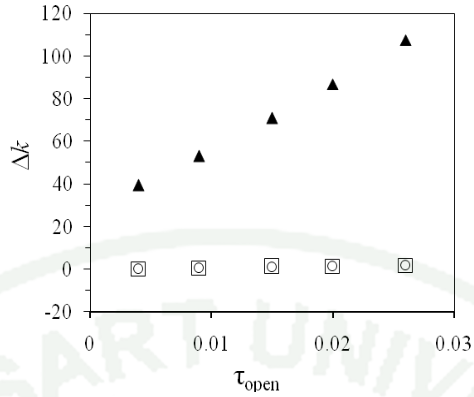

Figure 17 Plots of Δk vs. τ_{open} at conversion equal to 50% and r_{Di} = 1 using the unit-area normalized response fitting for different procedures: procedure 1.1 (open circles), procedure 1.2 (open squares) and procedure 2 (solid triangles)

2.2 Effect of conversion on accuracy of estimated parameters determined from different procedures

Calculated values of ΔD_e^{inert} obtained from different procedures at τ_{open} =0.015 are shown in Figure 18. The information in Figure 18 represents the case in which r_{Di} equal to 1. The quantities ΔD_e^{inert} obtained from procedure 1.1 and procedure 1.2 are constant throughout the range of conversion. The underestimate of ΔD_e^{inert} is observed for procedure 2 using the unit-area normalized response fitting. Procedure 2 using the exit flow rate curve fitting give overestimate of ΔD_e^{inert}. The quantities $\left|\Delta D_e^{inert}\right|$ obtained from procedure 1.1 and procedure 1.2 are very close to each other. The quantities $\left|\Delta D_e^{inert}\right|$ obtained from procedure 2 using the exit flow rate curve fitting and the unit-area normalized response fitting are increased with increasing the conversion except at conversion greater than 80%. Procedure 1.1 provides the most accuracy of the gas diffusivity in inert zone. In addition, procedure

2 using the unit-area normalized response fitting gives large $\left|\Delta D_e^{inert}\right|$ than those using the exit flow rate curve fitting.

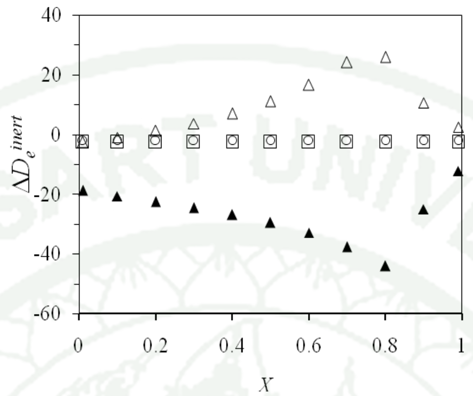

Figure 18 Plots of ΔD_e^{inert} vs. conversion at r_{Di} = 1.0 and τ_{open} = 0.015 for different procedures: procedure 1.1 (open circles), procedure 1.2 (open squares), procedure 2 (open triangles) using the exit flow rate curve fitting and procedure 2 (solid triangles) using the unit-area normalized response fitting

Figure 19 shows the plots of ΔD_e^{cat} obtained from different procedures at r_{Di} = 1.0 and τ_{open} =0.015. The underestimate of Δk is observed for all procedures except procedure 2 using the unit-area normalized response fitting. The quantities ΔD_e^{cat} obtained from procedure 1.1 and procedure 1.2 are constant throughout the range of conversion. The overestimate of ΔD_e^{inert} is observed for procedure 2 using the unit-area normalized response fitting. Procedure 2 using the exit flow rate curve fitting give underestimate of ΔD_e^{inert}. Similarly to Figure 18, the quantities $\left|\Delta D_e^{cat}\right|$ obtained from procedure 1.1 and procedure 1.2 are very close to each other. The quantities $\left|\Delta D_e^{cat}\right|$ obtained from procedure 2 using the exit flow rate curve fitting and the unit-area normalized response fitting are increased with increasing the conversion except at conversion greater than 80%. Procedure 1.1 and procedure 1.2 gives low value of

$\left|\Delta D_e^{cat}\right|$. In addition, procedure 2 using the unit-area normalized response fitting provides the highest $\left|\Delta D_e^{cat}\right|$. Procedure 2 using the unit-area normalized response fitting gives large $\left|\Delta D_e^{cat}\right|$ than those using the exit flow rate curve fitting except at conversion equal to 0.9.

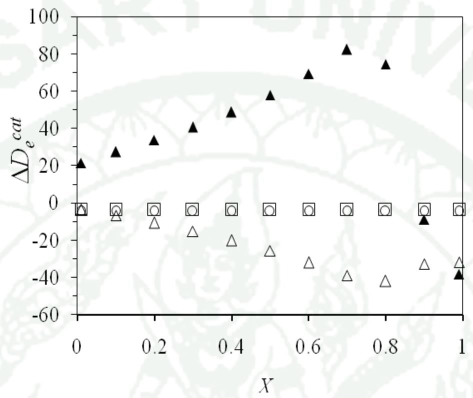

Figure 19 Plots of ΔD_e^{cat} vs. conversion at r_{Di} = 1.0 and τ_{open} = 0.015 for different procedures: procedure 1.1 (open circles), procedure 1.2 (open squares), procedure 2 (open triangles) using the exit flow rate curve fitting and procedure 2 (solid triangles) using the unit-area normalized response fitting

Considering the effect of conversion on accuracy of estimated reaction rate constant, Figure 20 shows the plots of Δk obtained from different procedures using the exit flow rate curve fitting versus conversion at r_{Di} = 1.0 and τ_{open} = 0.015. The underestimate of Δk is observed for all procedures using the exit flow rate curve fitting. When the conversions are increased, the quantities $\left|\Delta k\right|$ determined from all different procedures decrease. The quantities $\left|\Delta k\right|$ obtained from all different procedures using the exit flow rate curve fitting are not very different. The quantities Δk change drastically with conversion at the conversion range between 1 and 10%. $\left|\Delta k\right|$ at 10% conversion is approximately 10% which is much smaller than that at 1%

conversion ($|\Delta k|$ = 100%). At conversion equal to 0.01, the highest $|\Delta k|$ is observed for all procedures due to the small κ_{real} at this conversion.

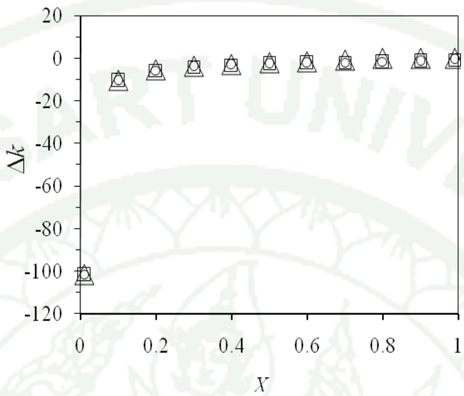

Figure 20 Plots of Δk vs. conversion at r_{Di} = 1.0 and τ_{open} = 0.015 using the exit flow rate curve fitting for different procedures: procedure 1.1 (open circles), procedure 1.2 (open squares) and procedure 2 (open triangles)

For the unit-area normalized response fitting, calculated values of Δk obtained from different procedures at r_{Di} = 1.0 and τ_{open} = 0.015 are shown in Figure 21. The quantities $|\Delta k|$ obtained from procedure 1.1 and procedure 1.2 are very close to each other. When the conversions are increased, the quantities $|\Delta k|$ obtained from all procedures using the unit-area normalized response fitting decrease. The quantities $|\Delta k|$ obtained from procedure 1.1 and procedure 1.2 are very small. The largest error of $|\Delta k|$ is observed from procedure 2 using the unit-area normalized response fitting especially at conversion equal to 1% ($|\Delta k|$ = 1300%).

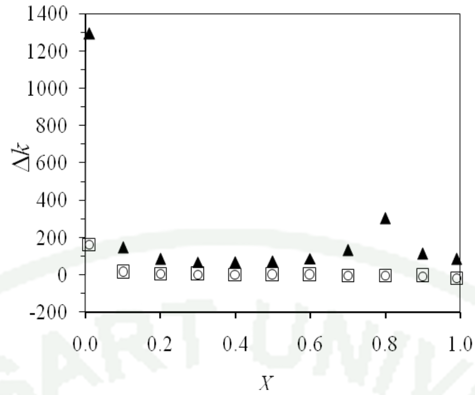

Figure 21 Plots of Δk vs. conversion at r_{Di} = 1.0 and τ_{open} = 0.015 using the unit-area normalized response fitting for different procedures: procedure 1.1 (open circles), procedure 1.2 (open squares) and procedure 2 (solid triangles)

The results mentioned above, it can be concluded that the best procedure is procedure 1.1 which gives the highest accuracy of ΔD_e^{inert} , ΔD_e^{cat} and Δk. And procedure 1.2 is better than procedure 2 using both of the exit flow rate curve fitting and the unit-area normalized response fitting. The lowest accuracy of ΔD_e^{inert} , ΔD_e^{cat} and Δk is observed from procedure 2 using the unit-area normalized response fitting. This can be suggested that procedure 1.1 should be used to determine the estimated parameters.

2.3 Effect of r_{Di} on accuracy of estimated parameters determined from different procedures

Calculated values of ΔD_e^{inert} obtained from different procedures at τ_{open} =0.015 are shown in Figure 22. The information in Figure 22 represents the case in which conversion equal to 50%. The results show that the quantities ΔD_e^{inert} of procedure 1.1 are constant with all the magnitude of r_{Di} since this experimental response is generated from the diffusion response from the one-zone model. When increasing

r_{Di}, the quantities $\left|\Delta D_e^{inert}\right|$ obtained from procedure 2 using the exit flow rate curve fitting and the unit-area normalized response fitting are also increased. Procedure 1.1 provides the most accuracy of the gas diffusivity in inert zone compared with procedure 1.2 and procedure 2. In addition, procedure 2 using the unit-area normalized response fitting gives higher $\left|\Delta D_e^{inert}\right|$ than those using the exit flow rate curve fitting. It can be found that good accuracy of ΔD_e^{inert} is observed when r_{Di} is less than or equal to 1. At r_{Di} equal to 1, the values of $\left|\Delta D_e^{inert}\right|$ obtained from procedure 1.1 and procedure 1.2 are the same.

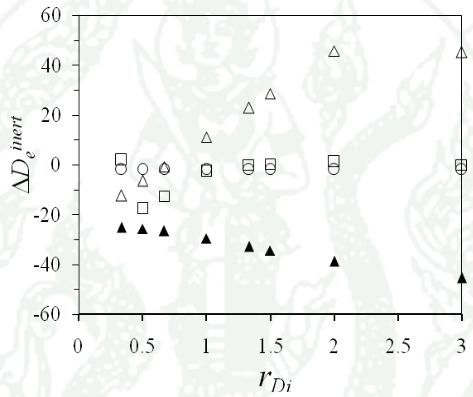

Figure 22 Plots of ΔD_e^{inert} vs. r_{Di} at conversion equal to 50% and τ_{open}=0.015 for different procedures: procedure 1.1 (open circles), procedure 1.2 (open squares), procedure 2 (open triangles) using the exit flow rate curve fitting and procedure 2 (solid triangles) using the unit-area normalized response fitting

Figure 23 shows the plots of ΔD_e^{cat} obtained from different procedures at conversion equal to 50% and τ_{open}=0.015. Similarly to Figure 22, procedure 1.1 gives the lowest $\left|\Delta D_e^{cat}\right|$ and procedure 2 using the unit-area normalized response fitting provides the highest $\left|\Delta D_e^{cat}\right|$. The overestimate of ΔD_e^{cat} is observed for procedure 2 using the unit-area normalized response fitting. It can be seen from this figure that at

r_{Di} equal to 1, the quantities $\left|\Delta D_e^{cat}\right|$ has high accuracy except $\left|\Delta D_e^{cat}\right|$ obtained from procedure 2 using the unit-area normalized response fitting and the values of $\left|\Delta D_e^{cat}\right|$ obtained from procedure 1.1 and procedure 1.2 are the same at this magnitude of r_{Di} .

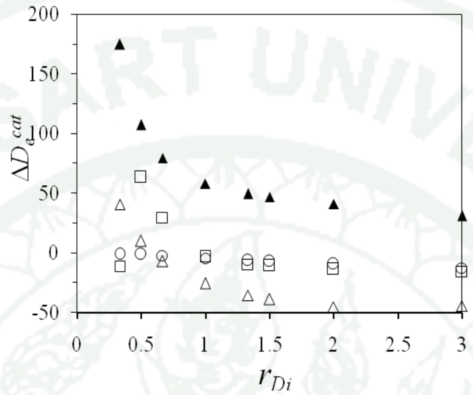

Figure 23 Plots of ΔD_e^{cat} vs. r_{Di} at conversion equal to 50% and τ_{open} =0.015 for different procedures: procedure 1.1 (open circles), procedure 1.2 (open squares), procedure 2 (open triangles) using the exit flow rate curve fitting and procedure 2 (solid triangles) using the unit-area normalized response fitting

Considering the effect of r_{Di} on accuracy of estimated reaction rate constant, Figure 24 shows the plots of Δk obtained from different procedures using the exit flow rate curve fitting versus r_{Di} at τ_{open} =0.015 and conversion equal to 50%. For the exit flow rate curve fitting, when increasing the magnitude of r_{Di} , the quantities $|\Delta k|$ determined from procedure 1.1 and procedure 1.2 are increased. The quantities $|\Delta k|$ obtained from all different procedures seem to be not different. The magnitudes of $|\Delta k|$ at the r_{Di} range between 1/3 and 3/1 are considerably small which not exceed 4% for all procedures. In addition, when r_{Di} is less than or equal to 1, the numerical results show good accuracy of $|\Delta k|$. Similarly to Figure 22 and 23, the values of $|\Delta k|$ obtained from procedure 1.1 and procedure 1.2 are the same at r_{Di} equal to 1.

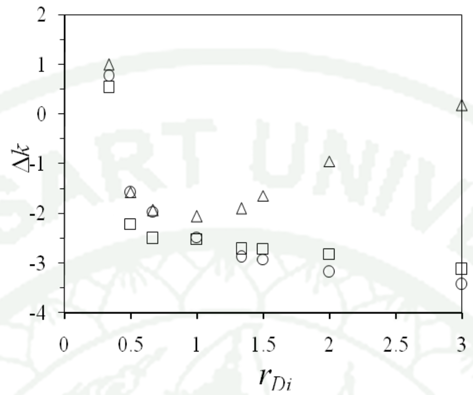

Figure 24 Plots of Δk vs. r_{Di} at conversion equal to 50% and τ_{open} =0.015 using the exit flow rate curve fitting for different procedures: procedure 1.1 (open circles), procedure 1.2 (open squares) and procedure 2 (open triangles)

For the unit-area normalized response fitting, calculated values of Δk obtained from different procedures at τ_{open} =0.015 and x=0.5 are shown in Figure 25. The overestimate of Δk is observed for procedure 2. The quantities $|\Delta k|$ obtained from procedure 1.1 and procedure 1.2 are not very different. Similarly to Figure 23, 24 and 25, the values of $|\Delta k|$ obtained from procedure 1.1 and procedure 1.2 are the same at r_{Di} equal to 1. When the magnitudes of r_{Di} are increased, the quantities $|\Delta k|$ obtained from procedure 2 using the unit-area normalized response fitting also increase. The large error of $|\Delta k|$ is observed from procedure 2 using the unit-area normalized response fitting. At r_{Di} equal to 1/3, all procedures give high accuracy of $|\Delta k|$. The lowest $|\Delta k|$ obtained from procedure 1.1 and procedure 1.2 are observed at r_{Di} equal to 1.

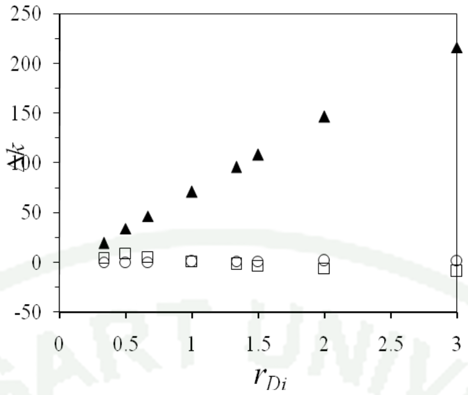

Figure 25 Plots of Δk vs. r_{Di} at conversion equal to 50% and τ_{open} =0.015 using the unit-area normalized response fitting for different procedures: procedure 1.1 (open circles), procedure 1.2 (open squares) and procedure 2 (solid triangles)

For the results of effect of r_{Di} on accuracy of estimated parameters, it can be found that although procedure 2 using the unit-area normalized response fitting gives large error of parameters but it is not as bad when r_{Di} equal to 1. At r_{Di} equal to 1, the parameters obtained from procedure 1.1 and procedure 1.2 are the same value.

3. Three-zone reactor ($L_{cat}/L_{reactor}$ =1/30)

3.1 Effect of τ_{open} on accuracy of estimated parameters determined from different procedures

The cases shown in this section have the magnitude of r_{Di} equal to 1.0 and conversion equal to 0.5. The quantities ΔD_e^{inert} obtained from different procedures at r_{Di} = 1 and x=0.5 are shown in Figure 26. Numerical values of ΔD_e^{inert} are shown in Appendix G. The linear relationship between ΔD_e^{inert} and τ_{open} is observed for procedure 1.1, procedure 1.2 and procedure 2 using the unit-area normalized response fitting. The underestimate of ΔD_e^{inert} is observed for procedure 2 using the unit-area normalized response fitting. But procedure 2 using the exit flow rate curve fitting gives overestimate of ΔD_e^{inert}. The quantities $\left|\Delta D_e^{inert}\right|$ obtained from procedure 1.1 and procedure 2 using the unit-area normalized response fitting are increased with increasing the magnitude of τ_{open}. Procedure 1.1 gives the lowest $\left|\Delta D_e^{inert}\right|$ but procedure 2 using the unit-area normalized response fitting gives the highest $\left|\Delta D_e^{inert}\right|$. For procedure 2, the exit flow rate curve fitting provides less $\left|\Delta D_e^{inert}\right|$ than the unit-area normalized response fitting.

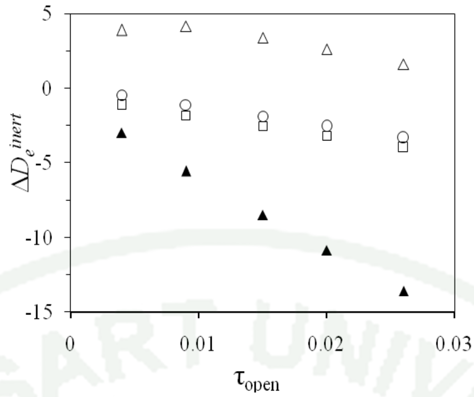

Figure 26 Plots of ΔD_e^{inert} vs. τ_{open} at r_{Di} = 1.0 and x=0.5 for different procedures: procedure 1.1 (open circles), procedure 1.2 (open squares), procedure 2 (open triangles) using the exit flow rate curve fitting and procedure 2 (solid triangles) using the unit-area normalized response fitting

Figure 27 shows the plots of ΔD_e^{cat} obtained from different procedures versus τ_{open} at r_{Di} = 1.0 and x=0.5. Numerical values of ΔD_e^{cat} are shown in Appendix H. The relationship between ΔD_e^{cat} and τ_{open} is close to linear for procedure 1.1, procedure 1.2 and procedure 2 using the unit-area normalized response fitting. The overestimate of ΔD_e^{inert} is observed for procedure 2 using the unit-area normalized response fitting. Procedure 2 using the exit flow rate curve fitting gives underestimate of ΔD_e^{inert}. When the magnitudes of τ_{open} are increased, the quantities $\left|\Delta D_e^{cat}\right|$ obtained from all also increase. From this figure, procedure 1.2 gives the lowest of $\left|\Delta D_e^{cat}\right|$ and $\left|\Delta D_e^{cat}\right|$ obtained from procedure 2 using the exit flow rate curve fitting is high.

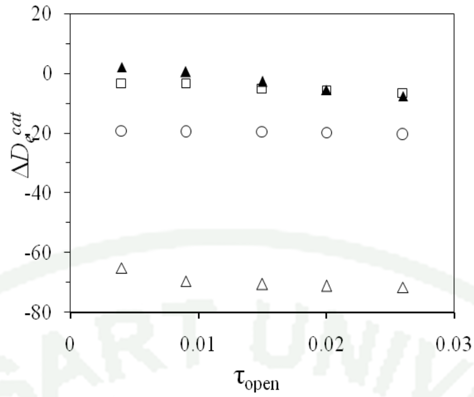

Figure 27 Plots of ΔD_e^{cat} vs. τ_{open} at r_{Di} = 1.0 and x=0.5 for different procedures: procedure 1.1 (open circles), procedure 1.2 (open squares), procedure 2 (open triangles) using the exit flow rate curve fitting and procedure 2 (solid triangles) using the unit-area normalized response fitting

Considering the effect of τ_{open} on accuracy of estimated reaction rate constant, Figure 28 shows the plots of Δk obtained from different procedures using the exit flow rate curve fitting versus τ_{open} at r_{Di} = 1.0 and conversion equal to 50%. Numerical values of Δk using the exit flow rate curve fitting are shown in Appendix I. The relationship between Δk and τ_{open} is close to linear for all procedures. The underestimate of Δk is observed for all procedures. When increasing the magnitude of τ_{open}, the quantities $|\Delta k|$ determined from all different procedures also increase. The quantities $|\Delta k|$ obtained from all different procedures are not very different. The magnitudes of $|\Delta k|$ obtained all different procedures are small within which $|\Delta k|$ does not exceed 4%.

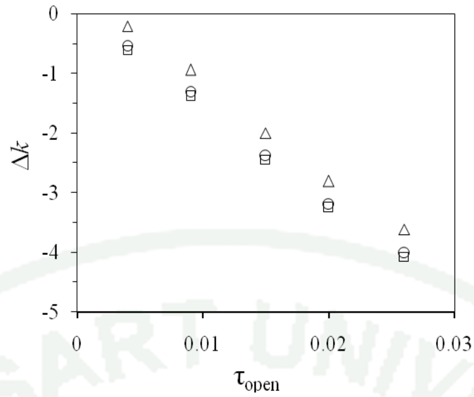

Figure 28 Plots of Δk vs. τ_{open} at conversion equal to 50% and r_{Di} = 1.0 using the exit flow rate curve fitting for different procedures: procedure 1.1 (open circles), procedure 1.2 (open squares) and procedure 2 (open triangles)

For the unit-area normalized response fitting, calculated values of Δk obtained from different procedures at r_{Di} = 1.0 and x = 0.5 are shown in Figure 29. Numerical values of Δk using the unit-area normalized response fitting are shown in Appendix J. The overestimate of Δk is observed for all procedures. The quantities $|\Delta k|$ obtained from procedure 1.1 and procedure 1.2 are very close to each other. When the magnitudes of τ_{open} are increased, the quantities $|\Delta k|$ obtained from all procedures using the unit-area normalized response fitting also increase. The quantities $|\Delta k|$ obtained from procedure 1.1 and procedure 1.2 are very small. The largest error of $|\Delta k|$ is observed from procedure 2 using the unit-area normalized response fitting.

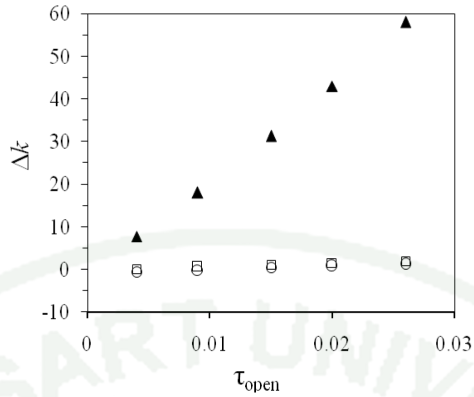

Figure 29 Plots of Δk vs. τ_{open} at conversion equal to 50% and r_{Di} = 1 using the unit-area normalized response fitting for different procedures: procedure 1.1 (open circles), procedure 1.2 (open squares) and procedure 2 (solid triangles)

3.2 Effect of conversion on accuracy of estimated parameters determined from different procedures

Calculated values of ΔD_e^{inert} obtained from different procedures at τ_{open} =0.015 are shown in Figure 30. The information in Figure 30 represents the case in which r_{Di} equal to 1. The quantities ΔD_e^{inert} obtained from procedure 1.1 and procedure 1.2 are constant throughout the range of conversion. The quantities $\left|\Delta D_e^{inert}\right|$ obtained from procedure 1.1 and procedure 1.2 are very close to each other. The underestimate of ΔD_e^{inert} is observed for procedure 2 using the unit-area normalized response fitting. But procedure 2 using the exit flow rate curve fitting gives overestimate of ΔD_e^{inert}. The quantities $\left|\Delta D_e^{inert}\right|$ obtained from procedure 2 using the exit flow rate curve fitting and the unit-area normalized response fitting are increased with increasing the conversion except at conversion greater than 90%. Procedure 1.1 provides the most accuracy of the gas diffusivity in inert zone. In addition, procedure 2 using the unit-area normalized response fitting gives large $\left|\Delta D_e^{inert}\right|$ than those using the exit flow rate curve fitting.

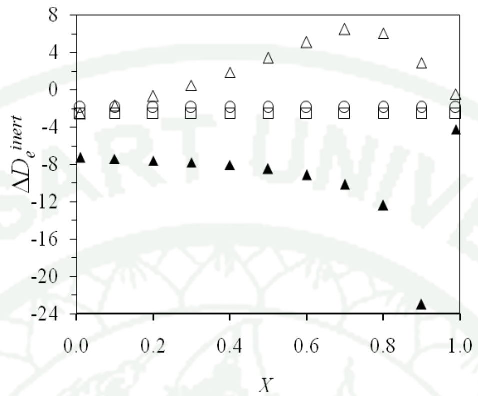

Figure 30 Plots of ΔD_e^{inert} vs. conversion at r_{Di} = 1.0 and τ_{open} = 0.015 for different procedures: procedure 1.1 (open circles), procedure 1.2 (open squares), procedure 2 (open triangles) using the exit flow rate curve fitting and procedure 2 (solid triangles) using the unit-area normalized response fitting

Figure 31 shows the plots of ΔD_e^{cat} obtained from different procedures at r_{Di} = 1.0 and τ_{open} =0.015. The underestimate of Δk is observed for all procedures. The quantities ΔD_e^{cat} obtained from procedure 1.1 and procedure 1.2 are constant throughout the range of conversion. It can be seen that the quantities $\left|\Delta D_e^{cat}\right|$ obtained from procedure 2 using the exit flow rate curve fitting are increased with increasing the conversion. Procedure 1.2 gives low value of $\left|\Delta D_e^{cat}\right|$ and procedure 2 using the exit flow rate curve fitting provides the highest $\left|\Delta D_e^{cat}\right|$. Procedure 2 using the exit flow rate curve fitting gives large $\left|\Delta D_e^{cat}\right|$ than those using the unit-area normalized response fitting except at conversion equal to 0.99.

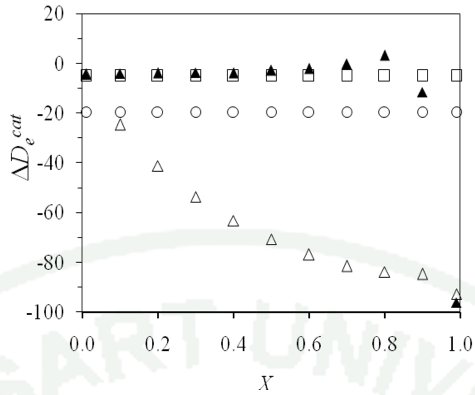

Figure 31 Plots of ΔD_e^{cat} vs. conversion at r_{Di} = 1.0 and τ_{open} = 0.015 for different procedures: procedure 1.1 (open circles), procedure 1.2 (open squares), procedure 2 (open triangles) using the exit flow rate curve fitting and procedure 2 (solid triangles) using the unit-area normalized response fitting

Considering the effect of conversion on accuracy of estimated reaction rate constant, Figure 32 shows the plots of Δk obtained from different procedures using the exit flow rate curve fitting versus conversion at r_{Di} = 1.0 and τ_{open} = 0.015. The underestimate of Δk is observed for all procedures using the exit flow rate curve fitting. When increasing the conversion, the quantities $|\Delta k|$ determined using the exit flow rate curve fitting is slightly decreased except at x=0.01 for all procedures. The quantities $|\Delta k|$ obtained from all different procedures using the exit flow rate curve fitting are not very different. At conversion equal to 0.01, the highest $|\Delta k|$ is observed for all procedures due to the small κ_{real} at this conversion and $|\Delta k|$ in this conversion is dramatically increased for all procedures.

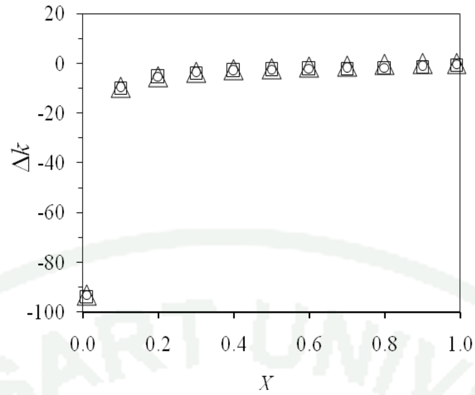

Figure 32 Plots of Δk vs. conversion at r_{Di} = 1.0 and τ_{open} = 0.015 using the exit flow rate curve fitting for different procedures: procedure 1.1 (open circles), procedure 1.2 (open squares) and procedure 2 (open triangles)

For the unit-area normalized response fitting, calculated values of Δk obtained from different procedures at r_{Di} = 1.0 and τ_{open} = 0.015 are shown in Figure 33. The quantities $|\Delta k|$ obtained from procedure 1.1 and procedure 1.2 are very close to each other. When the conversions are increased, the quantities $|\Delta k|$ obtained from procedure 2 using the unit-area normalized response fitting decrease except at conversion equal to 80%. The quantities $|\Delta k|$ obtained from procedure 1.1 and procedure 1.2 are very small. The largest error of $|\Delta k|$ is observed from procedure 2 using the unit-area normalized response fitting especially at conversion equal to 1% ($|\Delta k|$ = 1000%). It is clearly seen that procedure 2 gives much higher $|\Delta k|$ than procedure 1.1 and 1.2.

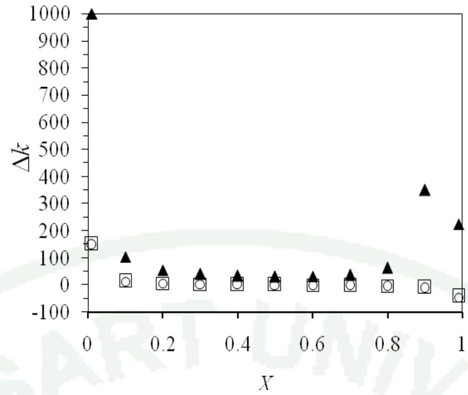

Figure 33 Plots of Δk vs. conversion at r_{Di} = 1.0 and τ_{open} = 0.015 using the unit-area normalized response fitting for different procedures: procedure 1.1 (open circles), procedure 1.2 (open squares) and procedure 2 (solid triangles)

The results mentioned above, it can be concluded that the best procedure is procedure 1.1 which gives the highest accuracy of ΔD_e^{inert} , ΔD_e^{cat} and Δk. And procedure 1.2 is better than procedure 2 using both of the exit flow rate curve fitting and the unit-area normalized response fitting. The lowest accuracy of ΔD_e^{inert} , ΔD_e^{cat} and Δk is observed from procedure 2 using the unit-area normalized response fitting. When comparing $L_{cat}/L_{reactor}$ between 1/3 and 1/30, the accuracy of parameters with $L_{cat}/L_{reactor}$ =1/30 is more than those with $L_{cat}/L_{reactor}$ =1/3. This can be suggested that procedure 1.1 should be used to determine the estimated parameters and the length of catalyst zone should be small.

3.3 Effect of r_{Di} on accuracy of estimated parameters determined from different procedures

Calculated values of ΔD_e^{inert} obtained from different procedures at τ_{open} =0.015 are shown in Figure 34. The information in Figure 34 represents the case in which conversion equal to 50%. The results show that the quantities ΔD_e^{inert} of procedure

1.1 are constant with all the magnitude of r_{Di} since this experimental response is generated from the diffusion response from the one-zone model. The underestimate of ΔD_e^{inert} is observed for procedure 2 using the unit-area normalized response fitting. But procedure 2 using the exit flow rate curve fitting gives overestimate of ΔD_e^{inert}. When increasing r_{Di}, the quantities $\left|\Delta D_e^{inert}\right|$ obtained from procedure 2 using the exit flow rate curve fitting and the unit-area normalized response fitting are also increased. Procedure 1.1 provides the most accuracy of the gas diffusivity in inert zone compared with procedure 1.2 and procedure 2. In addition, procedure 2 using the unit-area normalized response fitting gives higher $\left|\Delta D_e^{inert}\right|$ than those using the exit flow rate curve fitting. It can be found that good accuracy of ΔD_e^{inert} is observed when r_{Di} is less than or equal to 1.

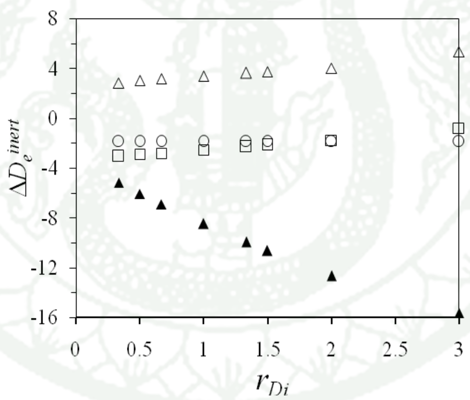

Figure 34 Plots of ΔD_e^{inert} vs. r_{Di} at conversion equal to 50% and τ_{open}=0.015 for different procedures: procedure 1.1 (open circles), procedure 1.2 (open squares), procedure 2 (open triangles) using the exit flow rate curve fitting and procedure 2 (solid triangles) using the unit-area normalized response fitting

Figure 35 shows the plots of ΔD_e^{cat} obtained from different procedures at conversion equal to 50% and τ_{open}=0.015. The overestimate of ΔD_e^{cat} is observed for procedure 2 using the unit-area normalized response fitting. Procedure 2 using the exit flow rate curve fitting gives underestimate of ΔD_e^{cat}. Similarly to Figure 34, procedure 1.1 gives the lowest of $\left|\Delta D_e^{cat}\right|$ and procedure 2 using the unit-area normalized response fitting provides the highest of $\left|\Delta D_e^{cat}\right|$. The underestimate of ΔD_e^{cat} is observed for procedure 2 using the exit flow rate curve fitting. It can be seen from this figure that at r_{Di} equal to 1, the quantities $\left|\Delta D_e^{cat}\right|$ has high accuracy except $\left|\Delta D_e^{cat}\right|$ obtained from procedure 2 using the unit-area normalized response fitting.

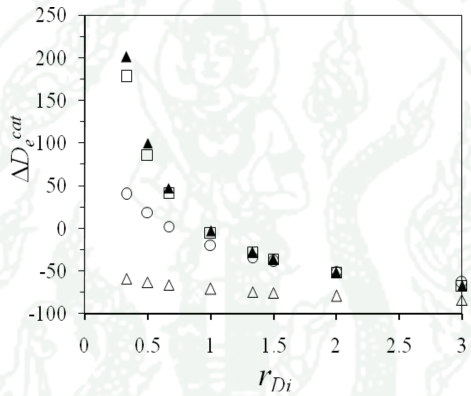

Figure 35 Plots of ΔD_e^{cat} vs. r_{Di} at conversion equal to 50% and τ_{open}=0.015 for different procedures: procedure 1.1 (open circles), procedure 1.2 (open squares), procedure 2 (open triangles) using the exit flow rate curve fitting and procedure 2 (solid triangles) using the unit-area normalized response fitting

Considering the effect of r_{Di} on accuracy of estimated reaction rate constant, Figure 36 shows the plots of Δk obtained from different procedures using the exit flow rate curve fitting versus r_{Di} at τ_{open}=0.015 and conversion equal to 50%. For the exit flow rate curve fitting, when increasing the magnitude of r_{Di}, the quantities $|\Delta k|$ determined from all procedures increase. The quantities $|\Delta k|$ obtained from all different procedures seem to be not different. In addition, when r_{Di} is less than or equal to 1, the numerical results show good accuracy of $|\Delta k|$.

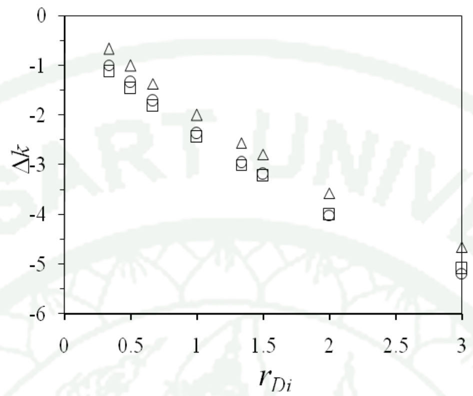

Figure 36 Plots of Δk vs. r_{Di} at conversion equal to 50% and τ_{open} =0.015 using the exit flow rate curve fitting for different procedures: procedure 1.1 (open circles), procedure 1.2 (open squares) and procedure 2 (open triangles)

For the unit-area normalized response fitting, calculated values of Δk obtained from different procedures at τ_{open} =0.015 and x=0.5 are shown in Figure 37. The overestimate of Δk is observed for procedure 2. The quantities $|\Delta k|$ obtained from procedure 1.1 and procedure 1.2 are not very different. When the magnitudes of r_{Di} are increased, the quantities $|\Delta k|$ obtained from procedure 2 using the unit-area normalized response fitting also increase. The large error of $|\Delta k|$ is observed from procedure 2 using the unit-area normalized response fitting. At r_{Di} equal to 1/3, all procedures give high accuracy of $|\Delta k|$. The lowest $|\Delta k|$ obtained from procedure 1.1 and procedure 1.2 are observed at r_{Di} equal to 1.

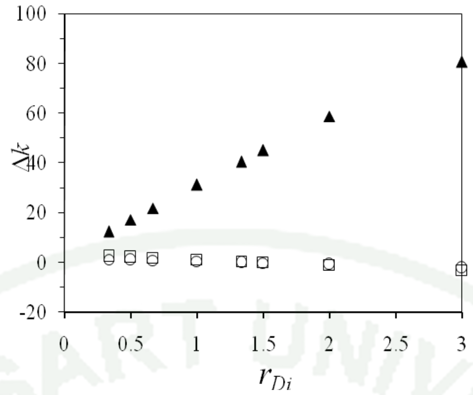

Figure 37 Plots of Δk vs. r_{Di} at conversion equal to 50% and τ_{open} =0.015 using the unit-area normalized response fitting for different procedures: procedure 1.1 (open circles), procedure 1.2 (open squares) and procedure 2 (solid triangles)

For the results of effect of r_{Di} on accuracy of estimated parameters, it can be found that although procedure 2 using the unit-area normalized response fitting gives large error of parameters but it is not as bad when r_{Di} equal to 1. At r_{Di} equal to 1, the parameters obtained from procedure 1.1 and procedure 1.2 are the same value.

CONCLUSIONS AND RECOMMENDATION

Accuracy of different procedures for estimating parameters from TAP pulse responses has been investigated for the irreversible reaction case. The kinetic parameter from the TAP experimental response was determined by using different estimation procedures including determination of the kinetic parameter after transport parameter determination, and determination of the kinetic and transport parameters simultaneously. The TAP experimental response was simulated under the triangular inlet flow condition. The exit flow rate curves and the unit-area normalized response curves are applied for parameter estimations based on the least square fit. The quantities ΔD_e and $\Delta\kappa$ were used to indicate the accuracy of the estimated diffusivity and reaction rate constant respectively.

For the one-zone reactor, the relationship between ΔD_e and τ_{open} is close to linear for all different procedures. The linear relationship between Δk and τ_{open} is also observed for all procedures. The results indicate that the first procedure generally provides more accurate estimated diffusivity and reaction rate constant than the second procedure. The second procedure using the exit flow rate curve fitting provides more accurate estimated diffusivity and reaction rate constant than those using the unit-area normalized response fitting. It is suggested that the exit flow rate curve fitting should be involved in the quantitative interpretation. Determination of the gas diffusivity and the first order irreversible reaction rate constant using the first procedure is suggested for the one-zone reactor.

For the three-zone reactor, there are three different procedures including procedure 1.1 involving determination of the reaction rate constant after the gas diffusivities in the inert zone and the catalyst zone are determined sequentially, procedure 1.2 involving determination of the reaction rate constant after the gas diffusivities in the inert and catalyst zones are simultaneously determined, and procedure 2 involving determination of the reaction rate constant and gas diffusivities in inert and catalyst zones simultaneously. When the ratio of the length of catalyst zone to the length of reactor is equal to 1/3, procedure 1.1 generally gives the lowest $\left|\Delta D_e^{inert}\right|$, $\left|\Delta D_e^{cat}\right|$ and $\left|\Delta k\right|$. Procedure 1.2 is more accurate than procedure 2 for both exit flow rate curve fitting and unit-area normalized response fitting. The lowest accuracy of estimated D_e^{inert}, D_e^{cat} and k is observed from procedure 2 using the unit-area normalized response fitting. The quantities $\left|\Delta k\right|$ obtained all different procedures using the exit flow rate curve fitting are not much different. When using the unit-area normalized response fitting, procedure 2 gives much higher $\left|\Delta k\right|$ than procedure 1.1 and procedure 1.2. Considering effect of r_{Di} on accuracy of estimated parameters, it was found that although procedure 2 using the unit-area normalized response fitting gives large error of parameters but the error is small when r_{Di} is equal to 1. At r_{Di} equal to 1, the parameters obtained from procedure 1.1 and procedure 1.2 are the same. The results indicate that procedure 1.1 should be used to determine the estimated parameters in the three-zone reactor. For the three-zone reactor with ratio of the length of catalyst zone to the length of reactor equal to 1/30, procedure 1.1 also provides the most accuracy of D_e^{inert}, D_e^{cat} and k. In addition, determination of the gas diffusivities in each zone and the first order irreversible reaction rate constant using $L_{cat}/L_{reactor}$ =1/30 gives more accurate D_e^{inert}, D_e^{cat} and k than those using $L_{cat}/L_{reactor}$ =1/3.

In the case of the three-zone reactor, the results reported in this work show that using procedure 1.1 give more accurate estimated parameters when $L_{cat}/L_{reactor}$ is smaller. The advantage of using a thin catalyst zone has been reported including a uniform catalyst change across the catalyst bed during the experiment. However, there is no report on whether a thin catalyst zone can handle the temperature non-uniformity problem. Investigation on this problem will be useful for interpretation of TAP data.

LITERATURE CITED

Boonnumpha, Y. 2005. **Validity of the Dirac Delta Function for Describing the Inlet Flow in TAP Pulse.** M.Eng. Thesis, Kasetsart University.

Cunningham, R.E. and R.J.J. Williams. 1980. **Diffusion in Gases and Porous Media.** Plenum Press, New York.

Fierro, V., Y. Schuurman, C. Mirodatos, J.L. Duplan and J. Verstraete. 2002. Study of the cracking reaction of linear and branched hexanes under protolytic conditions by non-stationary kinetics. **J. Chem. Eng.** 90: 139.

Gleaves, J.T., J.R. Ebner and T.C., Kuechler. 1988. Temporal Analysis of Products (TAP) – A unique catalyst evaluation system with submillisecond time resolution. **Catal. Rev. Sci. Eng.** 30 (1): 49-116.

Gleaves, J.T., G.S. Yablonskii, P. Phanawadee and Y. Schuurman. 1997. TAP-2: An interrogative kinetics approach. **Appl. Catal. A: Gen** 160: 55-88.

Gleaves, J.T., G.S. Yablonsky, X. Zheng, R. Fushimi and P. L. Mills. 2010. Temporal Analysis of Products (TAP) – Recent advances in technology for kinetic analysis of multicomponent catalysts. **J. Mol. Catal. A: Chem.** 315: 108-134.

Huinink, J.P. 1995. **A Quantitative Analysis of Transient Kinetic Experiments: The Oxidation of CO by O_2/NO on Pt.** Ph.D. Thesis, Eindhoven University of Technology, Eindhoven.

Huizenga, D.G. and D.M. Smith. 1986. Knudsen diffusion in random assemblages of uniform spheres. **AIChE Journal** 32: 1-6.

Pérez-Ramírez, J., E.V. Kondratenko, V.A. Kondratenko and M. Baerns. 2004. Selectivity-directing factors of ammonia oxidation over PGM gauzes in the Temporal Analysis of Products reactor : Primary interactions of NH_3 and O_2. **J. Catal.** 227: 90-100.

Petzold, L.R. 1983. Automatic selection of methods for solving stiff and nonstiff systems of ordinary differential equations. **Siam J. Sci. Stat. Comput.** 4: 136-148.

Phanawadee, P. 1997. **Theory and Methodology of TAP Knudsen Pulse Response Experiments.** Ph.D. Thesis, Washington University, Saint Louis, Missouri, USA

Phanawadee, P., G.S. Yablonsky, P. Preechasanongkit and K. Somapa. 1999. A new correlation for determination of the effective Knudsen diffusivity of a gas in a TAP reactor. **Ind. Eng. Chem. Res.** 38: 2877.

Rothaemel, M. and M. Baerns. 1996. Modeling and simulation of transient adsorption and reaction in vacuum using the Temporal Analysis of Products reactor. Ind**. Eng. Chem. Res.** 3: 1556-1565.

Schuurman, Y. and J.T. Glaeves. 1997. A Comparison of steady-state and unsteady–steady-state reaction kinetics of n-butane oxidation over VPO catalysts using a TAP-2 reactor system. **Catal. Today.** 33: 25.

Shekhtman, S.O., A. Goguet, R. Burch, C. Hardacre, N. Maguire. 2008. CO multipulse TAP studies of 2% Pt/CeO_2 catalyst: Influence of catalyst pretreatment and temperature on the number of active sites observed. **J. Cat.** 253: 303-311.

Soick, M., D. Wolf and M. Baerns. 2000. Determination of kinetic parameters for complex heterogeneous catalytic reactions by numerical evaluation of TAP experiments. **Chem. Eng. Sci.** 55: 2875-2882.

Svoboda, G.D., J.T. Gleaves and P.L. Mills. 1992. New method for studying the pyrolysis of VPE/CVD Precursors under vacuum condition. Application to trimethylantimony and tetramethyltin. **Ind. Eng. Chem. Res.** 31: 19.

Tantake, P., P. Phanawadee, Y. Boonnumpha and J. Limtrakul. 2007. Comparison between regression analysis and moment analysis for transport and kinetic parameter estimation in TAP experiments under a non-ideal inlet condition. **Catal. Today** 121: 261-268.

Weerts, W.L.M., M.H.J.M. de Croon and G.B. Marin. 1996. The adsorption of silane, disilane and trisilane on polycrystalline silicon: a transient kinetic study. **J.Surf. Sci.** 367: 321.

Zou, B., M.P. Dudukovic and P.L. Mills. 1993. Modelling of evacuated pulse micro-reactor. **Chem. Eng. Sci.** 48: 2345-2355.

APPENDICES

Appendix A

Discretization of the Mathematical Model for Diffusion with First Order Irreversible Reaction in TAP Reactor

In this study, the set of PDEs describing the transport and kinetic processes in TAP reactor is numerically solved using the so-called Method of Lines (MOL). The method of lines is an important numerical procedure for the solution of evolutionary partial differential equations (PDEs). The idea is to discretize the partial derivatives with respect to all independent variables except the time variable which remains continuous. This process leads to a system of ordinary differential equations (ODEs) for the discretized variables which can then, in principle, be solved by the initial value method. The discretization of MOL can be accomplished using the method of finite differences.

According to the Taylor's expansion, we can write

$$\phi(\xi_{i+1},\tau) = \phi(\xi_i,\tau) + h_\xi \frac{\partial \phi(\xi_i,\tau)}{\partial \xi} + \frac{h_\xi^2}{2!}\frac{\partial^2 \phi(\xi_i,\tau)}{\partial \xi^2} + \cdots \qquad \text{A-1}$$

$$\phi(\xi_{i-1},\tau) = \phi(\xi_i,\tau) - h_\xi \frac{\partial \phi(\xi_i,\tau)}{\partial \xi} + \frac{h_\xi^2}{2!}\frac{\partial^2 \phi(\xi_i,\tau)}{\partial \xi^2} - \cdots \qquad \text{A-2}$$

From the Taylor's series written in Eqs. (A-1) and (A-2), the central finite difference approximation for the second order derivative is described by

$$\left(\frac{\partial^2 \phi(\tau)}{\partial \xi^2}\right)_i = \frac{\phi_{i+1}(\tau) - 2\phi_i(\tau) + \phi_{i-1}(\tau)}{h_\xi^2} - \frac{h_\xi^2}{12}\left(\frac{\partial^4 \phi(\tau)}{\partial \xi^4}\right)_i + \cdots$$

or,

$$\left(\frac{\partial^2 \phi(\tau)}{\partial \xi^2}\right)_i \cong \frac{\phi_{i+1}(\tau) - 2\phi_i(\tau) + \phi_{i-1}(\tau)}{h_\xi^2} \qquad \text{A-3}$$

The central finite difference approximation for first order derivative is given by

$$\left(\frac{\partial \phi(\tau)}{\partial \xi}\right)_i = \frac{\phi_{i+1}(\tau) - \phi_{i-1}(\tau)}{2h_\xi} + \frac{h_\xi^2}{6}\left(\frac{\partial^3 \phi(\tau)}{\partial \xi^3}\right)_i + \cdots$$

or, $$\left(\frac{\partial\phi(\tau)}{\partial\xi}\right)_i \cong \frac{\phi_{i+1}(\tau)-\phi_{i-1}(\tau)}{2h_\xi} \qquad \text{A-4}$$

According to Eq. (A-1), the forward finite difference approximation for the first order derivative is described by

$$\left(\frac{\partial\phi(\tau)}{\partial\xi}\right)_i = \frac{-\phi_{i+2}(\tau)+4\phi_{i+1}(\tau)-3\phi_i(\tau)}{2h_\xi} + \frac{h_\xi^2}{6}\left(\frac{\partial^3\phi(\tau)}{\partial\xi^3}\right)_i + \cdots$$

or, $$\left(\frac{\partial\phi(\tau)}{\partial\xi}\right)_i \cong \frac{-\phi_{i+2}(\tau)+4\phi_{i+1}(\tau)-3\phi_i(\tau)}{2h_\xi} \qquad \text{A-5}$$

According to Eq. (A-2), the backward finite difference approximation for first order derivative is given by

$$\left(\frac{\partial\phi(\tau)}{\partial\xi}\right)_i = \frac{3\phi_i(\tau)-4\phi_{i-1}(\tau)+\phi_{i-2}(\tau)}{2h_\xi} - \frac{h_\xi^2}{6}\left(\frac{\partial^3\phi(\tau)}{\partial\xi^3}\right)_i + \cdots$$

or, $$\left(\frac{\partial\phi(\tau)}{\partial\xi}\right)_i \cong \frac{3\phi_i(\tau)-4\phi_{i-1}(\tau)+\phi_{i-2}(\tau)}{2h_\xi} \qquad \text{A-6}$$

where h_ξ is the step size between the axial coordinate of the reactor.

Discretization for one-zone reactor

The mass balance equation for diffusion in a one-zone reactor is described in the generalized dimensionless form as

$$\frac{\partial C^*}{\partial\tau} = \frac{\partial^2 C^*}{\partial\xi^2} \qquad \text{A-7}$$

If the reaction is first order irreversible reaction, the mass balance equation can be described in the generalized dimensionless by

$$\frac{\partial C^*}{\partial \tau} = \frac{\partial^2 C^*}{\partial \xi^2} - \kappa C^* \qquad \text{A-8}$$

The dimensionless initial and boundary conditions are described by

Initial condition: $\tau = 0;\quad C^* = 0$ A-11

Boundary condition: $\xi = 0;\quad -\frac{\partial C^*}{\partial \xi} = \delta(\tau - 0^+)$ A-12

$\xi = 0;\quad -\frac{\partial C^*}{\partial \xi} = X(\tau)$ (for non-ideal inlet condition) A-13

$\xi = 1;\quad C^* = 0$ A-14

The dimensionless exit flow rate of the gas is calculated using

$$F^* = -\left.\frac{\partial C^*}{\partial \xi}\right|_{\xi=1} \qquad \text{A-15}$$

1. Discretization along the axial coordinate

$$\left(\frac{dC^*}{d\tau}\right)_i = \frac{C^*_{i+1} - 2C^*_i + C^*_{i-1}}{h_\xi^2} - \kappa C^*_i \qquad \text{A-16}$$

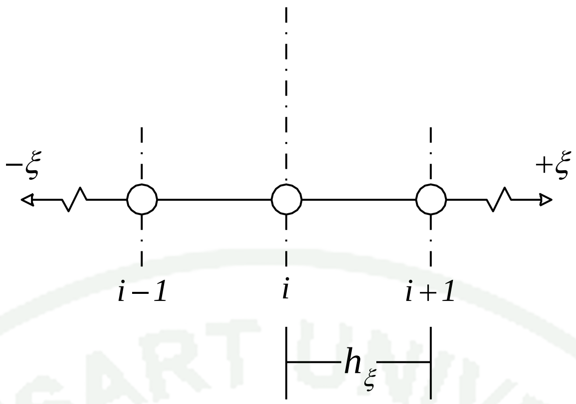

Appendix Figure A1 Discretization along the axial coordinate of the reactor.

2. Discretization at the initial condition

At initial condition: $$\left(\frac{dC^*}{d\tau}\right)_{i=inlet} = 0 \qquad \text{A-17}$$

The initial condition in Eq. (A-17) explains that there is no flux at t=0.

3. Discretization at the boundary condition

3.1 Inlet boundary condition

3.1.1 Discretization at the reactor inlet and the Delta function

Discretization at the reactor inlet and the Delta function is shown in Figure A2. The area of rectangular is unity. The definition of Delta function is described by

$$\int_0^1 F^*_{A,in} d\tau = \int_{-\infty}^{+\infty} \delta(\tau - 0^+) d\tau \equiv 1 \qquad \text{A-18}$$

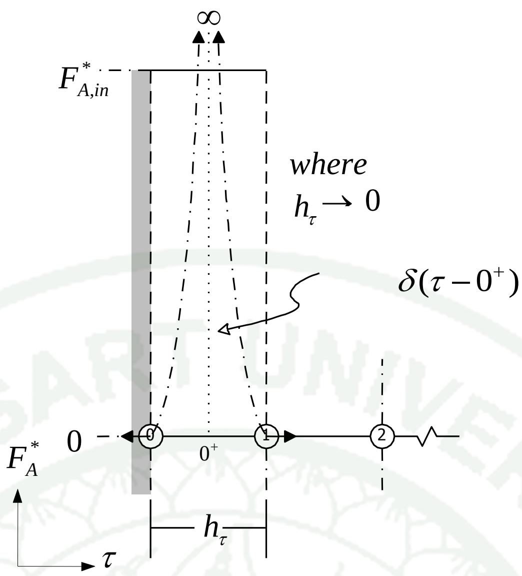

Appendix Figure A2 Discretization at the reactor inlet and the Delta function.

From Eq. A-18 and Figure A2, we obtain

$$F^*_{A,in}.h_\tau = 1 \tag{A-19}$$

From Eqs. A-12 and A-18, the relationship between $F^*_{A,in}$ and C^*_A is discretized as follows:

$$F^*_{A,in} = \frac{C^*_{A,1} - C^*_{A,0}}{h_\xi} \tag{A-20}$$

Substituting Eq. A-20 into Eq. A-19 ($h_\xi = h_\tau$)

$$C^*_{A,1} - C^*_{A,0} = \begin{cases} 1 & 0 \le \tau_i \le h_\tau \\ 0 & h_\tau < \tau_i \le 1 \end{cases} \tag{A-21}$$

Therefore, the equation describe the boundary at the reactor inlet is

$$\left(\frac{d(C^*_{A,1}-C^*_{A,0})}{d\tau}\right)_{i=inlet}=\begin{cases}1 & 0\le\tau_i\le h_\tau\\ 0 & h_\tau<\tau_i\le 1\end{cases} \quad \text{(A-22)}$$

3.1.2 Discretization at the reactor inlet and the triangular function

$$\int_0^1 F^*_{A,in}d\tau=\int_{-\infty}^{+\infty}X(\tau)d\tau\equiv 1 \quad \text{(A-23)}$$

The definition of inlet flow rate under the triangular function is described by Eq. (23). Discretization at the reactor inlet and the triangular function is shown in Figure A3. The area of triangular is unity.

$$\tau_{open}=\tau_{open1}+\tau_{open2}+\tau_{open3}+\tau_{open4}+.......$$

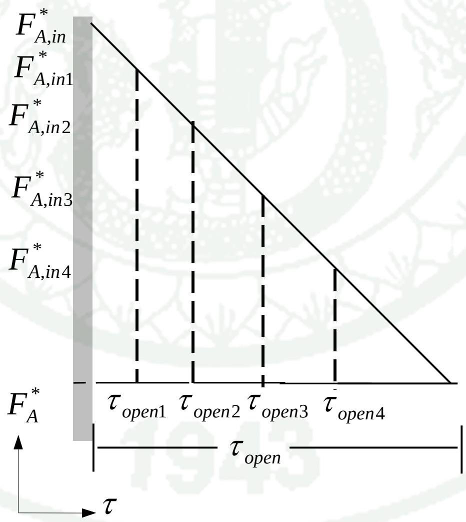

Appendix Figure A3 Discretization at the reactor inlet and the triangular function.

From Eq. A-23 and Figure A3, we obtain

$$F^*_{A,in1}\ \tau_{open1}+F^*_{A,in2}\tau_{open2}+F^*_{A,in3}\tau_{open3}+F^*_{A,in4}\tau_{open4}+.......=1 \quad \text{(A-24)}$$

$$A1+A2+A3+A4+.......=1$$

where $\tau_{open} = h_\tau$

From Eqs. A-13 and A-24, the relationship between $F^*_{A,in}$ and C^*_A is discretized as follows:

$$F^*_{A,in} = \frac{C^*_{A,1} - C^*_{A,0}}{h_\xi} \tag{A-25}$$

Substituting Eq. A-24 into Eq. A-25 ($h_\xi = h_\tau$)

$$C^*_{A,1} - C^*_{A,0} = \begin{cases} A1 & 0 \le \tau_{open1} \\ A2 & \tau_{open1} \le \tau_{open2} \\ A3 & \tau_{open2} \le \tau_{open3} \\ A4 & \tau_{open3} \le \tau_{open4} \\ ..... & \\ 0 & \tau_{openi} \le \tau \end{cases} \tag{A-26}$$

Therefore, the equation describe the boundary at the reactor inlet is

$$\left(\frac{d(C^*_{A,1} - C^*_{A,0})}{d\tau}\right)_{i=inlet} = \begin{cases} A1 & 0 \le \tau_{open1} \\ A2 & \tau_{open1} \le \tau_{open2} \\ A3 & \tau_{open2} \le \tau_{open3} \\ A4 & \tau_{open3} \le \tau_{open4} \\ ..... & \\ 0 & \tau_{openi} \le \tau \end{cases} \tag{A-27}$$

Discretization for three-zone reactor

The mass balance equation for diffusion in inert zone is described in the generalized dimensionless form as

$$\frac{\partial C^*}{\partial \tau} = r_{Di}\,\frac{\partial^2 C^*}{\partial \xi^2} \tag{A-28}$$

If the reaction is first order irreversible reaction, the mass balance equation can be described in the generalized dimensionless by

$$\frac{\partial C^*}{\partial \tau} = \frac{\partial^2 C^*}{\partial \xi^2} - \kappa C^* \tag{A-29}$$

Dimensionless boundary conditions;

$\xi = \xi_1\,;$ $$C^*\Big|_I = C^*\Big|_{II} \tag{A-30}$$

$$-r_{Di}\,\frac{\partial C^*}{\partial \xi}\bigg|_I = -\frac{\partial C^*}{\partial \xi}\bigg|_{II} \tag{A-31}$$

$\xi = \xi_2\,;$ $$C^*\Big|_{II} = C^*\Big|_{III} \tag{A-32}$$

$$-\frac{\partial C^*}{\partial \xi}\bigg|_{II} = -r_{Di}\,\frac{\partial C^*}{\partial \xi}\bigg|_{III} \tag{A-33}$$

The dimensionless exit flow rate can be calculated using

$$F^* = -r_{Di}\,\frac{\partial C^*}{\partial \xi}\bigg|_{\xi=1} \tag{A-34}$$

1. Discretization along the axial coordinate of the reactor

   Discretization along the axial coordinate of the inert bedsfor three zone reactor (Zone 1 and Zone 3) when $0 < \xi_i < \xi_1$ and $\xi_2 < \xi_i < 1$

For Knudsen diffusion : $$r_{\varepsilon i}\left(\frac{dC^*}{d\tau}\right) = r_{Di}\left(\frac{C^*_{i+1} - 2C^*_i + C^*_{I-1}}{h^2_\xi}\right) \quad \text{(A-35)}$$

For the catalyst bed (zone 2), which reaction takes place when $\xi_1 < \xi_i < \xi_2$

$$\left(\frac{dC^*}{d\tau}\right) = \frac{C^*_{i+1} - 2C_i + C_{i-1}}{h^2_\xi} - k^* C^*_i \quad \text{(A-36)}$$

2. Discretization of initial condition

At initial condition: $$\left(\frac{dC^*}{d\tau}\right)_{i=inlet} = 0 \quad \text{(A-37)}$$

The initial condition in Eq. (A-37) explains that there is no flux at t=0.

3. Discretization at the reactor boundaries

Boundary conditions at the boundaries between the three zones are described by A4(a) and A4(b) and discretized as follows

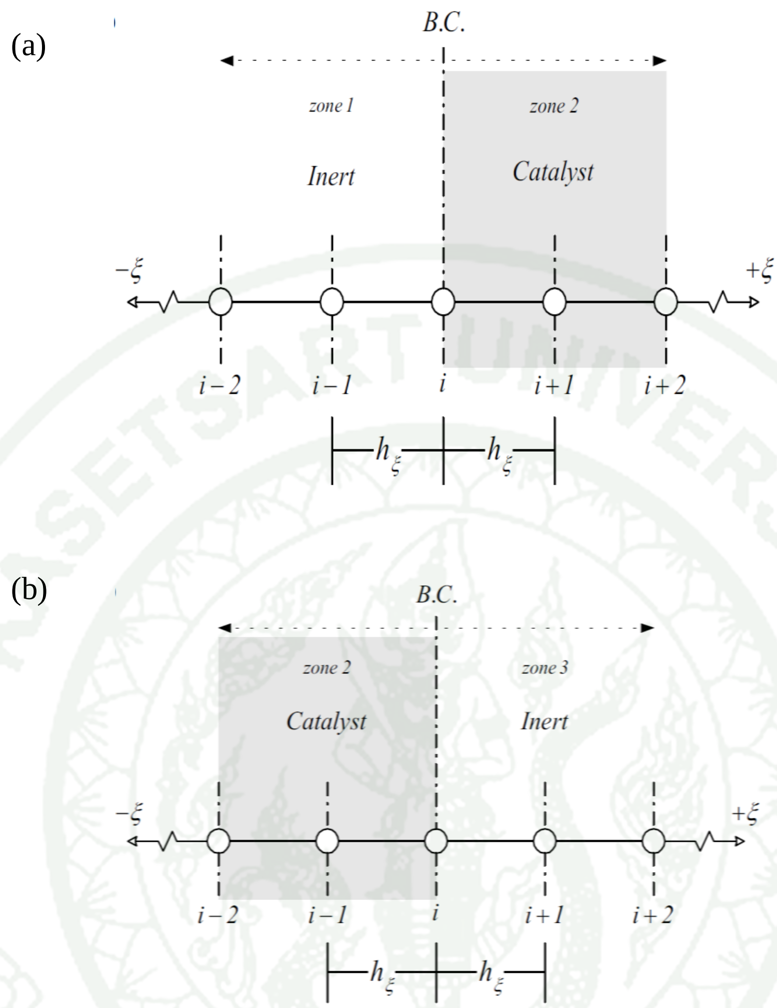

Appendix Figure A4 Discretization of the boundary conditions between the three zone (a) at the coordinate ξ_1 , (b) at the coordinate ξ_2

Boundary condition at ξ_1 : $$-r_{Di}\left.\frac{\partial C^*}{\partial \xi}\right|_{I} = -\left.\frac{\partial C^*}{\partial \xi}\right|_{II} \qquad \text{(A-38)}$$

$$-r_{Di}\left(\frac{3C_i^* - 4C_{i-1}^* + 2C_{i-2}^*}{2h_\xi}\right) = -\left(\frac{-C_{i+2}^* + 4C_{i+1}^* - 3C_i^*}{2h_\xi}\right) \qquad \text{(A-39)}$$

$$C_i^* = \frac{1}{3r_{Di}+3}\left(-C_{i+2}^* + 4C_{i+1}^* + 4r_{Di}C_{i-1}^* - r_{Di}C_{i-2}^*\right) \qquad \text{(A-40)}$$

Hence, the rate of change of dimensionless concentration with respect to time at ξ_1 is obtained

$$\left(\frac{dC^*}{d\tau}\right)_i = \frac{1}{3r_{Di}+3}\left[-\left(\frac{dC^*}{d\tau}\right)_{i+2} + 4\left(\frac{dC^*}{d\tau}\right)_{i+1} + 4r_{Di}\left(\frac{dC^*}{d\tau}\right)_{i-1} - r_{Di}\left(\frac{dC^*}{d\tau}\right)_{i-2}\right] \quad \text{(A-41)}$$

Boundary condition at ξ_2 :

$$-\left.\frac{\partial C^*}{\partial \xi}\right|_{II} = -r_{Di}\left.\frac{\partial C^*}{\partial \xi}\right|_{III} \quad \text{(A-42)}$$

In the same fashion as the boundary condition at ξ_1, the rate of change of dimensionless concentration with respect to time at ξ_2 can be described by

$$\left(\frac{dC^*}{d\tau}\right)_i = \frac{1}{3r_{Di}+3}\left[-\left(\frac{dC^*}{d\tau}\right)_{i+2} + 4\left(\frac{dC^*}{d\tau}\right)_{i+1} + 4r_{Di}\left(\frac{dC^*}{d\tau}\right)_{i-1} - r_{Di}\left(\frac{dC^*}{d\tau}\right)_{i-2}\right] \quad \text{(A-43)}$$

Discretization at the reactor exit

Flow rate at the reactor outlet for both one zone and three zone reactor is described by A5 and discretized as shown in Fig A5

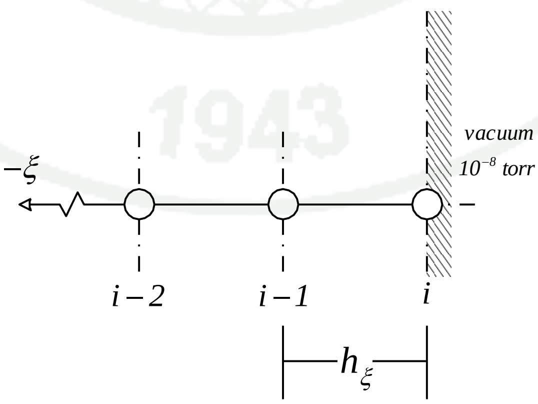

Appendix Figure A5 Discretization at the reactor exit.

At the reactor outlet of the one zone reactor, $C^*_{i=outlet} = 0$. The first order PDE describing the exit flow rate of the gas can be discretized using the backward finite approximation as follows:

$$F^* = -\frac{3C_i^* - 4C_{i-1}^* + C_{i-2}^*}{2h_\xi} = \frac{1}{2h_\xi}\left(4C_{i-1}^* - C_{i-2}^*\right) \qquad \text{(A-44)}$$

At the reactor outlet of the three zone reactor, $C^*_{i=outlet} = 0$. The exit flow rate is discretized as follows

$$F^* = -r_{Di}\frac{3C_i^* - 4C_{i-1}^* + C_{i-2}^*}{2h_\xi} = \frac{r_{Di}}{2h_\xi}\left(4C_{i-1}^* - C_{i-2}^*\right) \qquad \text{(A-45)}$$

Appendix B

Simulated Results for $D_{e,est}$ and ΔD_e Obtained from Different Procedures at Various τ_{open} and X for the One-Zone Reactor

Appendix Table B1 Simulated Results for $D_{e,est}$ and ΔD_e Obtained from Different Procedures at Various τ_{open} and X for One-Zone Reactor

τ_{open}	X	First procedure Exit flow rate curve fitting		Second procedure Exit flow rate curve fitting		Second procedure Unit-area normalized fitting	
		$D_{e,est}$	ΔD_e	$D_{e,est}$	ΔD_e	$D_{e,est}$	ΔD_e
0.004	0.01	0.9956±0.0001	-0.436	0.9956±0.0001	-0.437	0.9825±0.0001	-1.750
	0.25	0.9956±0.0001	-0.436	0.9950±0.0001	-0.503	0.9815±0.0001	-1.850
	0.50	0.9956±0.0001	-0.436	0.9940±0.0001	-0.601	0.9798±0.0001	-2.020
	0.75	0.9956±0.0001	-0.436	0.9923±0.0002	-0.770	0.9762±0.0002	-2.380
	0.99	0.9956±0.0001	-0.436	0.9840±0.0002	-1.597	0.9534±0.0002	-4.660
0.009	0.01	0.9892±0.0003	-1.081	0.9892±0.0003	-1.082	0.9610±0.0003	-3.900
	0.25	0.9892±0.0003	-1.081	0.9877±0.0003	-1.227	0.9590±0.0003	-4.100
	0.50	0.9892±0.0003	-1.081	0.9856±0.0003	-1.440	0.9554±0.0003	-4.460
	0.75	0.9892±0.0003	-1.081	0.9819±0.0003	-1.809	0.9477±0.0003	-5.890
	0.99	0.9892±0.0003	-1.081	0.9641±0.0004	-3.587	0.9019±0.0003	-9.810
0.015	0.01	0.9813±0.0005	-1.868	0.9813±0.0005	-1.871	0.9360±0.0004	-6.830
	0.25	0.9813±0.0005	-1.868	0.9789±0.0005	-2.107	0.9328±0.0004	-7.203
	0.50	0.9813±0.0005	-1.868	0.9754±0.0005	-2.457	0.9271±0.0005	-7.860
	0.75	0.9813±0.0005	-1.868	0.9694±0.0005	-3.060	0.9150±0.0005	-9.285
	0.99	0.9813±0.0005	-1.868	0.9407±0.0006	-5.928	0.8470±0.0004	-18.06
0.020	0.01	0.9747±0.0007	-2.531	0.9747±0.0007	-2.531	0.9161±0.0005	-8.390
	0.25	0.9747±0.0007	-2.531	0.9716±0.0007	-2.843	0.9119±0.0006	-8.810
	0.50	0.9747±0.0007	-2.531	0.9670±0.0007	-3.303	0.9046±0.0006	-9.540
	0.75	0.9747±0.0007	-2.531	0.9591±0.0007	-4.095	0.8892±0.0006	-11.10
	0.99	0.9747±0.0007	-2.531	0.9218±0.0007	-7.828	0.8069±0.0004	-19.30
0.026	0.01	0.9667±0.0009	-3.326	0.9668±0.0008	-3.322	0.8930±0.0007	-10.70
	0.25	0.9667±0.0009	-3.326	0.9628±0.0008	-3.722	0.8878±0.0007	-11.20
	0.50	0.9667±0.0009	-3.326	0.9569±0.0009	-4.311	0.8788±0.0007	-12.12
	0.75	0.9667±0.0009	-3.326	0.9468±0.0009	-5.322	0.8598±0.0007	-14.02
	0.99	0.9667±0.0009	-3.326	0.9000±0.0008	-10.00	0.7648±0.0003	-23.50

Appendix C

Simulated Results for κ_{est} and Δk Obtained from Different Procedures at Various τ_{open} and X for the One-Zone Reactor

Appendix Table C1 Simulated Results for κ_{est} and Δk Obtained from Different Procedures at Various τ_{open} and X for One-Zone Reactor

τ_{open}	X	First procedure Exit flow rate curve fitting		Second procedure Exit flow rate curve fitting		First procedure Unit-area normalized fitting		Second procedure Unit-area normalized fitting	
		κ_{est}	Δk	κ_{est}	Δk	κ_{est}	Δk	κ_{est}	Δk
0.004	0.01	0.0153±0.0004	-24.04	0.0153±0.0004	-24.04	0.0284±0.0005	40.99	0.0721±0.0005	257.3
	0.25	0.6227±0.0005	-1.571	0.6223±0.0005	-1.636	0.6378±0.0007	0.818	0.6903±0.0006	9.118
	0.50	1.7151±0.0007	-1.110	1.7123±0.0007	-1.273	1.7320±0.0011	-0.140	1.8042±0.0008	4.028
	0.75	4.2170±0.0011	-0.958	4.2028±0.0012	-1.290	4.2284±0.0022	-0.690	4.3632±0.0013	2.475
	0.99	27.835±0.0066	-0.844	27.509±0.0062	-2.004	27.362±0.0168	-2.529	28.765±0.0065	2.470
0.009	0.01	0.0097±0.0008	-51.71	0.0097±0.0008	-51.68	0.0381±0.0011	89.07	0.1322±0.0010	555.3
	0.25	0.6111±0.0010	-3.405	0.6102±0.0010	-3.543	0.6436±0.0015	1.740	0.7570±0.0012	19.67
	0.50	1.6925±0.0014	-2.414	1.6865±0.0015	-2.763	1.7283±0.0024	-0.349	1.8850±0.0016	8.685
	0.75	4.1690±0.0024	-2.084	4.1386±0.0025	-2.800	4.1915±0.0048	-1.556	4.4846±0.0027	5.328
	0.99	27.565±0.0142	-1.805	26.862±0.0126	-4.311	26.513±0.0350	-5.552	29.499±0.0121	5.085
0.015	0.01	0.0033±0.0013	-83.70	0.0033±0.0013	-83.65	0.0496±0.0018	145.7	0.2021±0.0016	-902.2
	0.25	0.5974±0.0016	-5.564	0.5960±0.0017	-5.784	0.6501±0.0025	2.770	0.8347±0.0019	31.94
	0.50	1.6657±0.0023	-3.958	1.6559±0.0024	-4.522	1.7229±0.0039	-0.663	1.9787±0.0026	14.09
	0.75	4.1123±0.0038	-3.418	4.0628±0.0040	-4.580	4.1446±0.0077	-2.659	4.6249±0.0042	8.623
	0.99	27.258±0.0229	-2.899	26.116±0.0192	-6.969	25.502±0.0542	-9.154	30.237±0.0159	7.713
0.020	0.01	0.0019±0.0017	-90.79	-0.0019±0.0017	-100.2	0.0589±0.0023	192.0	0.2582±0.0021	1180
	0.25	0.5863±0.0021	-7.317	0.5846±0.0022	-7.595	0.6552±0.0032	3.568	0.8969±0.0025	41.77
	0.50	1.6438±0.0030	-5.220	1.6312±0.0031	-5.950	1.7176±0.0051	-0.966	2.0537±0.0033	18.41
	0.75	4.0658±0.0050	-4.509	4.0014±0.0052	-6.022	4.1039±0.0101	-3.613	4.7362±0.0053	11.24
	0.99	27.017±0.0297	-3.757	25.525±0.0236	-9.072	24.682±0.0678	-12.08	30.717±0.0168	9.421
0.026	0.01	-0.0077±0.0021	-138.4	-0.0077±0.0021	-138.4	0.0696±0.0030	245.3	0.3229±0.0025	1501
	0.25	0.5734±0.0027	-9.359	0.5713±0.0027	-9.697	0.6606±0.0041	4.428	0.9684±0.0030	53.08
	0.50	1.6183±0.0037	-6.698	1.6023±0.0039	-7.613	1.7103±0.0065	-1.387	2.1396±0.0040	23.36
	0.75	4.0115±0.0063	-5.734	3.9299±0.0065	-7.699	4.0535±0.0127	-4.797	4.8627±0.0065	14.21
	0.99	26.748±0.0374	-4.717	24.855±0.0279	-11.46	23.731±0.0815	-15.46	31.125±0.0163	10.88

Appendix D

Simulated Results for $D_{e,est}^{inert}$ and ΔD_{e}^{inert} Obtained from Different Procedures at Various r_{Di}, τ_{open} and X for the Three-Zone Reactor with $L_{cat}/L_{reactor}$ = 1/3.

Appendix Table D1 Simulated Results for $D_{e,est}^{inert}$ and ΔD_e^{inert} Obtained from Different Procedures at Various r_{Di}, τ_{open} and X for Three-Zone Reactor with $L_{cat}/L_{reactor}$ = 1/3.

r_{Di}	τ_{open}	X	Procedure 1.1		Procedure 1.2		Procedure 2		Procedure 2	
			Exit flow rate curve fitting		Exit flow rate curve fitting		Exit flow rate curve fitting		Unit-area normalized fitting	
			$D_{e,est}^{inert}$	ΔD_e^{inert}	$D_{e,est}^{inert}$	ΔD_e^{inert}	$D_{e,est}^{inert}$	ΔD_e^{inert}	$D_{e,est}^{inert}$	ΔD_e^{inert}
1/1	0.004	0.01	0.9956±0.0005	-0.4353	1.0164±0.0047	1.6390	0.9899±1.7779	-1.0065	0.8680±0.6496	-13.199
		0.10	0.9956±0.0005	-0.4353	1.0164±0.0047	1.6390	1.0071±0.8736	0.7090	0.8468±0.4187	-15.325
		0.20	0.9956±0.0005	-0.4353	1.0164±0.0047	1.6390	1.0294±0.5147	2.9370	0.8271±0.3076	-17.291
		0.30	0.9956±0.0005	-0.4353	1.0164±0.0047	1.6390	1.0567±0.3556	5.6690	0.8066±0.2261	-19.337
		0.40	0.9956±0.0005	-0.4353	1.0164±0.0047	1.6390	1.0896±0.2361	8.9610	0.7848±0.1678	-21.516
		0.50	0.9956±0.0005	-0.4353	1.0164±0.0047	1.6390	1.1296±0.1379	12.961	0.7596±0.1242	-24.040
		0.60	0.9956±0.0005	-0.4353	1.0164±0.0047	1.6390	1.1383±0.0028	13.834	0.7270±0.0088	-27.303
		0.70	0.9956±0.0005	-0.4353	1.0164±0.0047	1.6390	1.0709±0.0074	7.0880	0.7571±0.0297	-24.286
		0.80	0.9956±0.0005	-0.4353	1.0164±0.0047	1.6390	1.0387±0.0043	3.8710	0.8416±0.0145	-15.844
		0.90	0.9956±0.0005	-0.4353	1.0164±0.0047	1.6390	1.0172±0.0028	1.7150	0.8898±0.0107	-11.023
		0.99	0.9956±0.0005	-0.4353	1.0164±0.0047	1.6390	0.9972±0.0019	-0.2806	0.9149±0.0111	-8.5135
	0.009	0.01	0.9892±0.0010	-1.0809	0.9822±3.3024	-1.7785	0.9830±3.3921	-1.7009	0.8418±0.0787	-15.819
		0.10	0.9892±0.0010	-1.0809	0.9822±3.3024	-1.7785	0.9996±1.5857	-0.0364	0.8226±0.5757	-17.742
		0.20	0.9892±0.0010	-1.0809	0.9822±3.3024	-1.7785	1.0215±0.9792	2.1520	0.8025±0.4195	-19.748
		0.30	0.9892±0.0010	-1.0809	0.9822±3.3024	-1.7785	1.0480±0.6786	4.7950	0.7823±0.3109	-21.775
		0.40	0.9892±0.0010	-1.0809	0.9822±3.3024	-1.7785	1.0809±0.4981	8.0910	0.7600±0.2289	-24.004
		0.50	0.9892±0.0010	-1.0809	0.9822±3.3024	-1.7785	1.1228±0.3573	12.279	0.7343±0.1649	-26.575
		0.60	0.9892±0.0010	-1.0809	0.9822±3.3024	-1.7785	1.1770±0.2272	17.704	0.7022±0.1115	-29.780
		0.70	0.9892±0.0010	-1.0809	0.9822±3.3024	-1.7785	1.2189±0.0638	21.893	0.6569±0.0690	-34.311
		0.80	0.9892±0.0010	-1.0809	0.9822±3.3024	-1.7785	1.1094±0.0105	10.944	0.7116±0.0157	-28.842
		0.90	0.9892±0.0010	-1.0809	0.9822±3.3024	-1.7785	1.0532±0.0052	5.3190	0.8130±0.0093	-18.698
		0.99	0.9892±0.0010	-1.0809	0.9822±3.3024	-1.7785	1.0099±0.0023	0.9850	0.8906±0.0922	-10.939

Appendix Table D1 (Continued)

r_{Di}	τ_{open}	X	Procedure 1.1 Exit flow rate curve fitting		Procedure 1.2 Exit flow rate curve fitting		Procedure 2 Exit flow rate curve fitting		Procedure 2 Unit-area normalized fitting	
			$D_{e,est}^{inert}$	ΔD_{e}^{inert}	$D_{e,est}^{inert}$	ΔD_{e}^{inert}	$D_{e,est}^{inert}$	ΔD_{e}^{inert}	$D_{e,est}^{inert}$	ΔD_{e}^{inert}
	0.015	0.01	0.9813±0.0017	-1.8683	0.9745±5.0812	-2.5530	0.9747±5.4801	-2.5347	0.8125±0.9924	-18.754
		0.10	0.9813±0.0017	-1.8683	0.9745±5.0812	-2.5530	0.9907±2.4462	-0.9288	0.7944±0.7259	-20.557
		0.20	0.9813±0.0017	-1.8683	0.9745±5.0812	-2.5530	1.0119±1.5139	1.1870	0.7748±0.5525	-22.517
		0.30	0.9813±0.0017	-1.8683	0.9745±5.0812	-2.5530	1.0377±1.0885	3.7670	0.7547±0.4061	-24.530
		0.40	0.9813±0.0017	-1.8683	0.9745±5.0812	-2.5530	1.0701±0.8366	7.0050	0.7321±0.3009	-26.788
		0.50	0.9813±0.0017	-1.8683	0.9745±5.0812	-2.5530	1.1114±0.6401	11.141	0.7056±0.2158	-29.440
		0.60	0.9813±0.0017	-1.8683	0.9745±5.0812	-2.5530	1.1667±0.4768	16.673	0.6717±0.1447	-32.834
		0.70	0.9813±0.0017	-1.8683	0.9745±5.0812	-2.5530	1.2418±0.2903	24.182	0.6244±0.0848	-37.558
		0.80	0.9813±0.0017	-1.8683	0.9745±5.0812	-2.5530	1.2596±0.0487	25.963	0.5603±0.0476	-43.971
		0.90	0.9813±0.0017	-1.8683	0.9745±5.0812	-2.5530	1.1067±0.0097	10.672	0.7504±0.0082	-24.962
		0.99	0.9813±0.0017	-1.8683	0.9745±5.0812	-2.5530	1.0253±0.0029	2.5260	0.8791±0.0075	-12.087
	0.020	0.01	0.9747±0.0022	-2.5310	1.0006±0.0104	0.0640	0.9678±7.0412	-3.2226	0.7895±1.0746	-21.050
		0.10	0.9747±0.0022	-2.5310	1.0006±0.0104	0.0640	0.9835±3.3290	-1.6500	0.7726±0.0806	-22.743
		0.20	0.9747±0.0022	-2.5310	1.0006±0.0104	0.0640	1.0042±2.0460	0.4210	0.7530±0.6135	-24.695
		0.30	0.9747±0.0022	-2.5310	1.0006±0.0104	0.0640	1.0293±1.4505	2.9330	0.7329±0.4651	-26.712
		0.40	0.9747±0.0022	-2.5310	1.0006±0.0104	0.0640	1.0607±1.1003	6.0710	0.7099±0.3448	-29.011
		0.50	0.9747±0.0022	-2.5310	1.0006±0.0104	0.0640	1.1013±0.8643	10.125	0.6827±0.2483	-31.727
		0.60	0.9747±0.0022	-2.5310	1.0006±0.0104	0.0640	1.1559±0.6756	15.593	0.6470±0.1650	-35.298
		0.70	0.9747±0.0022	-2.5310	1.0006±0.0104	0.0640	1.2329±0.4800	23.292	0.5977±0.0948	-40.230
		0.80	0.9747±0.0022	-2.5310	1.0006±0.0104	0.0640	1.3336±0.1982	33.364	0.5415±0.0410	-45.850
		0.90	0.9747±0.0022	-2.5310	1.0006±0.0104	0.0640	1.1639±0.0161	16.388	0.7173±0.0076	-28.268
		0.99	0.9747±0.0022	-2.5310	1.0006±0.0104	0.0640	1.0378±0.0035	3.7780	0.8775±0.0070	-12.254

Appendix Table D1 (Continued)

r_{Di}	τ_{open}	X	Procedure 1.1		Procedure 1.2		Procedure 2		Procedure 2	
			Exit flow rate curve fitting		Exit flow rate curve fitting		Exit flow rate curve fitting		Unit-area normalized fitting	
			$D_{e,est}^{inert}$	ΔD_{e}^{inert}	$D_{e,est}^{inert}$	ΔD_{e}^{inert}	$D_{e,est}^{inert}$	ΔD_{e}^{inert}	$D_{e,est}^{inert}$	ΔD_{e}^{inert}
	0.026	0.01	0.9667±0.0028	-3.3256	0.9606±7.7240	-3.9409	0.9595±9.7506	-4.0494	0.7642±1.1503	-23.581
		0.10	0.9667±0.0028	-3.3256	0.9606±7.7240	-3.9409	0.9749±4.3794	-2.5128	0.7475±0.8903	-25.247
		0.20	0.9667±0.0028	-3.3256	0.9606±7.7240	-3.9409	0.9946±2.5884	-0.5425	0.7283±0.6762	-27.174
		0.30	0.9667±0.0028	-3.3256	0.9606±7.7240	-3.9409	1.0190±1.8342	1.9010	0.7078±0.5106	-29.218
		0.40	0.9667±0.0028	-3.3256	0.9606±7.7240	-3.9409	1.0495±1.4061	4.9450	0.6845±0.3786	-31.546
		0.50	0.9667±0.0028	-3.3256	0.9606±7.7240	-3.9409	1.0890±1.1219	8.8980	0.6562±0.2717	-34.383
		0.60	0.9667±0.0028	-3.3256	0.9606±7.7240	-3.9409	1.1426±0.9088	14.257	0.6193±0.1802	-38.069
		0.70	0.9667±0.0028	-3.3256	0.9606±7.7240	-3.9409	1.2191±0.6942	21.905	0.5677±0.0998	-43.232
		0.80	0.9667±0.0028	-3.3256	0.9606±7.7240	-3.9409	1.3335±0.4039	33.354	0.5211±0.0308	-47.888
		0.90	0.9667±0.0028	-3.3256	0.9606±7.7240	-3.9409	1.2561±0.0314	25.607	0.6945±0.0070	-30.548
		0.99	0.9667±0.0028	-3.3256	0.9606±7.7240	-3.9409	1.0523±0.0043	5.2300	0.8816±0.0075	-11.838
1/3	0.015	0.50	0.9813±±0.0017	-1.8683	1.0199±0.0043	1.9910	0.8771±0.0325	-12.292	0.7497±0.4541	-25.028
1/2			0.9813±±0.0017	-1.8683	0.8246±0.6253	-17.541	0.9367±0.1246	-6.3299	0.7444±0.3598	-25.562
2/3			0.9813±±0.0017	-1.8683	0.8739±1.5208	-12.610	0.9943±0.2492	-0.5676	0.7349±0.2938	-26.513
4/3			0.9813±±0.0017	-1.8683	1.0001±0.0091	0.0090	1.2288±1.0850	22.882	0.6725±0.1681	-32.754
3/2			0.9813±±0.0017	-1.8683	1.0042±0.0106	0.4180	1.2874±1.2302	28.744	0.6564±0.1516	-34.357
2/1			0.9813±±0.0017	-1.8683	1.0121±0.0149	1.2070	1.4577±1.0947	45.765	0.6125±0.1252	-38.754
3/1			0.9813±±0.0017	-1.8683	1.0009±0.0194	0.0880	1.4522±0.0737	45.223	0.5471±0.1019	-45.293

Appendix E

Simulated Results for $D_{e,est}^{cat}$ and ΔD_{e}^{cat} Obtained from Different Procedures at Various r_{Di}, τ_{open} and X for the Three-Zone Reactor with $L_{cat}/L_{reactor}$ = 1/3.

Appendix Table E1 Simulated Results for $D_{e,est}^{cat}$ and ΔD_{e}^{cat} Obtained from Different Procedures at Various r_{Di}, τ_{open} and X for Three-Zone Reactor with $L_{cat}/L_{reactor}$ = 1/3.

r_{Di}	τ_{open}	X	Procedure 1.1		Procedure 1.2		Procedure 2		Procedure 2	
			Exit flow rate curve fitting		Exit flow rate curve fitting		Exit flow rate curve fitting		Unit-area normalized fitting	
			$D_{e,est}^{cat}$	ΔD_{e}^{cat}	$D_{e,est}^{cat}$	ΔD_{e}^{cat}	$D_{e,est}^{cat}$	ΔD_{e}^{cat}	$D_{e,est}^{cat}$	ΔD_{e}^{cat}
1/1	0.004	0.01	0.9687±0.0018	-3.1259	0.9024±0.0047	-9.7640	0.9796±3.4687	-2.0442	1.2289±2.1464	22.886
		0.10	0.9687±0.0018	-3.1259	0.9024±0.0047	-9.7640	0.9462±1.5690	-5.3847	1.2980±1.5466	29.796
		0.20	0.9687±0.0018	-3.1259	0.9024±0.0047	-9.7640	0.9060±0.8334	-9.3967	1.3658±1.2572	36.580
		0.30	0.9687±0.0018	-3.1259	0.9024±0.0047	-9.7640	0.8614±5.0996	-13.864	1.4409±1.0267	44.087
		0.40	0.9687±0.0018	-3.1259	0.9024±0.0047	-9.7640	0.8131±0.2946	-18.693	1.5246±0.8493	52.459
		0.50	0.9687±0.0018	-3.1259	0.9024±0.0047	-9.7640	0.7611±0.1469	-23.890	1.6255±0.7094	62.553
		0.60	0.9687±0.0018	-3.1259	0.9024±0.0047	-9.7640	0.7441±0.0029	-25.586	1.7621±0.5807	76.206
		0.70	0.9687±0.0018	-3.1259	0.9024±0.0047	-9.7640	0.8177±0.0108	-18.235	1.5077±0.1306	50.767
		0.80	0.9687±0.0018	-3.1259	0.9024±0.0047	-9.7640	0.8580±0.0077	-14.200	1.1657±0.0318	16.573
		0.90	0.9687±0.0018	-3.1259	0.9024±0.0047	-9.7640	0.8832±0.0061	-11.678	1.0121±0.0125	1.2100
		0.99	0.9687±0.0018	-3.1259	0.9024±0.0047	-9.7640	0.8837±0.0055	-11.629	0.8473±0.0085	-15.273
	0.009	0.01	0.9624±0.0033	-3.7561	0.9757±0.0649	-2.4251	0.9741±6.6341	-2.5851	1.2252±2.7058	22.521
		0.10	0.9624±0.0033	-3.7561	0.9757±0.0649	-2.4251	0.9409±2.8562	-5.9131	1.2873±2.1872	28.725
		0.20	0.9624±0.0033	-3.7561	0.9757±0.0649	-2.4251	0.9005±1.5892	-9.9544	1.3557±1.7690	35.571
		0.30	0.9624±0.0033	-3.7561	0.9757±0.0649	-2.4251	0.8561±0.9765	-14.388	1.4280±1.4526	42.800
		0.40	0.9624±0.0033	-3.7561	0.9757±0.0649	-2.4251	0.8068±0.6215	-19.325	1.5106±1.1933	51.061
		0.50	0.9624±0.0033	-3.7561	0.9757±0.0649	-2.4251	0.7519±0.3761	-24.814	1.6077±0.9677	60.770
		0.60	0.9624±0.0033	-3.7561	0.9757±0.0649	-2.4251	0.6911±0.0195	-30.894	1.7271±0.7455	72.710
		0.70	0.9624±0.0033	-3.7561	0.9757±0.0649	-2.4251	0.6450±0.0475	-35.496	1.8817±0.5311	88.172
		0.80	0.9624±0.0033	-3.7561	0.9757±0.0649	-2.4251	0.7299±0.0123	-27.010	1.3717±0.0505	37.166
		0.90	0.9624±0.0033	-3.7561	0.9757±0.0649	-2.4251	0.7799±0.0082	-22.015	0.9863±0.0096	-1.3725
		0.99	0.9624±0.0033	-3.7561	0.9757±0.0649	-2.4251	0.7813±0.0053	-21.871	0.7250±0.0080	-27.505

Appendix Table E1 (Continued)

r_{Di}	τ_{open}	X	Procedure 1.1 Exit flow rate curve fitting		Procedure 1.2 Exit flow rate curve fitting		Procedure 2 Exit flow rate curve fitting		Procedure 2 Unit-area normalized fitting	
			$D_{e,est}^{inert}$	ΔD_{e}^{inert}	$D_{e,est}^{inert}$	ΔD_{e}^{inert}	$D_{e,est}^{inert}$	ΔD_{e}^{inert}	$D_{e,est}^{inert}$	ΔD_{e}^{inert}
	0.015	0.01	0.9557±0.0052	-4.4297	0.9687±0.9992	-3.1281	0.9685±10.765	-3.1499	1.2175±3.5510	21.751
		0.10	0.9557±0.0052	-4.4297	0.9687±0.9992	-3.1281	0.9351±4.4266	-6.4937	1.2751±2.8553	27.512
		0.20	0.9557±0.0052	-4.4297	0.9687±0.9992	-3.1281	0.8949±2.4705	-10.508	1.3403±2.4041	34.031
		0.30	0.9557±0.0052	-4.4297	0.9687±0.9992	-3.1281	0.8501±1.5733	-14.987	1.4093±1.9534	40.933
		0.40	0.9557±0.0052	-4.4297	0.9687±0.9992	-3.1281	0.8002±1.0468	-19.979	1.4886±1.6122	48.863
		0.50	0.9557±0.0052	-4.4297	0.9687±0.9992	-3.1281	0.7446±0.6748	-25.543	1.5817±1.2970	58.169
		0.60	0.9557±0.0052	-4.4297	0.9687±0.9992	-3.1281	0.6817±0.0405	-31.834	1.6965±0.9902	69.653
		0.70	0.9557±0.0052	-4.4297	0.9687±0.9992	-3.1281	0.6115±0.1895	-38.850	1.8249±0.6486	82.491
		0.80	0.9557±0.0052	-4.4297	0.9687±0.9992	-3.1281	0.5804±0.0300	-41.960	1.7473±0.2726	74.728
		0.90	0.9557±0.0052	-4.4297	0.9687±0.9992	-3.1281	0.6737±0.0109	-32.634	0.9139±0.0061	-8.6118
		0.99	0.9557±0.0052	-4.4297	0.9687±0.9992	-3.1281	0.6843±0.0051	-31.569	0.6193±0.0064	-38.065
	0.020	0.01	0.9495±0.0067	-5.0518	0.8921±0.0104	-10.793	0.9633±13.870	-3.6671	1.2099±3.9661	20.987
		0.10	0.9495±0.0067	-5.0518	0.8921±0.0104	-10.793	0.9296±6.0375	-7.0384	1.2630±3.2503	26.304
		0.20	0.9495±0.0067	-5.0518	0.8921±0.0104	-10.793	0.8891±3.3438	-11.090	1.3267±2.7350	32.672
		0.30	0.9495±0.0067	-5.0518	0.8921±0.0104	-10.793	0.8445±2.1001	-15.552	1.3935±2.2887	39.351
		0.40	0.9495±0.0067	-5.0518	0.8921±0.0104	-10.793	0.7946±1.3805	-20.540	1.4711±1.8898	47.110
		0.50	0.9495±0.0067	-5.0518	0.8921±0.0104	-10.793	0.7390±0.9120	-26.097	1.5606±1.5253	56.059
		0.60	0.9495±0.0067	-5.0518	0.8921±0.0104	-10.793	0.6753±0.5738	-32.469	1.6731±1.1529	67.307
		0.70	0.9495±0.0067	-5.0518	0.8921±0.0104	-10.793	0.6034±0.3096	-39.665	1.7794±0.7190	77.941
		0.80	0.9495±0.0067	-5.0518	0.8921±0.0104	-10.793	0.5268±0.0926	-47.319	1.5642±0.1768	56.418
		0.90	0.9495±0.0067	-5.0518	0.8921±0.0104	-10.793	0.5963±0.0132	-40.375	0.8389±0.0041	-16.114
		0.99	0.9495±0.0067	-5.0518	0.8921±0.0104	-10.793	0.6201±0.0050	-37.992	0.5562±0.0056	-44.385

Appendix Table E1 (Continued)

r_{Di}	τ_{open}	X	Procedure 1.1 Exit flow rate curve fitting $D_{e,est}^{inert}$	Procedure 1.1 Exit flow rate curve fitting ΔD_e^{inert}	Procedure 1.2 Exit flow rate curve fitting $D_{e,est}^{inert}$	Procedure 1.2 Exit flow rate curve fitting ΔD_e^{inert}	Procedure 2 Exit flow rate curve fitting $D_{e,est}^{inert}$	Procedure 2 Exit flow rate curve fitting ΔD_e^{inert}	Procedure 2 Unit-area normalized fitting $D_{e,est}^{inert}$	Procedure 2 Unit-area normalized fitting ΔD_e^{inert}
	0.026	0.01	0.9418±0.0084	-5.8161	0.9534±0.1514	-4.6600	0.9553±19.210	-4.4652	1.1980±4.3791	19.804
		0.10	0.9418±0.0084	-5.8161	0.9534±0.1514	-4.6600	0.9221±7.9498	-7.7858	1.2493±3.6965	24.926
		0.20	0.9418±0.0084	-5.8161	0.9534±0.1514	-4.6600	0.8822±4.2426	-11.783	1.3104±3.0984	31.044
		0.30	0.9418±0.0084	-5.8161	0.9534±0.1514	-4.6600	0.8377±2.6679	-16.233	1.3757±2.5830	37.570
		0.40	0.9418±0.0084	-5.8161	0.9534±0.1514	-4.6600	0.7877±1.7696	-21.226	1.4503±2.1290	45.034
		0.50	0.9418±0.0084	-5.8161	0.9534±0.1514	-4.6600	0.7318±1.1862	-26.821	1.5386±1.7156	53.857
		0.60	0.9418±0.0084	-5.8161	0.9534±0.1514	-4.6600	0.6683±0.7728	-33.174	1.6404±1.2791	64.044
		0.70	0.9418±0.0084	-5.8161	0.9534±0.1514	-4.6600	0.5953±0.4456	-40.475	1.7170±0.7364	71.695
		0.80	0.9418±0.0084	-5.8161	0.9534±0.1514	-4.6600	0.5118±0.1790	-48.822	1.3641±0.0877	36.414
		0.90	0.9418±0.0084	-5.8161	0.9534±0.1514	-4.6600	0.5130±0.0172	-48.698	0.7515±0.0029	-24.846
		0.99	0.9418±0.0084	-5.8161	0.9534±0.1514	-4.6600	0.5575±0.0005	-44.249	0.5003±0.0052	-49.967
1/3	0.015	0.50	0.9557±0.0052	-1.8683	1.0199±0.0043	1.9910	0.8771±0.2073	-12.292	0.7497±10.662	-25.028
1/2			0.9557±0.0052	-1.8683	0.8246±9.8956	-17.541	0.9367±0.4180	-6.3299	0.7444±4.4632	-25.562
2/3			0.9557±0.0052	-1.8683	0.8739±6.6904	-12.610	0.9943±0.5215	-0.5676	0.7349±2.5484	-26.513
4/3			0.9557±0.0052	-1.8683	1.0001±0.0091	0.0090	1.2288±0.6955	22.882	0.6725±0.8402	-32.754
3/2			0.9557±0.0052	-1.8683	1.0042±0.0106	0.4180	1.2874±0.6422	28.744	0.6564±0.9097	-34.357
2/1			0.9557±0.0052	-1.8683	1.0121±0.0149	1.2070	1.4577±0.3492	45.765	0.6125±0.5069	-38.754
3/1			0.9557±0.0052	-1.8683	1.0009±0.0193	0.0880	1.4522±0.0223	45.223	0.5471±0.3303	-45.293

Appendix F

Simulated Results for κ_{est} and Δk Obtained from Different Procedures using the Exit Flow Rate Curve Fitting at Various r_{Di}, τ_{open} and X for the Three-Zone Reactor with $L_{cat}/L_{reactor}$ = 1/3.

Appendix Table F1 Simulated Results for κ_{est} and Δk Obtained from Different Procedures using the Exit Flow Rate Curve Fitting at Various r_{Di}, τ_{open} and X for the Three-Zone Reactor with $L_{cat}/L_{reactor}$ = 1/3.

r_{Di}	τ_{open}	X	κ_{real}	Procedure 1.1		Procedure 1.2		Procedure 2	
				κ_{est}	Δk	κ_{est}	Δk	κ_{est}	Δk
1/1	0.004	0.01	0.0606	0.0411±0.0048	-32.166	0.0415±0.0082	-31.445	0.0411±0.0048	-32.168
		0.10	0.6599	0.6380±0.0052	-3.3176	0.6389±0.0085	-3.1814	0.6382±0.0053	-3.2925
		0.20	1.4666	1.4414±0.0058	-1.7217	1.4429±0.0089	-1.6167	1.4424±0.0058	-1.6501
		0.30	2.4760	2.4463±0.0065	-1.1983	2.4489±0.0092	-1.0957	2.4498±0.0063	-1.0586
		0.40	3.7760	3.7412±0.0075	-0.9219	3.7453±0.0095	-0.8120	3.7502±0.0067	-0.6825
		0.50	5.5167	5.4756±0.0089	-0.7446	5.4824±0.0098	-0.6217	5.4971±0.0069	-0.3553
		0.60	7.9770	7.9269±0.0110	-0.6287	7.9382±0.0099	-0.4860	7.9730±0.0075	-0.0498
		0.70	11.740	11.678±0.0144	-0.5230	11.698±0.0101	-0.3535	11.739±0.0093	-0.0043
		0.80	18.311	18.234±0.0208	-0.4216	18.272±0.0118	-0.2141	18.309±0.0128	-0.0109
		0.90	33.458	33.361±0.0360	-0.2908	33.447±0.0230	-0.0323	33.450±0.0202	-0.0245
		0.99	126.03	125.96±0.1266	-0.0563	126.33±0.1254	0.2372	125.97±0.0543	-0.0508
	0.009	0.01	0.0606	0.0244±0.0088	-59.732	0.0244±0.0088	-59.660	0.0244±0.0089	-59.779
		0.10	0.6599	0.6190±0.0096	-6.1987	0.6188±0.0096	-6.2275	0.6192±0.0098	-6.1637
		0.20	1.4666	1.4191±0.0107	-3.2401	1.4187±0.0107	-3.2688	1.4203±0.0109	-3.1556
		0.30	2.4760	2.4199±0.0121	-2.2662	2.4191±0.0122	-2.2981	2.4237±0.0121	-2.1139
		0.40	3.7760	3.7093±0.0140	-1.7669	3.7079±0.0141	-1.8038	3.7187±0.0133	-1.5167
		0.50	5.5167	5.4363±0.0166	-1.4579	5.4339±0.0167	-1.5007	5.4582±0.0143	-1.0604
		0.60	7.9770	7.8771±0.0204	-1.2530	7.8730±0.0204	-1.3036	7.9270±0.0151	-0.6273
		0.70	11.740	11.613±0.0264	-1.0792	11.606±0.0264	-1.1406	11.727±0.0160	-0.1090
		0.80	18.311	18.144±0.0375	-0.9142	18.130±0.0371	-0.9896	18.317±0.0205	0.0317
		0.90	33.458	33.225±0.0643	-0.6976	33.193±0.0627	-0.7917	33.466±0.0305	0.0248
		0.99	126.03	125.72±0.2198	-0.2515	125.58±0.2088	-0.3586	126.01±0.0626	-0.0182

Appendix Table F1 (Continued)

r_{Di}	τ_{open}	X	κ_{real}	Procedure 1.1		Procedure 1.2		Procedure 2	
				κ_{est}	Δk	κ_{est}	Δk	κ_{est}	Δk
	0.015	0.01	0.0606	0.0115±0.0137	-74.791	0.0161±0.0137	-64.607	0.0161±0.0139	-64.483
		0.10	0.6599	0.4584±0.0150	-7.6223	0.4617±0.0150	-6.9541	0.4620±0.0153	-6.8881
		0.20	1.4666	1.0609±0.0168	-4.0362	1.0617±0.0168	-3.9602	1.0632±0.0173	-3.8272
		0.30	2.4760	1.8182±0.0191	-2.8750	1.8149±0.0191	-3.0524	1.8191±0.0193	-2.8259
		0.40	3.7760	2.8006±0.0220	-2.2805	2.7902±0.0221	-2.6441	2.8007±0.0215	-2.2791
		0.50	5.5167	4.1257±0.0260	-1.9635	4.1029±0.0261	-2.5058	4.1270±0.0239	-1.9321
		0.60	7.9770	6.0217±0.0319	-1.6873	5.9762±0.0320	-2.4292	6.0311±0.0262	-1.5326
		0.70	11.740	8.9639±0.0412	-1.4631	8.8742±0.0412	-2.4488	9.0033±0.0281	-1.0302
		0.80	18.311	14.205±0.0583	-1.2884	14.018±0.0579	-2.5851	14.348±0.0314	-0.2933
		0.90	33.458	26.661±0.0991	-1.0676	26.206±0.0976	-2.7585	26.957±0.0444	0.0312
		0.99	126.03	108.08±0.3342	-0.4541	106.03±0.3233	-2.3358	108.58±0.0736	0.0120
	0.020	0.01	0.0606	-0.0204±0.0178	-133.63	-0.0198±0.0182	-132.71	-0.0204±0.0179	-133.72
		0.10	0.6599	0.5700±0.0194	-13.626	0.5710±0.0196	-13.468	0.5704±0.0199	-13.564
		0.20	1.4666	1.3617±0.0217	-7.1519	1.3635±0.0216	-7.0299	1.3634±0.0223	-7.0340
		0.30	2.4760	2.3524±0.0247	-4.9919	2.3554±0.0241	-4.8700	2.3571±0.0250	-4.8037
		0.40	3.7760	3.6314±0.0284	-3.8302	3.6362±0.0274	-3.7026	3.6421±0.0281	-3.5474
		0.50	5.5167	5.3382±0.0336	-3.2365	5.3461±0.0319	-3.0921	5.3615±0.0371	-2.8127
		0.60	7.9770	7.7618±0.0411	-2.6974	7.7752±0.0387	-2.5298	7.8126±0.0353	-2.0613
		0.70	11.740	11.455±0.0531	-2.4294	11.478±0.0498	-2.2283	11.569±0.0390	-1.4523
		0.80	18.311	17.934±0.0747	-2.0583	17.979±0.0509	-1.8109	18.218±0.0424	-0.5073
		0.90	33.458	32.917±0.1267	-1.6161	33.022±0.1244	-1.3022	33.463±0.0558	0.0149
		0.99	126.03	125.28±0.4263	-0.5943	125.77±0.4528	-0.2095	126.04±0.0835	0.0048

Appendix Table F1 (Continued)

r_{Di}	τ_{open}	X	κ_{real}	Procedure 1.1		Procedure 1.2		Procedure 2	
				κ_{est}	Δk	κ_{est}	Δk	κ_{est}	Δk
	0.026	0.01	0.0606	-0.0342±0.0224	-156.45	-0.0341±0.0223	-156.39	-0.0342±0.0224	-156.53
		0.10	0.6599	0.5501±0.0245	-16.634	0.5499±0.0245	-16.669	0.5507±0.0248	-16.553
		0.20	1.4666	1.3393±0.0274	-8.6799	1.3389±0.0274	-8.7099	1.3414±0.0281	-8.5395
		0.30	2.4760	2.3239±0.0311	-6.1414	2.3232±0.0311	-6.1712	2.3291±0.0317	-5.9313
		0.40	3.7760	3.5984±0.0358	-4.7023	3.5972±0.0359	-4.7352	3.6100±0.0357	-4.3975
		0.50	5.5167	5.3023±0.0423	-3.8867	5.3002±0.0424	-3.9239	5.3266±0.0405	-3.4455
		0.60	7.9770	7.7071±0.0518	-3.3841	7.7036±0.0518	-3.4276	7.7586±0.0459	-2.7384
		0.70	11.740	11.394±0.0667	-2.9481	11.387±0.0667	-3.0009	11.507±0.0516	-1.9796
		0.80	18.311	17.839±0.0938	-2.5755	17.828±0.0934	-2.6400	18.117±0.0570	-1.0584
		0.90	33.458	32.804±0.1587	-1.9538	32.777±0.1573	-2.0360	33.486±0.0686	0.0840
		0.99	126.03	125.19±0.5324	-0.6720	125.06±0.5219	-0.7728	126.09±0.0949	0.0452
1/3	0.015	0.50	2.4635	2.4825±0.0051	0.7721	2.4767±0.0061	0.5350	2.4882±0.0367	1.0030
1/2			3.4034	3.3498±0.0109	-1.5746	3.3282±0.0150	-2.2101	3.3501±0.0107	-1.5676
2/3			4.2083	4.1257±0.0162	-1.9635	4.1029±0.0182	-2.5058	4.1270±0.0163	-1.9321
4/3			6.5430	6.3551±0.0347	-2.8715	6.3653±0.0341	-2.7153	6.4190±0.0279	-1.8952
3/2			6.9800	6.7760±0.0388	-2.9225	6.7910±0.0376	-2.7082	6.8658±0.0291	-1.6358
2/1			8.0610	7.8046±0.0497	-3.1805	7.8339±0.0470	-2.8169	7.9848±0.0322	-0.9448
3/1			9.5600	9.2323±0.0675	-3.4280	9.2614±0.0632	-3.1238	9.5775±0.0421	0.1831

Appendix G

Simulated Results for κ_{est} and Δk Obtained from Different Procedures using the Unit-Area Normalized Response Fitting at Various r_{Di} , τ_{open} and X for the Three-Zone Reactor with $L_{cat}/L_{reactor}$ = 1/3.

Appendix Table G1 Simulated Results for κ_{est} and Δk Obtained from Different Procedures using the Unit-Area Normalized Response Fitting at Various r_{Di}, τ_{open} and X for the Three-Zone Reactor with $L_{cat}/L_{reactor}$ = 1/3.

r_{Di}	τ_{open}	X	κ_{real}	Procedure 1.1		Procedure 1.2		Procedure 2	
				κ_{est}	Δk	κ_{est}	Δk	κ_{est}	Δk
1/1	0.004	0.01	0.0606	0.0926±0.0064	52.889	0.0929±0.0064	53.499	0.3473±0.9998	473.61
		0.10	0.6599	0.6908±0.0073	4.6848	0.6921±0.0073	4.8754	1.0510±1.0114	59.264
		0.20	1.4666	1.4948±0.0086	1.9255	1.4977±0.0086	2.1206	2.0260±1.1388	38.140
		0.30	2.4760	2.4990±0.0102	0.9269	2.5039±0.0103	1.1260	3.3086±1.2837	33.625
		0.40	3.7760	3.7898±0.0125	0.3655	3.7981±0.0126	0.5845	5.0746±1.4953	34.392
		0.50	5.5167	5.5137±0.0158	-0.0547	5.5273±0.0161	0.1920	7.6894±1.8440	39.384
		0.60	7.9770	7.9400±0.0209	-0.4642	7.9627±0.0213	-0.1793	12.061±2.4423	51.191
		0.70	11.740	11.631±0.0294	-0.9268	11.671±0.0302	-0.5860	17.240±1.1615	46.856
		0.80	18.311	18.020±0.0459	-1.5870	18.099±0.0478	-1.1594	23.885±0.6806	30.441
		0.90	33.458	32.515±0.0895	-2.8197	32.712±0.0951	-2.2300	42.574±1.0827	27.245
		0.99	126.03	116.58±0.4371	-7.5020	118.05±0.4865	-6.3348	180.67±10.187	43.353
	0.009	0.01	0.0606	0.1227±0.0119	102.69	0.1231±0.0119	103.35	0.5684±1.4559	838.74
		0.10	0.6599	0.7218±0.0136	9.3848	0.7233±0.0136	9.6005	1.3064±1.6086	97.966
		0.20	1.4666	1.5265±0.0159	4.0850	1.5295±0.0160	4.2854	2.3394±1.7888	59.511
		0.30	2.4760	2.5306±0.0191	2.2036	2.5357±0.0192	2.4116	3.7037±2.0230	49.584
		0.40	3.7760	3.8199±0.0235	1.1613	3.8284±0.0237	1.3867	5.6033±2.3487	48.392
		0.50	5.5167	5.5390±0.0298	0.4037	5.5528±0.0301	0.6547	8.4514±2.8455	53.196
		0.60	7.9770	7.9532±0.0396	-0.2984	7.9762±0.0401	-0.0105	13.273±3.6515	66.395
		0.70	11.740	11.614±0.0561	-1.0741	11.654±0.0571	-0.7334	23.593±5.5343	100.97
		0.80	18.311	17.915±0.0884	-2.1610	17.993±0.0907	-1.7383	34.631±1.8037	89.125
		0.90	33.458	32.056±0.1742	-4.1909	32.248±0.1811	-3.6171	54.732±1.6045	63.585
		0.99	126.03	111.08±0.8166	-11.863	112.43±0.9786	-10.791	212.82±10.785	68.857

Appendix Table G1 (Continued)

r_{Di}	τ_{open}	X	κ_{real}	Procedure 1.1		Procedure 1.2		Procedure 2	
				κ_{est}	Δk	κ_{est}	Δk	κ_{est}	Δk
	0.015	0.01	0.0606	0.1589±0.0187	162.38	0.1597±0.0187	163.67	0.8438±2.2324	1293.6
		0.10	0.6599	0.7589±0.0213	15.008	0.7607±0.0213	15.271	1.6273±2.4048	146.60
		0.20	1.4666	1.5640±0.0251	6.6439	1.5674±0.0251	6.8758	2.7315±2.7636	86.248
		0.30	2.4760	2.5676±0.0301	3.6991	2.5734±0.0302	3.9326	4.2007±3.0923	69.658
		0.40	3.7760	3.8543±0.0370	2.0747	3.8637±0.0372	2.3220	6.2708±3.6317	66.071
		0.50	5.5167	5.5667±0.0470	0.9058	5.5817±0.0474	1.1788	9.4321±4.4361	70.973
		0.60	7.9770	7.9647±0.0624	-0.1538	7.9894±0.0631	0.1551	14.964±5.8426	87.594
		0.70	11.740	11.586±0.0884	-1.3109	11.628±0.0897	-0.9498	27.444±8.9347	133.77
		0.80	18.311	17.776±0.1395	-2.9207	17.857±0.1424	-2.4783	74.013±24.221	304.20
		0.90	33.458	31.489±0.2737	-5.8850	31.686±0.2821	-5.2971	71.352±2.3510	113.26
		0.99	126.03	104.89±1.2250	-16.778	106.19±1.2975	-15.748	235.02±9.9123	86.474
	0.020	0.01	0.0606	0.1886±0.0243	211.52	0.1895±0.0243	212.89	1.0797±2.8071	1683.2
		0.10	0.6599	0.7892±0.0277	19.595	0.7912±0.0278	19.897	1.9018±3.0462	188.20
		0.20	1.4666	1.5945±0.0326	8.7229	1.5981±0.0327	8.9690	3.0691±3.4840	109.27
		0.30	2.4760	2.5973±0.0392	4.8986	2.6033±0.0393	5.1418	4.6325±4.0221	87.096
		0.40	3.7760	3.8815±0.0481	2.7945	3.8911±0.0483	3.0490	6.8592±4.7574	81.652
		0.50	5.5167	5.5874±0.0611	1.2807	5.6026±0.0615	1.5565	10.312±5.9221	86.929
		0.60	7.9770	7.9712±0.0811	-0.0733	7.9959±0.0818	0.2364	16.548±7.9741	107.45
		0.70	11.740	11.556±0.1148	-1.5614	11.599±0.1163	-1.2028	31.371±12.715	167.22
		0.80	18.311	17.654±0.1804	-3.5891	17.733±0.1835	-3.1555	86.213±26.651	370.83
		0.90	33.458	31.011±0.3513	-7.3133	31.200±0.3605	-6.7479	84.715±2.9322	153.20
		0.99	126.03	100.15±1.5063	-20.541	101.33±1.5810	-19.599	242.81±9.4127	92.657

Appendix Table G1 (Continued)

r_{Di}	τ_{open}	X	κ_{real}	Procedure 1.1		Procedure 1.2		Procedure 2	
				κ_{est}	Δk	κ_{est}	Δk	κ_{est}	Δk
	0.026	0.01	0.0606	0.2238±0.0308	269.62	0.2250±0.0309	271.56	1.3667±3.5340	2157.1
		0.10	0.6599	0.8248±0.0353	24.995	0.8270±0.0353	25.318	2.2405±3.9177	239.53
		0.20	1.4666	1.6301±0.0415	11.148	1.6337±0.0416	11.395	3.4869±4.4501	137.75
		0.30	2.4760	2.6315±0.0498	6.2791	2.6375±0.0499	6.5222	5.1732±5.1333	108.94
		0.40	3.7760	3.9122±0.0612	3.6067	3.9216±0.0614	3.8565	7.6018±6.1185	101.32
		0.50	5.5167	5.6098±0.0776	1.6878	5.6245±0.0780	1.9548	11.458±7.7507	107.69
		0.60	7.9770	7.9746±0.1028	-0.0306	7.9980±0.1036	0.2638	18.645±10.782	133.73
		0.70	11.740	11.518±0.1451	-1.8902	11.557±0.1466	-1.5529	36.962±17.972	214.84
		0.80	18.311	17.500±0.2270	-4.4280	17.574±0.2302	-4.0260	103.10±26.635	463.07
		0.90	33.458	30.450±0.4364	-8.9910	30.622±0.4456	-8.4775	97.401±3.4016	191.11
		0.99	126.03	94.923±1.7783	-24.684	95.940±1.8500	-23.877	242.55±9.5445	92.453
1/3	0.015	0.50	2.4635	2.4769±0.0092	0.5435	2.5879±0.0043	5.0505	2.9445±1.9796	19.525
1/2			3.4034	3.4220±0.0184	0.5456	3.7143±0.0169	9.1335	4.5627±2.6842	34.063
2/3			4.2083	4.2353±0.0281	0.6406	4.4531±0.0295	5.8173	6.1701±3.2845	46.616
4/3			6.5430	6.6204±0.0644	1.1826	6.4165±0.0567	-1.9337	12.823±5.4224	95.980
3/2			6.9800	7.0725±0.0724	1.3251	6.7620±0.0591	-3.1232	14.562±5.8791	108.63
2/1			8.0610	8.1970±0.0947	1.6865	7.5926±0.0621	-5.8104	19.894±7.5763	146.79
3/1			9.5600	9.7684±0.1058	2.1794	8.6946±0.0648	-9.0520	30.266±11.011	216.58

Appendix H

Simulated Results for $D_{e,est}^{inert}$ and ΔD_{e}^{inert} Obtained from Different Procedures at Various r_{Di}, τ_{open} and X for the Three-Zone Reactor with $L_{cat}/L_{reactor} = 1/30$.

Appendix Table H1 Simulated Results for $D_{e,est}^{inert}$ and ΔD_{e}^{inert} Obtained from Different Procedures at Various r_{Di}, τ_{open} and X for Three-Zone Reactor with $L_{cat}/L_{reactor}$ = 1/30.

r_{Di}	τ_{open}	X	Procedure 1.1		Procedure 1.2		Procedure 2		Procedure 2	
			Exit flow rate curve fitting		Exit flow rate curve fitting		Exit flow rate curve fitting		Unit-area normalized fitting	
			$D_{e,est}^{inert}$	ΔD_{e}^{inert}	$D_{e,est}^{inert}$	ΔD_{e}^{inert}	$D_{e,est}^{inert}$	ΔD_{e}^{inert}	$D_{e,est}^{inert}$	ΔD_{e}^{inert}
1/1	0.004	0.01	0.9956±0.0005	-0.4353	0.9887±0.5605	-1.1312	0.9894±0.2854	-1.0616	0.9739±0.2539	-2.6142
		0.10	0.9956±0.0005	-0.4353	0.9887±0.5605	-1.1312	0.9982±0.0676	-0.1839	0.9734±0.2468	-2.6564
		0.20	0.9956±0.0005	-0.4353	0.9887±0.5605	-1.1312	1.0091±0.0338	0.9110	0.9729±0.6890	-2.7115
		0.30	0.9956±0.0005	-0.4353	0.9887±0.5605	-1.1312	1.0209±0.0199	2.0900	0.9722±0.3589	-2.7830
		0.40	0.9956±0.0005	-0.4353	0.9887±0.5605	-1.1312	1.0323±0.0118	3.2340	0.9715±0.4348	-2.8474
		0.50	0.9956±0.0005	-0.4353	0.9887±0.5605	-1.1312	1.0391±0.0062	3.9110	0.9704±0.4852	-2.9613
		0.60	0.9956±0.0005	-0.4353	0.9887±0.5605	-1.1312	1.0324±0.0027	3.2410	0.9683±0.7663	-3.1735
		0.70	0.9956±0.0005	-0.4353	0.9887±0.5605	-1.1312	1.0191±0.0013	1.9050	0.9654±0.7502	-3.4648
		0.80	0.9956±0.0005	-0.4353	0.9887±0.5605	-1.1312	1.0081±0.0007	0.8090	0.9596±0.7756	-4.0380
		0.90	0.9956±0.0005	-0.4353	0.9887±0.5605	-1.1312	0.9993±0.0004	-0.0750	0.9408±0.6043	-5.9168
		0.99	0.9956±0.0005	-0.4353	0.9887±0.5605	-1.1312	0.9915±0.0001	-0.8513	0.9318±0.0001	-6.8230
	0.009	0.01	0.9892±0.0010	-1.0809	0.9820±1.2278	-1.7953	0.9823±0.6857	-1.7699	0.9521±0.7479	-4.7854
		0.10	0.9892±0.0010	-1.0809	0.9820±1.2278	-1.7953	0.9910±0.1522	-0.9003	0.9517±0.7818	-4.8326
		0.20	0.9892±0.0010	-1.0809	0.9820±1.2278	-1.7953	1.0018±0.0753	0.1770	0.9504±1.2548	-4.9639
		0.30	0.9892±0.0010	-1.0809	0.9820±1.2278	-1.7953	1.0140±0.0477	1.4000	0.9492±0.9277	-5.0813
		0.40	0.9892±0.0010	-1.0809	0.9820±1.2278	-1.7953	1.0275±0.0314	2.7480	0.9472±1.2071	-5.2837
		0.50	0.9892±0.0010	-1.0809	0.9820±1.2278	-1.7953	1.0419±0.0206	4.1910	0.9447±1.2771	-5.5279
		0.60	0.9892±0.0010	-1.0809	0.9820±1.2278	-1.7953	1.0539±0.0122	5.3860	0.9409±1.5500	-5.9093
		0.70	0.9892±0.0010	-1.0809	0.9820±1.2278	-1.7953	1.0527±0.0057	5.2740	0.9346±1.7058	-6.5354
		0.80	0.9892±0.0010	-1.0809	0.9820±1.2278	-1.7953	1.0333±0.0024	3.3250	0.9221±1.3748	-7.7945
		0.90	0.9892±0.0010	-1.0809	0.9820±1.2278	-1.7953	1.0121±0.0010	1.2050	0.8672±0.4256	-13.276
		0.99	0.9892±0.0010	-1.0809	0.9820±1.2278	-1.7953	0.9932±0.0002	-0.6778	0.9419±0.0014	-5.8072

Appendix Table H1 (Continued)

r_{Di}	τ_{open}	X	Procedure 1.1 Exit flow rate curve fitting		Procedure 1.2 Exit flow rate curve fitting		Procedure 2 Exit flow rate curve fitting		Procedure 2 Unit-area normalized fitting	
			$D_{e,est}^{inert}$	ΔD_{e}^{inert}	$D_{e,est}^{inert}$	ΔD_{e}^{inert}	$D_{e,est}^{inert}$	ΔD_{e}^{inert}	$D_{e,est}^{inert}$	ΔD_{e}^{inert}
	0.015	0.01	0.9813±0.0017	-1.8683	0.9749±1.8109	-2.5106	0.9746±1.3457	-2.5428	0.9276±1.2481	-7.2367
		0.10	0.9813±0.0017	-1.8683	0.9749±1.8109	-2.5106	0.9827±0.2629	-1.7274	0.9263±1.6749	-7.3715
		0.20	0.9813±0.0017	-1.8683	0.9749±1.8109	-2.5106	0.9932±0.1302	-0.6780	0.9245±1.2506	-7.5465
		0.30	0.9813±0.0017	-1.8683	0.9749±1.8109	-2.5106	1.0050±0.0814	0.5030	0.9223±1.5123	-7.7681
		0.40	0.9813±0.0017	-1.8683	0.9749±1.8109	-2.5106	1.0187±0.0552	1.8660	0.9196±1.4386	-8.0427
		0.50	0.9813±0.0017	-1.8683	0.9749±1.8109	-2.5106	1.0342±0.0384	3.4220	0.9152±1.5480	-8.4752
		0.60	0.9813±0.0017	-1.8683	0.9749±1.8109	-2.5106	1.0510±0.0258	5.0970	0.9091±1.1317	-9.0864
		0.70	0.9813±0.0017	-1.8683	0.9749±1.8109	-2.5106	1.0650±0.0151	6.5030	0.8987±2.1651	-10.134
		0.80	0.9813±0.0017	-1.8683	0.9749±1.8109	-2.5106	1.0605±0.0066	6.0490	0.8763±1.0006	-12.374
		0.90	0.9813±0.0017	-1.8683	0.9749±1.8109	-2.5106	1.0292±0.0022	2.9200	0.7703±0.0003	-22.971
		0.99	0.9813±0.0017	-1.8683	0.9749±1.8109	-2.5106	0.9955±0.0003	-0.4498	0.9576±0.0009	-4.2406
	0.020	0.01	0.9747±0.0022	-2.5310	0.9684±2.2356	-3.1592	0.9684±1.5345	-3.1579	0.9076±1.2409	-9.2434
		0.10	0.9747±0.0022	-2.5310	0.9684±2.2356	-3.1592	0.9761±0.3509	-2.3857	0.9059±2.3517	-9.4144
		0.20	0.9747±0.0022	-2.5310	0.9684±2.2356	-3.1592	0.9862±0.1745	-1.3842	0.9037±1.6059	-9.6309
		0.30	0.9747±0.0022	-2.5310	0.9684±2.2356	-3.1592	0.9977±0.1086	-0.2350	0.9007±1.5481	-9.9251
		0.40	0.9747±0.0022	-2.5310	0.9684±2.2356	-3.1592	1.0109±0.0745	1.0920	0.8969±2.2390	-10.310
		0.50	0.9747±0.0022	-2.5310	0.9684±2.2356	-3.1592	1.0264±0.0529	2.6400	0.8917±2.1036	-10.831
		0.60	0.9747±0.0022	-2.5310	0.9684±2.2356	-3.1592	1.0439±0.0368	4.3920	0.8835±2.2727	-11.646
		0.70	0.9747±0.0022	-2.5310	0.9684±2.2356	-3.1592	1.0624±0.0236	6.2390	0.8697±1.7733	-13.035
		0.80	0.9747±0.0022	-2.5310	0.9684±2.2356	-3.1592	1.0717±0.0118	7.1740	0.8376±2.6613	-16.236
		0.90	0.9747±0.0022	-2.5310	0.9684±2.2356	-3.1592	1.0436±0.0037	4.3640	0.7701±0.0007	-22.988
		0.99	0.9747±0.0022	-2.5310	0.9684±2.2356	-3.1592	0.9975±0.0004	-0.2529	0.9644±0.0008	-3.5621

Appendix Table H1 (Continued)

r_{Di}	τ_{open}	X	Procedure 1.1 Exit flow rate curve fitting		Procedure 1.2 Exit flow rate curve fitting		Procedure 2 Exit flow rate curve fitting		Procedure 2 Unit-area normalized fitting	
			$D_{e,est}^{inert}$	ΔD_{e}^{inert}	$D_{e,est}^{inert}$	ΔD_{e}^{inert}	$D_{e,est}^{inert}$	ΔD_{e}^{inert}	$D_{e,est}^{inert}$	ΔD_{e}^{inert}
	0.026	0.01	0.9667±0.0028	-3.3256	0.9604±2.9364	-3.9620	0.9599±2.5081	-4.0118	0.8846±1.5820	-11.542
		0.10	0.9667±0.0028	-3.3256	0.9604±2.9364	-3.9620	0.9676±0.4740	-3.2389	0.8824±2.0722	-11.756
		0.20	0.9667±0.0028	-3.3256	0.9604±2.9364	-3.9620	0.9772±0.2259	-2.2800	0.8796±2.4024	-12.043
		0.30	0.9667±0.0028	-3.3256	0.9604±2.9364	-3.9620	0.9883±0.1401	-1.1716	0.8762±3.2364	-12.378
		0.40	0.9667±0.0028	-3.3256	0.9604±2.9364	-3.9620	1.0012±0.0967	0.1240	0.8712±2.1331	-12.881
		0.50	0.9667±0.0028	-3.3256	0.9604±2.9364	-3.9620	1.0165±0.0694	1.6460	0.8643±3.0312	-13.574
		0.60	0.9667±0.0028	-3.3256	0.9604±2.9364	-3.9620	1.0341±0.0495	3.4070	0.8539±2.5170	-14.611
		0.70	0.9667±0.0028	-3.3256	0.9604±2.9364	-3.9620	1.0544±0.0335	5.4390	0.8357±1.8329	-16.426
		0.80	0.9667±0.0028	-3.3256	0.9604±2.9364	-3.9620	1.0727±0.0189	7.2660	0.7888±2.8817	-21.120
		0.90	0.9667±0.0028	-3.3256	0.9604±2.9364	-3.9620	1.0596±0.0062	5.9640	0.7918±0.0023	-20.822
		0.99	0.9667±0.0028	-3.3256	0.9604±2.9364	-3.9620	1.0000±0.0004	-0.0031	0.9712±0.0009	-2.8836
1/3	0.015	0.50	0.9813±0.0017	-1.8683	0.9696±0.2735	-3.0359	1.0287±0.0113	2.8680	0.9485±0.2724	-5.1461
1/2			0.9813±0.0017	-1.8683	0.9711±0.8088	-2.8899	1.0305±0.0177	3.0490	0.9395±0.5861	-6.0497
2/3			0.9813±0.0017	-1.8683	0.9721±1.2893	-2.7883	1.0319±0.0244	3.1910	0.9312±0.8071	-6.8845
4/3			0.9813±0.0017	-1.8683	0.9772±2.6757	-2.2845	1.0366±0.0531	3.6550	0.9007±3.7164	-9.9327
3/2			0.9813±0.0017	-1.8683	0.9787±2.9725	-2.1303	1.0375±0.0606	3.7470	0.8937±2.6280	-10.630
2/1			0.9813±0.0017	-1.8683	0.9823±3.8784	-1.7653	1.0404±0.0868	4.0430	0.8736±4.0168	-12.643
3/1			0.9813±0.0017	-1.8683	0.9922±5.3448	-0.7833	1.0537±0.1390	5.3710	0.8438±2.0874	-15.617

Appendix I

Simulated Results for $D_{e,est}^{cat}$ and ΔD_{e}^{cat} Obtained from Different Procedures at Various r_{Di}, τ_{open} and X for the Three-Zone Reactor with $L_{cat}/L_{reactor}$ = 1/30.

Appendix Table I1 Simulated Results for $D_{e,est}^{cat}$ and ΔD_{e}^{cat} Obtained from Different Procedures at Various r_{Di} , τ_{open} and X for Three-Zone Reactor with $L_{cat}/L_{reactor}$ = 1/30

r_{Di}	τ_{open}	X	Procedure 1.1		Procedure 1.2		Procedure 2		Procedure 2	
			Exit flow rate curve fitting		Exit flow rate curve fitting		Exit flow rate curve fitting		Unit-area normalized fitting	
			$D_{e,est}^{cat}$	ΔD_{e}^{cat}	$D_{e,est}^{cat}$	ΔD_{e}^{cat}	$D_{e,est}^{cat}$	ΔD_{e}^{cat}	$D_{e,est}^{cat}$	ΔD_{e}^{cat}
1/1	0.004	0.01	0.8089±0.0066	-19.109	0.9675±15.517	-3.2465	0.9483±7.5958	-5.1700	1.0063±7.8041	0.6300
		0.10	0.8089±0.0066	-19.109	0.9675±15.517	-3.2465	0.7526±1.1454	-24.736	1.0099±7.6266	0.9940
		0.20	0.8089±0.0066	-19.109	0.9675±15.517	-3.2465	0.5935±0.3623	-40.652	1.0141±21.403	1.4060
		0.30	0.8089±0.0066	-19.109	0.9675±15.517	-3.2465	0.4780±0.1417	-52.195	1.0197±16.886	1.9690
		0.40	0.8089±0.0066	-19.109	0.9675±15.517	-3.2465	0.3958±0.0594	-60.421	1.0177±15.530	1.7680
		0.50	0.8089±0.0066	-19.109	0.9675±15.517	-3.2465	0.3491±0.0253	-65.094	1.0224±15.159	2.2360
		0.60	0.8089±0.0066	-19.109	0.9675±15.517	-3.2465	0.3579±0.0128	-64.213	1.0430±24.734	4.2950
		0.70	0.8089±0.0066	-19.109	0.9675±15.517	-3.2465	0.4024±0.0091	-59.762	1.0587±24.668	5.8730
		0.80	0.8089±0.0066	-19.109	0.9675±15.517	-3.2465	0.4393±0.0073	-56.074	1.0890±26.342	8.9040
		0.90	0.8089±0.0066	-19.109	0.9675±15.517	-3.2465	0.4360±0.0054	-56.405	1.2065±23.303	20.653
		0.99	0.8089±0.0066	-19.109	0.9675±15.517	-3.2465	0.2431±0.0015	-75.692	0.1942±0.0876	-80.583
	0.009	0.01	0.8044±0.0143	-19.556	0.9672±34.423	-3.2754	0.9595±18.937	-4.0492	0.9955±23.471	-0.4534
		0.10	0.8044±0.0143	-19.556	0.9672±34.423	-3.2754	0.7544±2.6260	-24.561	0.9874±24.124	-1.2562
		0.20	0.8044±0.0143	-19.556	0.9672±34.423	-3.2754	0.5911±0.8231	-40.894	0.9970±39.436	-0.2986
		0.30	0.8044±0.0143	-19.556	0.9672±34.423	-3.2754	0.4692±0.3306	-53.075	0.9938±28.950	-0.6229
		0.40	0.8044±0.0143	-19.556	0.9672±34.423	-3.2754	0.3768±0.1444	-62.321	1.0039±38.357	0.3910
		0.50	0.8044±0.0143	-19.556	0.9672±34.423	-3.2754	0.3048±0.0646	-69.519	1.0066±40.694	0.6620
		0.60	0.8044±0.0143	-19.556	0.9672±34.423	-3.2754	0.2535±0.0282	-74.650	1.0165±50.164	1.6480
		0.70	0.8044±0.0143	-19.556	0.9672±34.423	-3.2754	0.2320±0.0124	-76.804	1.0311±56.425	3.1120
		0.80	0.8044±0.0143	-19.556	0.9672±34.423	-3.2754	0.2433±0.0069	-75.674	1.0568±47.007	5.6840
		0.90	0.8044±0.0143	-19.556	0.9672±34.423	-3.2754	0.2407±0.0041	-75.933	1.2759±18.517	27.591
		0.99	0.8044±0.0143	-19.556	0.9672±34.423	-3.2754	0.1194±0.0006	-88.058	0.0350±0.0026	-96.504

Appendix Table I1 (Continued)

r_{Di}	τ_{open}	X	Procedure 1.1 Exit flow rate curve fitting		Procedure 1.2 Exit flow rate curve fitting		Procedure 2 Exit flow rate curve fitting		Procedure 2 Unit-area normalized fitting	
			$D_{e,est}^{cat}$	ΔD_{e}^{cat}	$D_{e,est}^{cat}$	ΔD_{e}^{cat}	$D_{e,est}^{cat}$	ΔD_{e}^{cat}	$D_{e,est}^{cat}$	ΔD_{e}^{cat}
	0.015	0.01	0.8056±0.0242	-19.437	0.9504±49.754	-4.9557	0.9589±37.669	-4.1062	0.9567±38.114	-4.3266
		0.10	0.8056±0.0242	-19.437	0.9504±49.754	-4.9557	0.7545±4.6106	-24.549	0.9606±51.589	-3.9371
		0.20	0.8056±0.0242	-19.437	0.9504±49.754	-4.9557	0.5887±1.4121	-41.126	0.9622±38.671	-3.7839
		0.30	0.8056±0.0242	-19.437	0.9504±49.754	-4.9557	0.4656±0.5642	-53.439	0.9644±46.994	-3.5564
		0.40	0.8056±0.0242	-19.437	0.9504±49.754	-4.9557	0.3693±0.2476	-63.069	0.9627±44.553	-3.7324
		0.50	0.8056±0.0242	-19.437	0.9504±49.754	-4.9557	0.2935±0.1132	-70.653	0.9736±49.055	-2.6428
		0.60	0.8056±0.0242	-19.437	0.9504±49.754	-4.9557	0.2327±0.0507	-76.725	0.9799±36.343	-2.0096
		0.70	0.8056±0.0242	-19.437	0.9504±49.754	-4.9557	0.1865±0.0211	-81.351	0.9977±72.007	-0.2347
		0.80	0.8056±0.0242	-19.437	0.9504±49.754	-4.9557	0.1623±0.0083	-83.767	1.0334±35.434	3.3430
		0.90	0.8056±0.0242	-19.437	0.9504±49.754	-4.9557	0.1530±0.0035	-84.695	0.8867±9.2512	-11.334
		0.99	0.8056±0.0242	-19.437	0.9504±49.754	-4.9557	0.0734±0.0003	-92.658	0.0393±0.0010	-96.069
	0.020	0.01	0.8032±0.0320	-19.680	0.9444±61.461	-5.5609	0.9487±42.542	-5.1316	0.9379±38.075	-6.2069
		0.10	0.8032±0.0320	-19.680	0.9444±61.461	-5.5609	0.7472±6.1100	-25.282	0.9420±72.764	-5.8011
		0.20	0.8032±0.0320	-19.680	0.9444±61.461	-5.5609	0.5833±1.8832	-41.667	0.9400±49.573	-6.0022
		0.30	0.8032±0.0320	-19.680	0.9444±61.461	-5.5609	0.4599±0.7448	-54.013	0.9441±48.247	-5.5905
		0.40	0.8032±0.0320	-19.680	0.9444±61.461	-5.5609	0.3646±0.3306	-63.540	0.9473±70.453	-5.2730
		0.50	0.8032±0.0320	-19.680	0.9444±61.461	-5.5609	0.2881±0.1525	-71.186	0.9458±66.154	-5.4167
		0.60	0.8032±0.0320	-19.680	0.9444±61.461	-5.5609	0.2259±0.0692	-77.409	0.9539±72.956	-4.6097
		0.70	0.8032±0.0320	-19.680	0.9444±61.461	-5.5609	0.1744±0.0290	-82.565	0.9680±58.883	-3.1959
		0.80	0.8032±0.0320	-19.680	0.9444±61.461	-5.5609	0.1363±0.0105	-86.366	1.0205±97.939	2.0530
		0.90	0.8032±0.0320	-19.680	0.9444±61.461	-5.5609	0.1169±0.0034	-88.306	0.0216±0.0015	-97.839
		0.99	0.8032±0.0320	-19.680	0.9444±61.461	-5.5609	0.0554±0.0002	-94.456	0.0352±0.0006	-96.482

Appendix Table I1 (Continued)

r_{Di}	τ_{open}	X	Procedure 1.1 Exit flow rate curve fitting		Procedure 1.2 Exit flow rate curve fitting		Procedure 2 Exit flow rate curve fitting		Procedure 2 Unit-area normalized fitting	
			$D_{e,est}^{cat}$	ΔD_e^{cat}	$D_{e,est}^{cat}$	ΔD_e^{cat}	$D_{e,est}^{cat}$	ΔD_e^{cat}	$D_{e,est}^{cat}$	ΔD_e^{cat}
	0.026	0.01	0.7946±0.0403	-20.543	0.9360±80.637	-6.3993	0.9525±71.278	-4.7512	0.9153±48.590	-8.4721
		0.10	0.7946±0.0403	-20.543	0.9360±80.637	-6.3993	0.7457±8.3579	-25.429	0.9171±53.990	-8.2899
		0.20	0.7946±0.0403	-20.543	0.9360±80.637	-6.3993	0.5795±2.4482	-42.051	0.9198±47.803	-8.0214
		0.30	0.7946±0.0403	-20.543	0.9360±80.637	-6.3993	0.4559±0.9606	-54.411	0.9122±68.741	-8.7822
		0.40	0.7946±0.0403	-20.543	0.9360±80.637	-6.3993	0.3597±0.4250	-64.028	0.9199±66.947	-8.0136
		0.50	0.7946±0.0403	-20.543	0.9360±80.637	-6.3993	0.2830±0.1696	-71.702	0.9247±96.993	-7.5271
		0.60	0.7946±0.0403	-20.543	0.9360±80.637	-6.3993	0.2200±0.0898	-78.001	0.9303±81.854	-6.9685
		0.70	0.7946±0.0403	-20.543	0.9360±80.637	-6.3993	0.1667±0.0382	-83.333	0.9418±61.745	-5.8186
		0.80	0.7946±0.0403	-20.543	0.9360±80.637	-6.3993	0.1225±0.0137	-87.751	1.0200±113.51	2.0030
		0.90	0.7946±0.0403	-20.543	0.9360±80.637	-6.3993	0.0917±0.0036	-90.833	0.0441±0.0033	-95.594
		0.99	0.7946±0.0403	-20.543	0.9360±80.637	-6.3993	0.0427±0.0002	-95.730	0.0309±0.0004	-96.906
1/3	0.015	0.50	0.8056±0.0242	-19.437	2.7803±65.011	178.03	0.4120±0.0666	-58.804	3.0129±78.563	201.29
1/2			0.8056±0.0242	-19.437	1.8660±86.308	86.599	0.3713±0.0845	-62.871	2.0030±75.846	100.30
2/3			0.8056±0.0242	-19.437	1.4191±79.406	41.907	0.3402±0.0973	-65.983	1.4767±57.471	47.669
4/3			0.8056±0.0242	-19.437	0.7217±42.193	-27.834	0.2587±0.1208	-74.128	0.7247±66.628	-27.529
3/2			0.8056±0.0242	-19.437	0.6426±37.057	-35.741	0.2448±0.1228	-75.522	0.6436±37.491	-35.645
2/1			0.8056±0.0242	-19.437	0.4856±27.402	-51.438	0.2112±0.1298	-78.882	0.4824±30.278	-51.764
3/1			0.8056±0.0242	-19.437	0.3281±16.919	-67.194	0.1636±0.1208	-83.642	0.3284±8.1633	-67.156

Appendix J

Simulated Results for κ_{est} and Δk Obtained from Different Procedures using the Exit Flow Rate Curve Fitting at Various r_{Di}, τ_{open} and X for the Three-Zone Reactor with $L_{cat}/L_{reactor}$ = 1/30.

Appendix Table J1 Simulated Results for κ_{est} and Δk Obtained from Different Procedures using the Exit Flow Rate Curve Fitting at Various r_{Di}, τ_{open} and X for the Three-Zone Reactor with $L_{cat}/L_{reactor}$ = 1/30

r_{Di}	τ_{open}	X	κ_{real}	Procedure 1.1		Procedure 1.2		Procedure 2	
				κ_{est}	Δk	κ_{est}	Δk	κ_{est}	Δk
1/1	0.004	0.01	0.6060	0.4572±0.0251	-24.548	0.4545±0.0354	-25.000	0.4573±0.0254	-24.533
		0.10	6.6586	6.4907±0.0276	-2.5220	6.4856±0.0392	-2.5975	6.4914±0.0279	-2.5112
		0.20	14.959	14.766±0.0312	-1.2943	14.756±0.0446	-1.3605	14.774±0.0311	-1.2408
		0.30	25.595	25.370±0.0363	-0.8800	25.354±0.0518	-0.9421	25.399±0.0340	-0.7636
		0.40	39.712	39.448±0.0438	-0.6658	39.420±0.0618	-0.7348	39.530±0.0363	-0.4588
		0.50	59.356	59.044±0.0554	-0.5269	58.996±0.0765	-0.6076	59.234±0.0379	-0.2066
		0.60	88.565	88.194±0.0751	-0.4186	88.107±0.0996	-0.5168	88.536±0.0411	-0.0324
		0.70	136.58	136.15±0.1120	-0.3159	135.98±0.1406	-0.4397	136.63±0.0495	0.0348
		0.80	230.22	229.78±0.1937	-0.1949	229.40±0.2267	-0.3578	230.37±0.0669	0.0614
		0.90	494.28	494.19±0.4464	-0.0174	493.11±0.4834	-0.2374	494.63±0.1040	0.0710
		0.99	3400.8	3407.5±2.6879	0.1946	3399.7±2.7066	-0.0341	3402.3±0.2194	0.0417
	0.009	0.01	0.6060	0.2896±0.0545	-52.203	0.2862±0.0770	-52.766	0.2885±0.0567	-52.395
		0.10	6.6586	6.2956±0.0604	-5.4512	6.2903±0.0857	-5.5314	6.2968±0.0614	-5.4339
		0.20	14.959	14.532±0.0688	-2.8572	14.522±0.0979	-2.9221	14.541±0.0697	-2.7950
		0.30	25.595	25.084±0.0957	-1.9958	25.068±0.1140	-2.0599	25.116±0.0789	-1.8700
		0.40	39.712	39.091±0.1190	-1.5642	39.063±0.1361	-1.6345	39.179±0.0894	-1.3436
		0.50	59.356	58.585±0.1564	-1.2993	58.537±0.1681	-1.3809	58.799±0.1007	-0.9383
		0.60	88.565	87.583±0.2238	-1.1088	87.495±0.2179	-1.2078	88.080±0.1129	-0.5475
		0.70	136.58	135.29±0.3686	-0.9434	135.12±0.3047	-1.0686	136.34±0.1282	-0.1724
		0.80	230.22	228.48±0.8092	-0.7591	228.10±0.4846	-0.9233	230.31±0.1584	0.0375
		0.90	494.28	491.94±0.0005	-0.4729	490.83±1.0157	-0.6986	494.79±0.2248	0.1037
		0.99	3400.8	3400.9±4.6952	0.0023	3392.7±5.5934	-0.2391	3402.6±0.3127	0.0523

Appendix Table J1 (Continued)

r_{Di}	τ_{open}	X	κ_{real}	Procedure 1.1		Procedure 1.2		Procedure 2	
				κ_{est}	Δk	κ_{est}	Δk	κ_{est}	Δk
	0.015	0.01	0.6060	0.0420±0.0899	-93.077	0.0386±0.1272	-93.627	0.0414±0.0909	-93.176
		0.10	6.6586	6.0147±0.0998	-9.6696	6.0091±0.1415	-9.7548	6.0163±0.1021	-9.6454
		0.20	14.959	14.181±0.1139	-5.2036	14.172±0.1619	-5.2658	14.192±0.1163	-5.1261
		0.30	25.595	24.665±0.1325	-3.6337	24.650±0.1883	-3.6930	24.701±0.1329	-3.4922
		0.40	39.712	38.605±0.1580	-2.7878	38.580±0.2244	-2.8510	38.698±0.1529	-2.5541
		0.50	59.356	57.950±0.1956	-2.3701	57.907±0.2769	-2.4424	58.170±0.1779	-1.9987
		0.60	88.565	86.755±0.2550	-2.0439	86.678±0.3585	-2.1307	87.269±0.2082	-1.4627
		0.70	136.58	134.17±0.3601	-1.7642	134.02±0.5002	-1.8740	135.39±0.2457	-0.8731
		0.80	230.22	226.75±0.5822	-1.5114	226.41±0.7936	-1.6574	229.52±0.2981	-0.3065
		0.90	494.28	489.00±1.2521	-1.0691	487.99±1.6606	-1.2724	494.34±0.3977	0.0113
		0.99	3400.8	3392.2±7.1335	-0.2552	3384.5±9.1587	-0.4802	3400.7±0.4279	-0.0035
	0.020	0.01	0.6060	-0.1550±0.1186	-125.58	-0.1589±0.1680	-126.22	-0.1569±0.1191	-125.89
		0.10	6.6586	5.8042±0.1315	-12.832	5.7983±0.1865	-12.920	5.8069±0.1343	-12.791
		0.20	14.959	13.938±0.1501	-6.8280	13.929±0.2131	-6.8888	13.952±0.1526	-6.7344
		0.30	25.595	24.383±0.1743	-4.7343	24.368±0.2476	-4.7925	24.424±0.1754	-4.5764
		0.40	39.712	38.228±0.2079	-3.7371	38.204±0.2951	-3.7986	38.326±0.2036	-3.4903
		0.50	59.356	57.468±0.2568	-3.1807	57.427±0.3637	-3.2504	57.693±0.2396	-2.8016
		0.60	88.565	86.093±0.3335	-2.7908	86.019±0.4701	-2.8740	86.608±0.2860	-2.2093
		0.70	136.58	133.29±0.4688	-2.4085	133.14±0.6548	-2.5147	134.51±0.3461	-1.5138
		0.80	230.22	225.51±0.7530	-2.0483	225.18±1.0368	-2.1894	228.56±0.4287	-0.7222
		0.90	494.28	487.05±1.6074	-1.4632	486.06±2.1667	-1.6627	493.98±0.5598	-0.0601
		0.99	3400.8	3389.2±9.0960	-0.3414	3381.5±11.949	-0.5681	3402.4±0.5255	0.0447

Appendix Table J1 (Continued)

r_{Di}	τ_{open}	X	κ_{real}	Procedure 1.1		Procedure 1.2		Procedure 2	
				κ_{est}	Δk	κ_{est}	Δk	κ_{est}	Δk
	0.026	0.01	0.6060	-0.305±0.1513	-150.36	-0.3093±0.2139	-151.04	-0.3047±0.1555	-150.28
		0.10	6.6586	5.5898±0.1682	-16.051	5.5846±0.2383	-16.130	5.5936±0.1701	-15.995
		0.20	14.959	13.702±0.1913	-8.4023	13.693±0.2717	-8.4665	13.719±0.1948	-8.2893
		0.30	25.595	24.083±0.2224	-5.9052	24.068±0.3157	-5.9666	24.128±0.2244	-5.7306
		0.40	39.712	37.857±0.2648	-4.6711	37.833±0.3758	-4.7330	37.962±0.2615	-4.4077
		0.50	59.356	56.983±0.3266	-3.9986	56.942±0.4627	-4.0680	57.214±0.3100	-3.6094
		0.60	88.565	85.477±0.4231	-3.4862	85.404±0.5970	-3.5688	85.989±0.3741	-2.9085
		0.70	136.58	132.38±0.5921	-3.0748	132.24±0.8295	-3.1795	133.57±0.4621	-2.2006
		0.80	230.22	224.15±0.9472	-2.6381	223.83±1.3114	-2.7793	227.21±0.5881	-1.3090
		0.90	494.28	484.93±2.0124	-1.8921	483.93±2.7374	-2.0950	493.14±0.7702	-0.2315
		0.99	3400.8	3384.3±11.366	-0.4878	3376.2±15.133	-0.7254	3401.5±0.6280	0.0200
1/3	0.015	0.50	20.358	20.157±0.0246	-0.9879	20.128±0.0384	-1.1284	20.224±0.0215	-0.6578
1/2			30.339	29.933±0.0531	-1.3404	29.895±0.0774	-1.4631	30.036±0.0477	-1.0000
2/3			40.173	39.486±0.0916	-1.7115	39.442±0.1311	-1.8197	39.626±0.0832	-1.3607
4/3			77.995	75.693±0.3288	-2.9525	75.658±0.4651	-2.9975	76.001±0.2987	-2.5578
3/2			87.146	84.366±0.4066	-3.1904	84.341±0.5755	-3.2185	84.720±0.3611	-2.7842
2/1			113.79	109.23±0.6743	-4.0115	109.24±0.9564	-4.0019	109.74±0.6130	-3.5669
3/1			163.96	155.46±1.2160	-5.1879	155.62±1.7334	-5.0861	156.34±1.0717	-4.6512

Appendix K

Simulated Results for κ_{est} and Δk Obtained from Different Procedures using the Unit-Area Normalized Response Fitting at Various r_{Di} , τ_{open} and X for the Three-Zone Reactor with $L_{cat}/L_{reactor}$ = 1/30

Appendix Table K1 Simulated Results for κ_{est} and Δk Obtained from Different Procedures using the the Unit-Area Normalized Response Fitting at Various r_{Di}, τ_{open} and X for the Three-Zone Reactor with $L_{cat}/L_{reactor}$ = 1/30

r_{Di}	τ_{open}	X	κ_{real}	Procedure 1.1		Procedure 1.2		Procedure 2	
				κ_{est}	Δk	κ_{est}	Δk	κ_{est}	Δk
1/1	0.004	0.01	0.6060	0.8514±0.0338	40.504	0.8570±0.0477	41.421	2.2200±0.0367	266.34
		0.10	6.6586	6.8828±0.0392	3.3671	6.9109±0.0554	3.7889	8.5042±1.3212	27.718
		0.20	14.959	15.140±0.0472	1.2112	15.205±0.0668	1.6437	17.149±8.1787	14.638
		0.30	25.595	25.699±0.0583	0.4050	25.821±0.0827	0.8821	28.273±11.801	10.464
		0.40	39.712	39.672±0.0744	-0.1009	39.890±0.1059	0.4470	43.117±16.734	8.5740
		0.50	59.356	59.041±0.0993	-0.5318	59.425±0.1420	0.1152	63.957±33.123	7.7506
		0.60	88.565	87.674±0.1416	-1.0056	88.378±0.2028	-0.2109	95.431±97.813	7.7525
		0.70	136.58	134.31±0.2239	-1.6602	135.72±0.3254	-0.6264	148.51±199.26	8.7339
		0.80	230.22	223.73±0.4249	-2.8214	227.15±0.6279	-1.3372	258.59±548.84	12.319
		0.90	494.28	465.21±1.2225	-5.8823	478.33±1.8822	-3.2272	666.18±2528.4	34.777
		0.99	3400.8	2444.3±18.992	-28.127	2769.2±35.734	-18.574	17518±2369.3	5051.2
	0.009	0.01	0.6060	1.1494±0.0740	89.670	1.1612±0.1047	91.622	4.2092±2.1541	594.60
		0.10	6.6586	7.1944±0.0861	8.0464	7.2304±0.1221	8.5882	10.800±5.6249	62.189
		0.20	14.959	15.466±0.1039	3.3878	15.542±0.1474	3.8931	19.908±18.224	33.082
		0.30	25.595	26.032±0.1287	1.7080	26.169±0.1829	2.2445	31.688±24.033	23.806
		0.40	39.712	40.000±0.1648	0.7252	40.238±0.2349	1.3251	47.558±54.906	19.756
		0.50	59.356	59.327±0.2211	-0.0494	59.741±0.3161	0.6479	70.087±103.10	18.078
		0.60	88.565	87.823±0.3169	-0.8378	88.572±0.4553	0.0078	104.74±236.47	18.258
		0.70	136.58	134.03±0.5056	-1.8660	135.51±0.7289	-0.7794	165.35±562.71	21.063
		0.80	230.22	221.87±0.9595	-3.6306	225.40±1.4074	-2.0943	302.68±1345.9	31.472
		0.90	494.28	453.93±2.7488	-8.1638	467.04±4.1604	-5.5121	1327.9±7159.5	168.65
		0.99	3400.8	2121.6±35.927	-37.615	2380.4±64.549	-30.006	33891±4539.0	896.54

Appendix Table K1 (Continued)

r_{Di}	τ_{open}	X	κ_{real}	Procedure 1.1		Procedure 1.2		Procedure 2	
				κ_{est}	Δk	κ_{est}	Δk	κ_{est}	Δk
	0.015	0.01	0.6060	1.5082±0.1224	148.89	1.5269±0.1735	151.97	6.6824±5.6229	1002.7
		0.10	6.6586	7.5680±0.1426	13.658	7.6113±0.2021	14.309	13.665±15.997	105.22
		0.20	14.959	15.852±0.1722	5.9708	15.935±0.2444	6.5223	23.363±22.489	56.175
		0.30	25.595	26.424±0.2133	3.2376	26.567±0.3033	3.7967	36.000±47.887	40.651
		0.40	39.712	40.378±0.2732	1.6768	40.620±0.3892	2.2850	53.164±78.797	33.872
		0.50	59.356	59.640±0.3666	0.4783	60.052±0.5238	1.1714	77.956±151.49	31.336
		0.60	88.565	87.946±0.5252	-0.6982	88.680±0.7534	0.1297	117.01±213.76	32.113
		0.70	136.58	133.59±0.8325	-2.1852	135.02±1.2017	-1.1382	188.80±934.71	38.236
		0.80	230.22	219.44±1.5758	-4.6840	222.78±2.3004	-3.2336	376.14±1537.7	63.381
		0.90	494.28	440.43±4.3953	-10.895	452.28±6.5891	-8.4983	17905±8268.7	3522.4
		0.99	3400.8	1822.4±43.527	-46.415	2005.2±80.026	-41.038	11040±502.95	224.64
	0.020	0.01	0.6060	1.8044±0.1625	197.75	1.8283±0.2306	201.70	8.7987±7.5391	1351.9
		0.10	6.6586	7.8748±0.1892	18.265	7.9247±0.2683	19.015	16.120±27.725	142.09
		0.20	14.959	16.168±0.2284	8.0799	16.258±0.3242	8.6808	26.334±34.325	76.038
		0.30	25.595	26.740±0.2828	4.4754	26.892±0.4021	5.0665	39.728±57.653	55.217
		0.40	39.712	40.676±0.3622	2.4265	40.926±0.5161	3.0558	58.097±143.29	46.296
		0.50	59.356	59.875±0.4856	0.8735	60.295±0.6937	1.5821	84.929±241.41	43.083
		0.60	88.565	88.008±0.6945	-0.6283	88.750±0.9960	0.2087	128.21±514.39	44.762
		0.70	136.58	133.16±1.0973	-2.5037	134.59±1.5829	-1.4574	211.49±965.37	54.852
		0.80	230.22	217.36±2.0598	-5.5900	220.64±3.0015	-4.1640	466.38±6384.8	102.58
		0.90	494.28	429.61±5.6029	-13.084	440.87±8.3716	-10.805	12932±107.91	2516.3
		0.99	3400.8	1632.0±50.937	-52.013	1778.3±85.692	-47.711	8118.6±259.75	138.72

Appendix Table K1 (Continued)

r_{Di}	τ_{open}	X	κ_{real}	Procedure 1.1		Procedure 1.2		Procedure 2	
				κ_{est}	Δk	κ_{est}	Δk	κ_{est}	Δk
	0.026	0.01	0.6060	2.1517±0.2098	255.07	2.1840±0.2974	260.40	11.383±12.727	1778.4
		0.10	6.6586	8.2328±0.2443	23.641	8.2905±0.3464	24.508	19.138±30.561	187.42
		0.20	14.959	16.534±0.2946	10.530	16.634±0.4184	11.192	30.003±62.711	100.57
		0.30	25.595	27.103±0.3647	5.8909	27.264±0.5187	6.5219	44.349±98.971	73.271
		0.40	39.712	41.009±0.4666	3.2660	41.272±0.6649	3.9265	64.258±163.26	61.808
		0.50	59.356	60.122±0.6247	1.2898	60.556±0.8925	2.0210	93.856±421.19	58.123
		0.60	88.565	88.032±0.8910	-0.6018	88.785±1.2776	0.2490	142.96±707.95	61.414
		0.70	136.58	132.57±1.4407	-2.9335	134.00±2.0197	-1.8858	243.70±1337.1	78.436
		0.80	230.22	214.75±2.6017	-6.7228	217.97±3.7886	-5.3212	655.14±3982.8	184.56
		0.90	494.28	417.06±6.8698	-15.623	427.68±10.235	-13.475	9741.3±1286.6	1870.8
		0.99	3400.8	1448.6±53.090	-57.403	1563.8±87.589	-54.016	6409.1±167.15	88.456
1/3	0.015	0.50	20.358	20.628±0.0442	1.3242	20.879±0.0630	2.5591	22.892±7.0040	12.449
1/2			30.339	30.674±0.0981	1.1039	31.005±0.1406	2.1949	35.569±23.986	17.237
2/3			40.173	40.530±0.1710	0.8895	40.926±0.2449	1.8733	48.992±47.046	21.952
4/3			77.995	78.048±0.6190	0.0679	78.396±0.8820	0.5137	109.61±53.844	40.529
3/2			87.146	87.041±0.7642	-0.1209	87.318±1.0874	0.1974	126.44±45.065	45.092
2/1			113.79	112.92±1.2692	-0.7688	112.88±1.7980	-0.8031	180.80±105.85	58.885
3/1			163.96	160.48±2.2348	-2.1250	159.00±3.2251	-3.0283	296.30±100.46	80.709

CURRICULUM VITAE

NAME : Miss Rapeeporn Ekjamnong

BIRTH DATE : May 24, 1985

BIRTH PLACE : Nakhonsawan, Thailand

EDUCATION :

YEAR	INSTITUTE	DEGREE/DIPLOMA
2006	Kasetsart Univ.	B.Sc. (Chemistry)
2010	Kasetsart Univ.	M.Eng. (Chemical Engineering)

SCHOLARSHIP : The National Center of Excellence for Petroleum, Petrochemicals, and Advanced Materials, Department of Chemical Engineering, Faculty of Engineering, Kasetsart University Scholarship 2005-2007